Metabolism studies in breast cancer

Thesis submitted by:
Anand Sharma
Green Templeton College

For the degree of:
Doctor of Philosophy
Department of Oncology
Trinity Term 2014
University of Oxford

Supervisor:
Professor Adrian L. Harris

Abstract

Metabolic reprogramming has emerged as a common phenotype of cancers. Otto Warburg in 1920s observed that cancer cells consume higher amounts of glucose for their metabolism producing high levels of lactate even in normal oxygen conditions, this has been termed as the Warburg effect. In breast cancer, this seemingly wasteful metabolism of glucose is mirrored by a similarly inefficient metabolism of glutamine.

Glutamine is the most abundant amino acid in plasma and it constitutes another important source of energy besides glucose. Glutamine serves as a precursor in nucleotide, glucose and amino acid biosynthesis, glutathione metabolism, protein synthesis and lipid synthesis through the mitochondrial or cytosolic conversion into citrate. It has long been known that tumour cells metabolize glutamine at significantly greater rates than any other amino acid.

Importantly, glutamine transporter and glutaminase expression has also been found to be upregulated in cancer versus normal tissues.

Our group has previously shown the anti-proliferative effect of metformin, which is enhanced in glutamine, deprived conditions; this has also been validated in a preclinical study. To investigate the active role of glutamine in breast cancer and the variable sensitivity in different cell lines, we worked on drugs affecting the glutamine metabolism. Breast cancer cell lines (MDA- MB 231, MDA MB-468, SKBR3, MCF 7, HCC 1806, T47D and BT474) were treated with glutamine dehydrogenase (GLUD) inhibitor bithionol (BT) and other drugs affecting glutamine metabolism including metformin and Phenylbutyrate.

The cytotoxic effects of BT against a panel of breast cancer cell lines were observed. Furthermore, apoptotic cell death was shown by expression of cPARP and confirmed by FACS. BT induced autophagy in breast cancer cell lines, which results in significant reduction in tumour growth as evidenced by LC3B and LAMP1 expression. Electron microscopy of the MCF 7 and MDA MB 231 cell lines (20 μM BT, 24 hour exposure) showed increased autophagosome, lysosomes and autolysosomes confirming autophagy in these treated cell lines.

Bithionol (BT) is an anthelmintic used to treat Fascioliasis (liver flukes) in humans. Fascioliasis is a trematode infection caused by Fasciola hepatica, involving the liver and biliary tract. However, recently due to the advent of newer drugs, this drug is used only in veterinary medicine. Mounting evidence suggests BT inhibits tumour growth in ovarian, melanoma and breast cancer cell lines.

Much of the interest in glutamine has stemmed from the discovery that the proto-oncogene Myc plays a role in the regulation of its metabolism. Myc transformed cells have been shown to be especially sensitive to glutamine withdrawal and subsequently it has been demonstrated that Myc induces the gene expression of several enzymes involved in glutamine metabolism. The importance of glutamine in supporting cancer cell proliferation and providing carbon for lipid synthesis has been shown to be of greater importance at times of mitochondrial stress with the reductive carboxylation pathway allowing glutamine to bypass the TCA cycle in its conversion to citrate.

My DPhil focuses on the sensitivity of different breast cancer subtypes on drugs/ conditions affecting glutamine metabolism and providing a unique opportunity in developing a new approach to increase anticancer efficacy by targeting glutamine metabolism in breast cancer. Also, BT may play a key role in inhibiting growth of breast cancer cells and targeting GLUD maybe a therapeutic option in this disease. Its role will be further validated *in vivo* xenograft models and in human samples in my DPhil study.

Acknowledgements

This thesis has been one of the most challenging experiences in my career and I have been lucky to have the opportunity to undertake it. Many people helped me along the way, and I would like to take a moment to thank them.

At first, I would like to thank Professor Adrian Harris, for his supervision, this thesis would not have been possible without his help and guidance. He has made me a better scientist and a clinician. His dedication towards research has inspired me in completing this work and taking up challenges in my career.

Dr Nikki Sibson, has been an important source of encouragement for me professionally and personally.

The two important members of Prof Adrian Harris's lab- Esther Bridges and Christos Zois have been my pillar of strength and have helped me immensely throughout my four years in oxford. These two scientists have not only imparted their technical expertise and scientific knowledge to me, but also have been around to support me in my difficult times. My thesis would not have been done without the help from these two members of the lab.

I would also like to thank Simon Wigfield and Alessandro Valli, for their help in the sea horse experiment and metabonomics. Also special thanks to James Mccullagh for his help for the Mass Spectroscopy. I would also like to thank Professor David Ferguson, for his help in electron microscopy.

Lisa Folkes for her help in the drug assay and pKa levels in the xenograft experiments. She was also instrumental for the HPLC experiments.

My fellow colleagues in the lab- Matteo Morotti, David Favara, Hugh Wright, Karim Bensaad, Helen Sheldon, Simon lord, Eugene Teoh, Alan McIntyre, Elena Favaro, and Katharina Feldinger, all of who were around to help and support me during the entire journey.

My family for their support and encouragement and in particular to my mother to whom, I am eternally indebted for always being there for me. Finally, I would like to thank my wife and daughter, who have always been a source of support and inspiration for me.

ABBREVIATIONS

μM	Micro molar
μm	Micrometre (s)
2DG	2 Deoxyglucose
α-KG	α-ketoglutarate
A	Adenosine
Ac	Acetyl
ACC	Acetyl CoA Carboxylase
ADP	Adenosine diphosphate
AE	Adverse Event
AICAR	5-Aminoimidazole-4-carboxamide ribonucleotide
ALT	Alanine Transaminase
AMP	Adenosine monophosphate
AMPK	5' Adenosine Monophosphate-activated Protein Kinase
ANC	Absolute Neutrophil Count
ANNOVA	Analysis of Variance
AOA	Amino-oxyacetate
APTT	Activated Partial Thromboplastin Time
Arg	Arginine
ATP	Adenosine Triphosphate
BOLD	Blood Oxygenation Level-Dependent
BP	Blood Pressure
BMI	Body Mass Index
BRCA1	Breast Cancer 1 gene

BPTES	Bis-2-(5-phenylacetamido-1,3,4-thiadiazol-2-yl)ethyl sulfide
BSA	Bovine serum albumin
BT	Bithionol
CAMMK	Calcium-calmodulin dependent protein kinase
CI	Confidence interval
CoA	Coenzyme A
CRUK	Cancer Research UK
CREB	cAMP response element-binding protein
CTP	Cytidine Triphosphate
dNTPs	deoxynucleotides
DAPI	4', 6-diamadino-2-phenylindole
DNA	Deoxyribonucleic Acid
DCE	Dynamic Contrast-Enhanced
DCA	Dichloroacetate
DEPC	Diethyl pyrocarbonate
DG	Diglyceride
2-DG	2-deoxyglucose
DMEM	Dulbecco's modified Eagle's minimal essential medium
DMSO	Dimethyl sulfoxide
DNL	De-novo Lipogenesis
ECOG	Eastern Cooperative Oncology Group
ECAR	Extracellular acidification rate
EDTA	Ethylenediaminetetraacetic acid
eGFR	estimated Glomerular Filtration Rate
ER	Oestrogen receptor

ETC	Electron transport chain
FAS	Fatty Acid Synthase
FACS	Fluorescence activated cell sorting
FBS	Foetal bovine serum
FCCP	Mesoxalonitrile 4-trifluoromethoxyphenylhydrazone
^{18}F-FDG	Fluorodeoxyglucose
FFPE	Formalin-Fixed Paraffin-Embedded
5FU	5-Fluorouracil
g	Grams
G	Guanine
G1	Gap 1 phase (cell cycle)
G6P	Glucose 6 phosphate
GDP	Glucose 6 phosphate
GO	Glucose Oxidation
GSTz1	Glutathione transferase zeta1
GC-IRMS	Chromatography-Isotope Ratio Mass Spectrometry
GC-MS	Gas Chromatography – Mass Spectrometry
GCP	Good Clinical Practice
GLUD	Glutamate dehydrogenase
Glu	Glutamic acid
GMD	Gross measurement diameter
GOT	Glutamate oxaloacetate transaminase
GPT	Glutamate pyruvate transaminase
GSH	Glutathione
GSSG	oxidized Glutathione

GTP	Guanosine triphosphate
H	Hypoxia (0.1% O_2)
h	Hour (s)
HDL	High-density lipoprotein
HER2	Human epidermal growth factor receptor 2
HEPES	4-(2-Hydroxyethyl)-1-piperazineethanesulphonic acid
Hb	Haemoglobin
HIF 1α	Hypoxia-inducible factor 1α
His	Histidine
HDL	High Density Lipoprotein
Hk	Hexokinase
HPLC	High Performance Liquid Chromatography
HRP	Horseradish peroxidase
^2H_2O	Deuterated water
H_2SO_4	Sulfuric acid
Hz	Hertz
IDH	Isocitrate dehydrogenase
IgG	Immunoglobin G
J	Coupling constant
kDa	Kilodalton (s)
KOH	Potassium hydroxide
Km	Michaelis constant
L	Litre (s)
LC	Liquid chromatography
LDH	Lactate dehydrogenase

LDL	Low Density Lipoprotein
LPA	Lysophophatidic acid
Lys	Lysine
M	Molar
m	Medium
MAPK	Mitogen-activated protein kinase
MDA-MB 231	Human breast adenocarcinoma line
MCF 7	Human breast adenocarcinoma line
MDA MB 468	Human breast adenocarcinoma line
MeOH	Methanol
mg	Milligram(s)
min	Minute(s)
mL	Millilitre(s)
mM	Millimetre(s)
mmol	Millimole(s)
mol	Mole(s)
m-TBST	Tris-buffered saline 0.1% Tween 20 and 5% milk powder
MnTMPyP	5,10,15,20-Tetrakis (1-methylpyridinium-4-yl)-21*H*, 23H-porphyrin manganese (III) pentachloride
MRI	Magnetic Resonance Imaging
mTOR	mammalian Target Of Rapamycin
mRNA	Messenger ribonucleic acid
MS	Mass Spectrometry
MW	Molecular Weight

N	Normoxia
NAD/NADH	Nicotinamide adenine dinucleotide
NADPH	Nicotinamide adenine dinucleotide phosphate
ng	Nanogram
NH4	Ammonium
NRF2	Nuclear factor (erythroid-derived 2)-like 2
ns	Not significant
OCR	Oxygen consumption rate
OXPHOS	Oxidative Phosphorylation
pAMPK	phosphorylated Adenosine Monophosphate-activated Protein Kinase
p53	Protein 53
PBS	Phosphate buffered saline solution
PCR	Polymerase chain reaction
PD	Pharmacodynamic
PDH	Pyruvate dehydrogenase
PDK	Pyruvate dehydrogenase kinase
PEP	Phosphoenolpyruvate
PET-CT	Positron Emission Tomography – Computed Tomography
PI3K	Phosphoinostide 3-kinase
PK	Pyruvate kinase
PL	Phospholipid
ppm	Parts per million
PPP	Pentose phosphate pathway
Pro	Proline

PTEN	Phosphate and tensin homolog
PVDF	Polyvinylidene fluoride
RFU	Relative fluorescence Unit
RCF	Relative centrifugal force
R&D	Research and Development
REC	Research Ethics Committee
RIPA	Radioimmunoprecipitation assay
RNA	Ribonucleic Acid
RNAseq	Next generation RNA sequencing
ROI	Region of interest
ROS	Reactive oxygen species
rpm	Rotations per minute
RPMI	Roswell Park Memorial Institute – 1640 medium
RT	Room Temperature
RT-PCR	Reverse transcription polymerase chain reaction
sat	Saturated
Scr	Non-targeting scramble siRNA control
SCD	Fatty Acid Desaturation
SDS-PAGE	Sodium dodecyl sulphate polyacrylamide gel electrophoresis
sec	Second
SEM	Standard error of the mean
Ser	Serine
S6K	S6 Kinase
shRNA	Small hairpin ribonucleic acid
siRNA	Small interfering ribonucleic acid

SIRT1	Silent Mating Type Information Regulation 2 Homolog 1
SKBR3	Human breast adenocarcinoma cell line
SOP	Standard Operating Procedure
SRB	Sulforhodamine B
SUV	Standardized Uptake Value
STAT3	Signal transducer and activator of transcription 3
T	Thymine
$t_{1/2}$	Half-life
TBST	Tris-buffered saline with 0.1% Tween 20
TCA cycle	Tricarboxylic acid cycle
TCA	Trichloroacetic acid
TG	Triglyceride
TIGAR	TP53-inducible glycolysis and apoptosis regulator
TLC	Thin layer chromatography
TPZ	Tirapazamine
TRIS	Tris (hydroxymethyl)aminomethane
TUNEL	Terminal deoxynucleotidyl transferase
U	Uracil
ULN	Upper Limit of Normal
V	Volume
VEGF	Vascular Endothelial Growth Factor
VOI	Volume of interest
W	Width

Table of Contents

List of Figures

CHAPTER 1

CHAPTER 3

CHAPTER 4

CHAPTER 5

CHAPTER 1: Introduction

1.1 Metabolic reprogramming

Warburg effect or enhanced glycolysis and impaired oxidative phosphorylation are a universal phenotype of cancer cells. The conventional cancer model defines metabolic reprogramming as a secondary response to cell cycle and proliferative signaling activated in cancer cells(Kroemer and Pouyssegur, 2008, Hanahan and Weinberg, 2011). In this model, the key role of metabolism is to provide energy, in order to support increased transcription and translation demands. Altered cellular metabolism seen in cancer cells, results in cells taking up glucose at higher rates resulting in increased aerobic glycolysis(Hsu and Sabatini, 2008, Kim and Dang, 2006, Warburg, 1956b).

Current evidence now supports an alternative model, in which altered metabolism constitutes a primary response to growth factor signaling primarily aimed at production of anabolic precursors for the synthesis of macromolecules essential for proliferation (e.g. nucleotides, proteins, lipids)(Ward and Thompson, 2012). The energy and biomass required for cell growth are provided by enhanced uptake of nutrients like glucose and glutamine. Glucose provides energy and some biosynthetic precursor molecules, whereas glutamine provides a major substrate for respiration and nitrogen for the production of proteins, hexosamines and macromolecules(Warburg, 1956a, Reitzer et al., 1979). Current research in cancer metabolism, have indicated the role of other energy sources, especially glutamine and other amino acids, in cell proliferation and survival(DeBerardinis et al., 2008, Sheen et al., 2011, Gao et al., 2009).

1.2 Glutamine metabolism

Glutamine is a critical amino acid for many processes in cancer cells(Souba, 1993). While many cancer cells depend on exogenous glutamine for survival to justify the therapeutic targeting of glutamine metabolism, the mechanisms of glutamine dependence and likely response and resistance of such glutamine-targeting strategies among cancers are largely unknown.

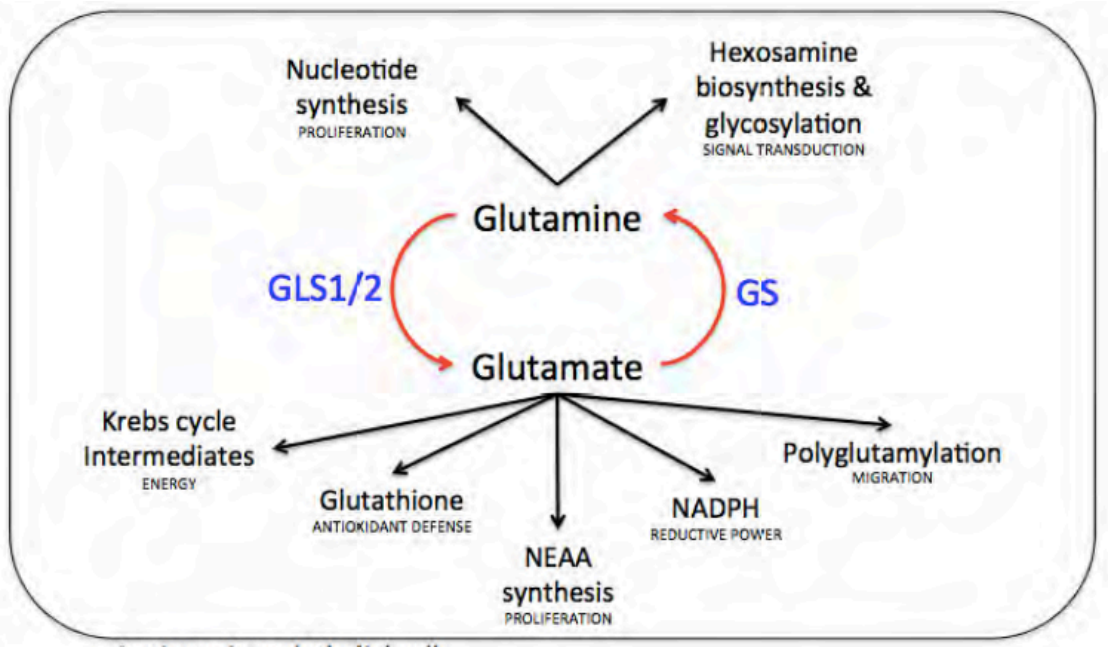

Fig 1.1: Role of glutamine in various metabolic pathways
GLS1/2- Glutaminase (the enzyme that catalyses the conversion of glutamine to glutamate in the glutaminolysis pathway)
GS- Glutamine Synthetase (is an enzyme that catalyses the condensation of glutamate with ammonia to form glutamine and ammonia has been shown to support transformed cells under conditions of glutamine deprivation)

It has long been known that tumour cells metabolise glutamine at significantly greater rates than any other amino acid(Eagle, 1955) but interest in the role of glutamine in

supporting cancer cell proliferation and the potential of glutamine metabolism is relatively recent. Much of this interest has stemmed from the discovery that the proto-oncogene Myc plays a role in the regulation of glutamine metabolism. Myc transformed cells have been shown to be especially sensitive to glutamine withdrawal (Yuneva et al., 2007) and subsequently it has been demonstrated that Myc induces the gene expression of several enzymes involved in glutamine metabolism (Wise et al., 2008, DeBerardinis and Cheng, 2010). The importance of glutamine in supporting cancer cell proliferation and providing carbon for lipid synthesis has been shown to be of greater importance at times of mitochondrial stress with the reductive carboxylation pathway allowing glutamine to bypass the TCA cycle in its conversion to citrate(Wang et al., 2010). Two key enzymes of the glutaminolysis pathway, glutaminase and glutamate dehydrogenase have been shown to be potential therapeutic targets in cancer cell. Glutamine, the most abundant amino acid in the body, plays an important role in cellular proliferation(Hensley et al., 2013). Even though glutamine is a non-essential amino acid, it accounts for more than 20% of the free amino acids pool in the plasma and 40% of the amino acids in the muscle(Bergstrom et al., 1974, Kuhn et al., 1999). It is also designated as a conditionally essential amino acid, as although most cells can synthesize glutamine, however in periods of rapid growth and illness, with increased demand, glutamine becomes essential(DeBerardinis and Cheng, 2010).

It is catabolized to a-ketoglutarate (aKG), an intermediate of the tricarboxylic acid (TCA) cycle, through two deamination reactions in a process termed glutamine Anaplerosis. The first reaction requires glutaminase (GLS) to generate glutamate, and the second occurs by the action of either glutamate dehydrogenase (GLUD) or

transaminases. Incorporation of aKG into the TCA cycle is the major anaplerotic step critical for the production of biomass building blocks including nucleotides, lipids, and amino acids(Ma and Vosseller, 2013, Wang et al., 2010, Zetterberg and Engstrom, 1981). Another important characteristic of glycolytic tumour cells is increased requirement of TCA cycle derived precursors and nicotinamide adenine dinucleotide phosphate (NADPH), for which they often rely on increased glutaminolysis(Jin et al., 2015, Frezza and Gottlieb, 2009).

In stress, inflammation, sepsis and injury, the requirement for glutamine increases, with marked increase in glutamine utilization by the kidneys, immune system and the alimentary tract. In such situations the intracellular pool of glutamine is depleted(Wilmore DW, 1983). Previous studies, have demonstrated that 50% of the dietary glutamine absorbed is retained in the splanchnic circulation (small intestine, liver), the requirement of glutamine by the immune system and the intestine in the post absorptive phase, is met by the skeletal muscle and liver(Hankard et al., 1995).

Glutamine also plays an important role in nucleotide metabolism, acting as a nitrogen donor in the de novo synthesis of purine and pyrimidine nucleotides(McCauley et al., 1998). The origin of cellular nucleic acids is from the following- nucleic acid degradation, diet and synthesis from amino acid precursors (glutamine, aspartate and glycine). In a healthy person, the de novo synthesis of purines and pyrimidines can be met by the amino acids and is capable of supporting the demand for nucleotides. However in periods of stress, the body increases the nucleotide synthesis from reducing the catabolism and increasing salvage of exogenous nucleotides, hence increasing the availability of glutamine for cellular needs(Boza et al., 2000, Grimble, 1993, LeLeiko and Walsh, 1996).

1.3 Glutamate dehydrogenase

GLUD resides within the inner mitochondrial matrix and catalyzes the reversible oxidative deamination of L-glutamate to 2-oxoglutarate using NADP as coenzyme(Hudson and Daniel, 1993). ATP and GTP inhibit it, whereas ADP acts as an activator of this enzyme(Dieter et al., 1981, Li et al., 2011b, Iwatsubo and Pantaloni, 1967, Koberstein and Sund, 1973). Steroid hormones and its analogs such as Diethylstilbestrol (DES) and palmitoyl coenzyme A are also potent inhibitors of this enzyme(Fahien and Kmiotek, 1981, Yielding and Tomkins, 1960). In contrast, ADP and Leucine are allosteric activators of this enzyme(Markau et al., 1972, Yielding and Tomkins, 1961, Prough et al., 1973), although Leucine is also a poor substrate for the enzyme(Smith and Stanley, 2008). mTOR (which is also activated by leucine availability) is also known to be an activator of this enzyme by suppressing SIRT4 expression(Csibi et al., 2013).

GLUD has been implicated in cancer cell proliferation, transformation and autophagy via various oncogenes and tumor suppressors such as mTORC1, SIRT4, K-RAS and p53(Csibi et al., 2014, Jeong et al., 2013, Son et al., 2013, Hu et al., 2010). Several studies have shown a clear relationship between GLUD expression and poorer outcomes(Liu et al., 2015, Pozniak et al., 2016). Two human GLUD genes have been identified, GLUD1 and GLUD2, of these GLUD1 is considered as a cancer therapeutic target, but the role of GLUD2 in cancer is unclear. GLUD in humans is encoded by a single functional GLUD1 gene expressed widely, humans have acquired an X linked GLUD2 gene expressed in brain astrocytes, in epithelial cells lining the convoluted tubules in renal cortex and testicular sertoli cells(Plaitakis et al., 2011). Although GTP inhibits GLUD1, GLUD2 is independent of GTP. Patients with

hyperinsulinism/ hyperammonemia (HI/HA) syndrome harbor GLUD1 mutations that attenuate GTP inhibition(Stanley, 2009). GLUD1 gene is located on the 10th Chromosome, whereas GLUD2 is X linked. It has been postulated that the GLUD1 was thought to derive from retroposition of the GLUD1 gene to the X chromosome where it gave rise to GLUD2 through random mutations and natural selection(Shashidharan et al., 1994). The structure of GLUD1 and 2 is homologous for all but 15 of the 505 amino acid residues. GLUD2 is markedly sensitive to estrogens and neuroleptic drugs(Borompokas et al., 2010).

The atomic structure of GLUD enzyme is in form of two trimers piled on top of each other with each subunit composed of three domains(Banerjee et al., 2003, Peterson and Smith, 1999). On top of the two domains is an antenna, which is exclusively seen in mammalian GLUD enzyme and it plays a vital role in GLUD regulation(Smith et al., 2002). The unique structure of GLUD enables it to undergo conformational changes to allow for binding sites for various allosteric regulators(Smith and Stanley, 2008).

Several GLUD1 inhibitors have been reported in literature (Li et al., 2011b), among these hexachlorophene (HCP), BT, GW5074 and Epigallocatechin gallate (EGCG) have shown significant GLUD1 inhibition, but these (Tsai et al., 2015, Choo et al., 2010) drugs have not shown yet been shown to be active in breast cancer. HCP forms a ring around the internal cavity in GLUD; in contrast GW5074 and BT bind as pairs of stacked compounds at hexameric 2 fold axes between the dimers of subunits(Li et al., 2009).

1.4 Transamination

Transaminases are enzymes that convert glutamate to aKG without producing ammonia. Of these, the two important ones in clinical medicine are glutamate-pyruvate transaminase (GPT or alanine aminotransaminase) and glutamate – oxaloacetate transaminase (GOT or aspartate transaminase)(Sorbi et al., 1999, Wroblewski and Ladue, 1956). The GPT transfers nitrogen from glutamate to pyruvate producing aKG and alanine, and the GOT transfers nitrogen from glutamate to oxaloacetate producing aKG and aspartate. GOT/ GPT both rely on Pyridoxal phosphate (PLP) the active form of vitamin B6, as a cofactor to transfer the amino group from aspartate of glutamate to the corresponding ketoacid (Figure 1.2).

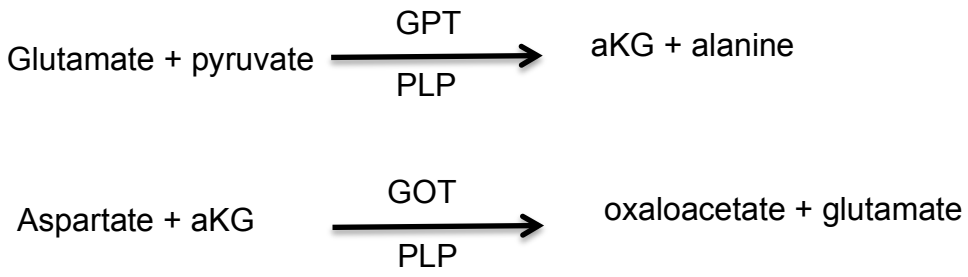

Figure 1.2: Schematic overview of the transaminase reaction, GOT-glutamate/oxaloacetate transaminase, PLP- pyridoxal phosphate

GLUD and transaminases compete for glutamate and the rate of amino acid synthesis depends on the activity of these enzymes(Coloff et al., 2016). Aminooxyacetate (AOA) is a pan-transaminase inhibitor and has shown some anticancer effects in c-myc-overexpressing breast cancer(Korangath et al., 2015, Sherry et al., 1998). AOA has also shown to have significant anti-tumour effects in pre-clinical studies as a single agent(Thornburg et al., 2008, Qing et al., 2012, Anso et al., 2013). In clinical trials in patients with tinnitus and Huntington's disease, the dosage of AOA used was 1-2mg/kg/day with manageable toxicity(Reed et al., 1985, Guth et al., 1990, Perry et al., 1980).

In pancreatic adenocarcinoma, mutant KRAS encourages utilization of glutamine through transamination, instead of the pathway involving the GLUD enzyme(Son et al., 2013). Genes representing the transamination pathway are highly expressed in pancreatic carcinoma as compared to other cancers and targeting this pathway has shown to have anti-tumour effects(Chakrabarti et al., 2015).

1.5 Reactive Oxygen Species (ROS)

ROS are byproducts of mitochondrial respiration and (Schumacker, 2015, Harris et al., 2015, Cairns et al., 2011) function differently at various concentrations. ROS are chemical species with one unpaired electron derived from molecular oxygen. Molecular oxygen contains two unpaired electrons in the outer shell. These electrons have the same spin; hence oxygen can react with one electron at a time. If any of these unpaired electrons gets excited, the oxygen molecule changes its basal state. This species formed is a singlet oxygen and works as a powerful oxidant reacting with other pairs of electrons(Turrens, 2003).

At low levels ROS act as signaling molecules, slightly higher levels they can damage DNA and at higher levels they can cause cell death(Wiseman and Halliwell, 1996, Sena and Chandel, 2012). Alteration of antioxidant capacity of malignant cells can cause drug resistance(Trachootham et al., 2009), targeting this redox modulation can be a therapeutic interventional strategy. Since the mitochondrion is the main source for ROS production, any damage to it will alter the electron transport chain, the ATP synthesis, as well as physical changes in proteins, enzymes and lipids as well as modify transductional pathways or DNA damage(Droge, 2002, Chatgilialoglu and O'Neill, 2001).

1.6 Glutathione

Glutathione (GSH) is a tripeptide thiol compound that is involved in protecting cells against free radical intermediaries and free radicals(Meister, 1983). GSH is a water-soluble tripeptide composed of glutamine, cysteine and glycine (Fig. 1.3). GSH synthesis entails the successive actions of two enzymes, ϒ-Glutamine cysteine synthetase and GSH synthetase. The bioavailability of cysteine is crucial rate limiting step for the synthesis of GSH. Glutathione is synthesized mainly in the cytoplasm, and then transported to the nucleus, endoplasmic reticulum, mitochondria and peroxisomes. More than 70% of the GSH remains in the cytoplasm and the mitochondria and nucleus store 30% and 10% of the total intracellular GSH content respectively(Lluis et al., 2005).

The thiol group is a very strong reducing agent, and is responsible for detoxification of various electrophilic compounds. The key mechanism of redox control of cell metabolism is the availability of the thiol groups to change reversibly their redox state with consequent changes in conformational catalytic and regulatory functions of a protein. The maintenance of the ratio of reduced GSH to oxidized glutathione (GSSG) is the chief mechanism by which the thiol groups control the redox balance of the cell(Janssen-Heininger et al., 2013, Nagy, 2013).

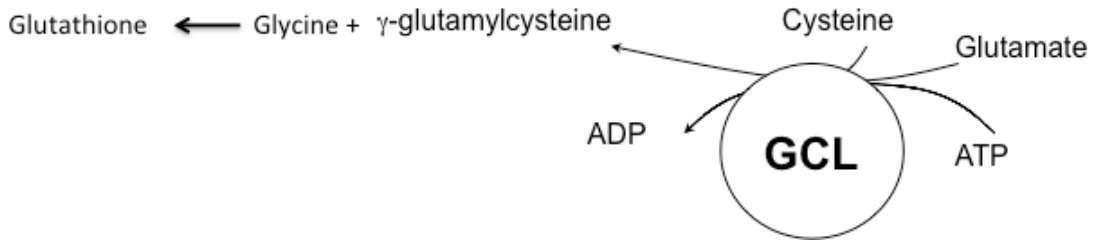

Figure 1.3: Synthesis of Glutathione from glutamate, cysteine and glycine. GCL-glutamate cysteine ligase.

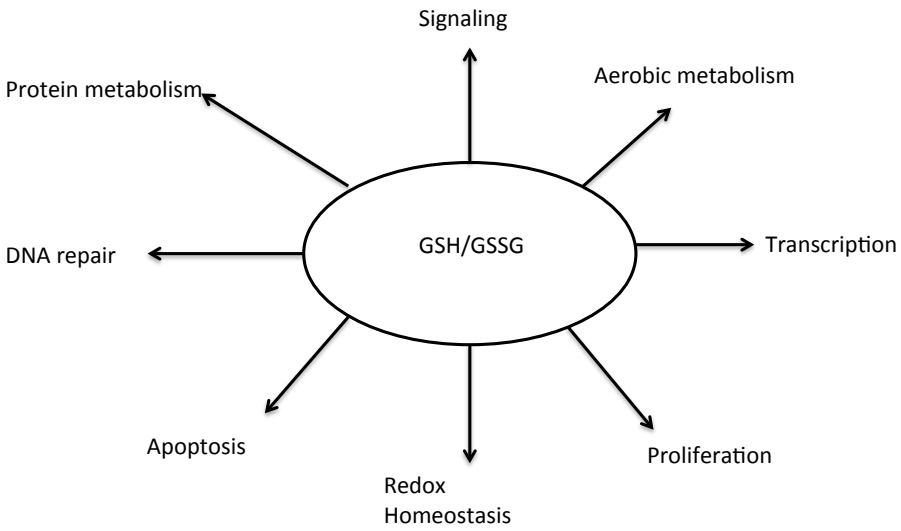

Figure 1.4: Role of glutathione in maintenance of the vital functions of cell organelles. GSH- reduced glutathione, GGSG- oxidized glutathione.

As GSH plays a dominant role in the oxidative defense mechanism of the cell, a reduction in the GSH levels can result in increased in the levels of ROS leading to oxidative stress(Meister, 1994, Townsend et al., 2003).

Altering glutathione synthesis is useful in chemotherapy, radiation and in protecting cells against effects of drugs, toxins and other chemicals(Townsend et al., 2003, Hawk et al., 2016).

1.7: Metformin effects in cancer metabolism

Metformin or 1,1-dimethylbiguanide hydrochloride is the most widely used drug for type 2 diabetes(Saeki et al., 2015). The United Kingdom Prospective Diabetes study (UKPDS) reported a lower all case mortality in patients taking metformin for type 2 diabetes compared to other therapies and also insulin(1998). The interest in the anti-tumour effects of metformin has been due to a series of epidemiological studies suggesting a protective effect of this drug against cancer (Noto et al., 2012, Franciosi et al., 2013, Evans et al., 2005, Libby et al., 2009, Landman et al., 2010, Decensi et al., 2010). The key study showing an important role of metformin in breast cancer was the Women's Health Initiative Trial, which involved 68,019 postmenopausal women in USA, including 3273 diabetics. This study showed that the incidence of invasive breast cancer was lower in diabetics taking metformin (HR, 0.75; 95% CI, 0.93-1.45)(Chlebowski et al., 2012).

Metformin targets mitochondrial oxidative phosphorylation affecting cellular synthesis of ATP, which in turn activates AMP-activated protein kinase (AMPK). Activated AMPK alters the cellular metabolism, in turn impairing proliferation of cancer cells and growth signaling through mammalian target of rapamycin (mTOR)(Mihaylova and Shaw, 2011, Hardie, 2013, Foretz et al., 2010, Miller et al., 2013).

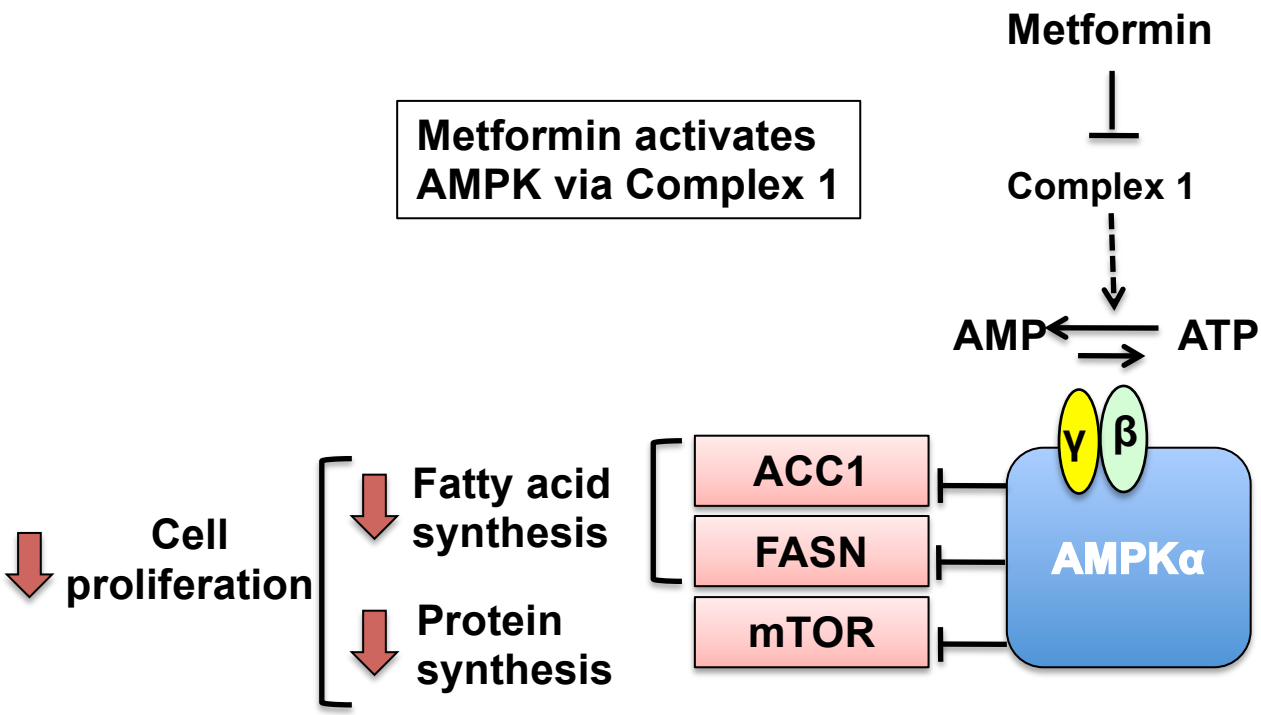

Figure 1.5:Metformin generates an energy stress by inhibition of complex 1 and subsequent activation of AMPK alters cellular metabolism from anabolic to catabolic through multiple transcriptional regulatory elements leading to inhibition of cell proliferation. ACC1- acetyl CoA carboxylase 1, FASN-fatty acid synthase, mTOR- mammalian target of rapamycin, AMP-activated protein kinase (AMPK).

1.8: Role of bithionol (BT) / GLUD targeting in cancer

BT (2,2'-thiobis (4,6-dichlorophenol)/ Bis (2-hydroxy-3,5-dichlorophenyl) sulphide, is a clinically approved anti-parasitic drug and previously has been shown to inhibit solid tumour growth in several preclinical cancer models(Saunders et al., 2008, Braddock, 2010, Bacq et al., 1991). It has a molecular weight of 356.04, and a molecular formula of $C_{12}H_6Cl_4O_2S$ (Figure 1.6).

Recently, there has been evidence of its activity in ovarian cancer by autotaxin inhibition(Ayyagari and Brard, 2014). Glutamate dehydrogenase (GLUD) is found in all living organisms and catalyzes the reversible oxidative deamination of L - glutamate to 2-oxoglutarate using NAD(P) as coenzyme.

In eukaryotic organisms, GLUD1 resides within the inner mitochondrial matrix where it catabolizes glutamate to feed 2-oxoglutarate to the Krebs cycle (Hudson and Daniel, 1993). BT is an inhibitor of GLUD1 and has shown activity in cancer through this mechanism(Li et al., 2007). X-ray crystallography has shown that the enzyme exists as a homo-hexamer and is composed of 2 trimers stacked together, base to base(Smith et al., 2001). GLUD1 activity is positively regulated by ADP and leucine; and by GTP and palmitoyl-coenzyme A negatively(Stanley, 2009).

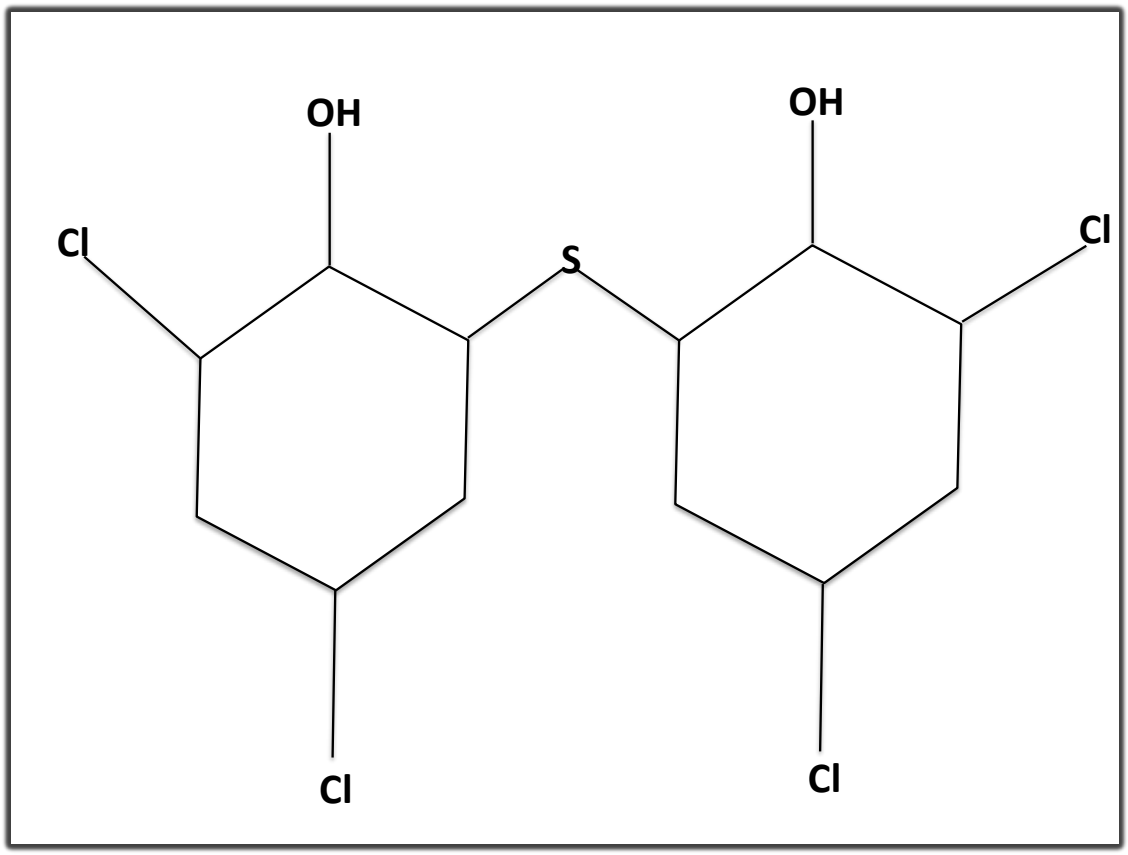

Figure 1.6: The two dimensional structure of Bithionol (2,2'-thiobis (4,6-dichlorophenol)

In 1962, Allen et al first reported that BT (2,2'-thiobis (4,6-dichlorophenol) was effective in treating tapeworm infestation in sheep(Allen et al., 1962). Since then numerous other drugs have been used in tapeworm infestations, hence this drug is not used in humans anymore(Martin, 1997, Bacq et al., 1991). BT is well tolerated in humans; with nausea, vomiting, dizziness and skin reactions being the most common reported size effects(Yokogawa et al., 1962, Kim, 1970). Even in individuals given multiple doses of BT, the reported toxicity was low. In recent publications, the anticancer potential of BT has been reported in various cancers, but the role of GLUD1 has not been exploited in any of them(Braddock, 2010, Saunders et al., 2008, Miller et al., 2010, Ayyagari and Brard, 2014). For instance, Ayyagari et al showed

that BT exerted cytotoxic effects by autotaxin inhibition (Ayyagari and Brard, 2014), ROS generation, and NF-kB inhibition.

After oral administration, BT is excreted partly as glucuronide and partly as sulphonic acid(Meshi et al., 1970, m, 1976).

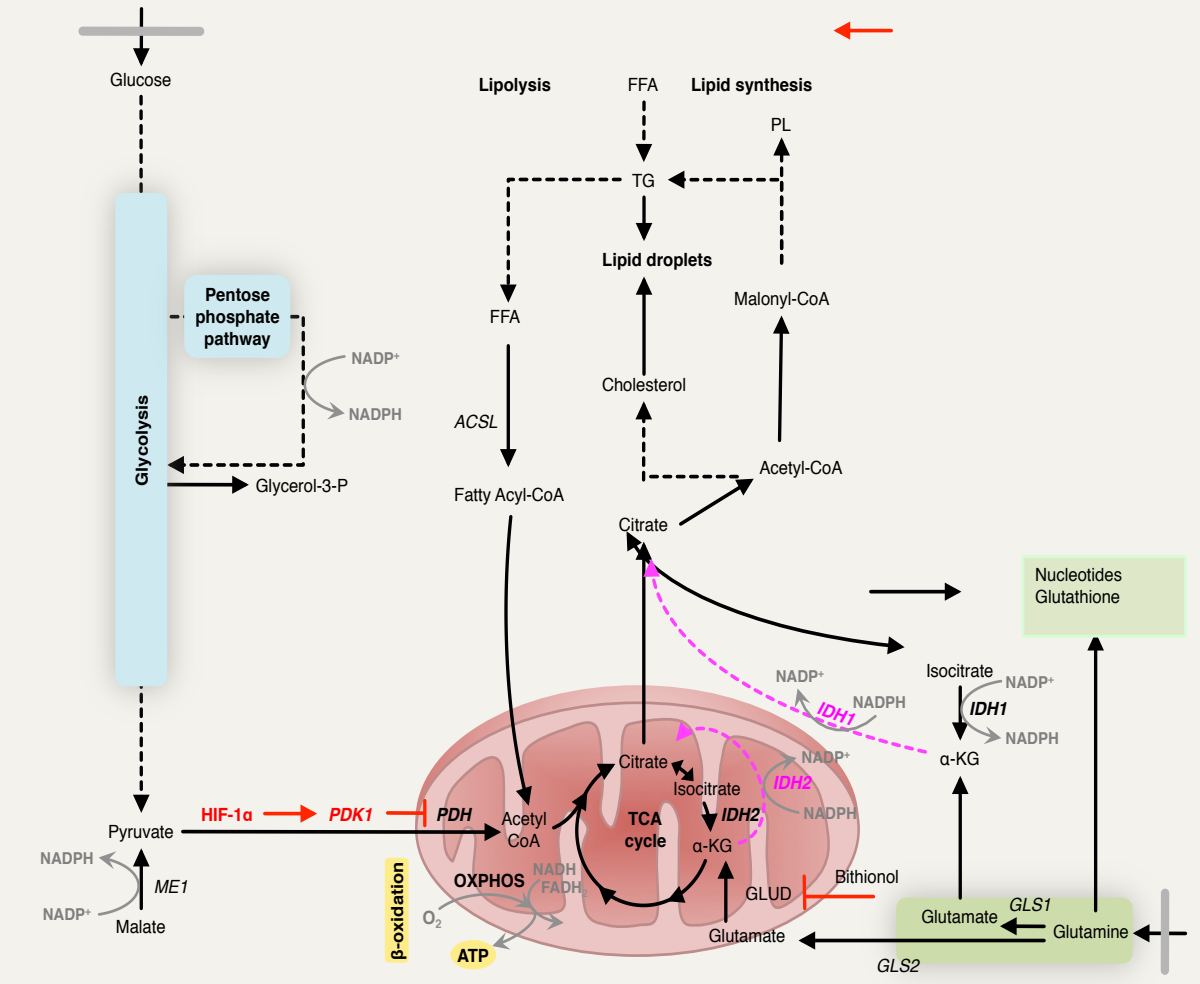

Figure 1.7: Overview of how glucose and glutamine carbons feed into the TCA cycle and subsequently lipid and cholesterol synthesis. A mitochondrial insult will disrupt the TCA cycle and consequently aerobic glycolysis becomes more essential for the generation of ATP. Glutamine's role as a substrate for lipid biosynthesis increases as it can be shunted via the reductive carboxylation

pathway away from the TCA cycle and to citrate. FFA- free fatty acid, TG- triglyceride, GLS- glutaminase, GLUD- glutamate dehydrogenase, IDH- Isocitrate dehydrogenase, PDK- pyruvate dehydrogenase kinase, HIF-1- hypoxia inducible factor 1.

1.9: Drugs affecting glutamine metabolism

1.9:1: Hexachlorophene (HCP)

The halogenated antibacterial compound HCP has been shown to be an uncoupler of oxidative phosphorylation(Kimbrough and Gaines, 1971), and is also known to be an inhibitor of lactate, formate, glucose and butanol dehydrogenases(Gould et al., 1953). It has also been shown that HCP inhibits glutamate dehydrogenase, alcohol dehydrogenase, Isocitrate dehydrogenase, glucose-6-phosphate dehydrogenase, lactate dehydrogenase and malate dehydrogenase(Wang and Buhler, 1978). HCP is hydrophobic and is chemically inert in solution. Six molecules of HCP form a ring and bind to the inner core of the GLUD hexamer(Li et al., 2011a).

HCP has previously shown to be an effective anti-helminthic drug, with activity against giardiasis and trichomoniasis(Takeuchi et al., 1985). Although HCP is known to be an uncoupler of oxidative phosphorylation, giardia and trichomonas parasites lack mitochondria and heme proteins; hence it is likely that there is a different mechanism of action. It is postulated, that it works by inhibiting aerobic metabolism in these worms. Recently metronidazole has found to be a better drug against these protozoa and has a better tolerability profile. HCP is also used as antimicrobial solution and is used as a compound in soaps and other cosmetic solutions(Silvernale et al., 1971, Jungermann, 1968). The use of HCP in humans is restricted due to the associated neurotoxicity(Nakaue et al., 1973). In bacteria, HCP inhibits both

endogenous and exogenous respiration and acts on various components of the electron transport chain. Exogenous menadione reverses the inhibition of the electron transport chain(Frederick et al., 1974). HCP by its mechanism of uncoupling of oxidative phosphorylation stimulates oxygen uptake and increases cytochrome reduction.

1.9.2:GW5074

GW5074 (5-Iodo-3-[(3,5-dibromo-4-hydroxyphenyl) methylene]-2-indolinone) is a GLUD enzyme inhibitor and also has been reported to be a c-Raf inhibitor(Jensen et al., 2015, Li et al., 2009). It has a brominated phenol group, which interacts with the GLUD aromatic ring, and hence inhibiting the enzyme by wedging into the junction points and keeping the stacked dimers from freely moving. Its use in humans is limited due to its neurotoxicity(Balderamos et al., 2008).

1.9.3: CB-839

CB-839 is a glutaminase inhibitor and has shown to have anti-proliferative effects on triple negative breast cancer cell lines(Gross et al., 2014). Its effects on HCC 1806 cell lines resulted in marked decrease in glutamine production, consumption, oxygen consumption, and levels of glutathione and tricarboxylic acid cycle intermediaries. This drug is currently in early phase trials in renal, breast, lung and myeloma(Thompson et al., 2017, Matre et al., 2016, Fung and Chan, 2017). It has been shown that high glutaminase expression is associated with poor prognosis(Yu et al., 2015, Huang et al., 2014).

1.9.4: Epigallocatechin-3-gallate (EGCG)

EGCG is a polyphenol is known to modulate inflammatory pathways through inhibition of Nf-kB activation(Liu et al., 2016, Ning et al., 2015). This polyphenol is is derived from green tea and is known to inhibit GLUD in vitro and is associated with blocking GDH mediated insulin secretion in wild type rat islets(Li et al., 2011a). Recent studies have shown that EGCG has activity in treating glioblastomas cells(Yang et al., 2009). This drug has found to be non-toxic and is being studied in treating various tumours. EGCG has also been useful in treating tuberous sclerosis.

1.10: Nucleotides and dNTPs

Nucleotides are the building blocks of DNA and RNA; these are composed of a nitrogenous base, a five-carbon sugar (ribose or deoxyribose) and a phosphate group. Nucleotides function in the energy metabolism via ATP, GTP, CTP and UTP (nucleoside triphosphates). In addition they are involved in cell signaling (cAMP, cGMP). Glutamine is a nitrogen donor in the synthesis of purine and pyrimidine nucleobases(Cory and Cory, 2006). Previously, it has been shown by attenuating glutamine synthesis in acute lymphoblastic leukemia (ALL), there is increased cytotoxicity and cell cycle arrest by blocking the nucleotide metabolism(Grigoryan et al., 2004).

Deoxyribonucleoside triphosphates (dNTPs), the building blocks of DNA are essential in maintain genomic integrity. Shift in the dNTP pool has been linked to many diseases, e.g. mitochondrial disorders, cancer and susceptibility to viral infections(Aye et al., 2015, Rampazzo et al., 2010). The dNTP pool peaks around the S phase, to assist nuclear DNA replication and failure of the cells to maintain

adequate dNTP levels can be damaging to the cell, leading to DNA breaks, mutagenesis and cell death(Mathews, 2006, Reichard, 1988).

1.11: Hypothesis

Besides the fact that glutamine metabolism has a multitude of effects on downstream pathways that are known to influence the growth and survival of cancer cells, there is now, in vitro, in vivo and growing clinical evidence for the anticancer effects with the use of various glutamine inhibitors.

I hypothesized that pharmacological inhibition of GLUD1 enzyme, with a small molecule GLUD1 inhibitor bithionol (BT); could elicit cancer cell death. My work focused on defining effects of BT via GLUD1 inhibition, on breast cancer metabolism using in vitro models to gain greater insight into its anticancer mechanism of action. This thesis also focused on developing an understanding of pathways that might be targeted to synergise with BT's anticancer effect. In future this thesis will enable me to set up a 'window of opportunity' clinical trial to study BT's effects on breast cancer metabolism to develop potential biomarkers and further investigate its in vivo effects.

Chapter 2: Material and Methods

2.1:Cell culture

MCF7, BT474, SKBR3, MDA-MB-231, HCC1806 and MDA-MB-468 cell lines were obtained from the American Type Culture Collection (LGC standards UK). All cell lines were cultured in Dulbecco's Modified Eagle Medium (DMEM) (Invitrogen) supplemented with 10% fetal bovine serum (FBS) at 37° C and 5% CO_2, in sterile flasks (Corning) in a humidified incubator. Cells were sub-cultured at about 80% confluency by treating with trypsin- EDTA (Invitrogen) to detach after a PBS wash. The cells were then spun in a centrifuge at 1000 rcf for 5 minutes prior to reseeding at 1 in 10. The Plasticware used in all experiments were procured from Corning.

2.2: Hypoxic exposure

INVIVO2 400 hypoxic chamber (Pro-Lab diagnostics) was used to create hypoxic conditions at 0.1% Oxygen (5%CO2)/37^{0}C. Media changes were performed under hypoxic conditions in the hypoxic chamber. Cells were allowed to adhere for at least 4 hours after reseeding, prior to hypoxic exposure.

2.3: Chemicals

For all laboratory studies bithionol, 2-deoxy-glucose and amino-oxyacetate was obtained from Sigma Aldrich. Bithionol was dissolved in DMSO. Metformin (Sigma) was dissolved in milli-Q water and applied at concentrations of 0.5 to 4 mm/L.

2.4: Antibodies

Mouse anti- LAMP and Rabbit anti- cleaved PARP antibody were obtained from Cell Signaling. Rabbit anti-LC3B antibody, Rabbit anti-GLUD, rabbit anti-Nf kB p65 and Mouse anti-VDAC1 antibody were obtained from abcam. All HRP- conjugated antibodies were obtained from DAKO and used at a concentration of 1:1000. For Western blot loading control, HRP conjugated monoclonal Anti-β actin (1:10,000) from Sigma was used.

2.5: Cell Counting

A 20µl aliquot of each sample was taken and then a cell count obtained using the Cellometer Auto T4 Cell Counter (Nexecelom bioscience), according to manufacturers instructions, between the particle size ranging from 9-22µm.

2.6: Cell Number Assays

100,000 cells per well were plated on to 6 well plates and the following day the media replaced with DMEM media containing drug concentrations as specified in the text. The media was supplemented with 5mM or 25mM glucose with or without 4mM glutamine. Cell number was counted daily to 96 hours. To maintain a more consistent glucose, glutamine and lactate concentration the media was replaced on a 24 hourly basis for all assays.

2.7: Oxygen Consumption and extracellular acidification experiments

Dependent upon the cell lines 17,500-20,000 cells were seeded per well on a 96 well plate and left to recover for 24 hours prior to media change with BT added at varying concentrations as specified in the text. After overnight drug treatment, the cells were assayed using the XF96 extracellular flux analyser (Seahorse Bioscience). This analyser uses solid-state probes only 200 µm above the cell monolayer to measure oxygen consumption and proton extrusion in real time. Compounds can be then pneumatically injected into the assay plate wells to assess specific mitochondrial and

glycolysis parameters (Oligomycin, Mesoxalonitrile 4-trifluoromethoxyphenylhydrazone (FCCP), Actinomycin A, rotenone, and 2-DG). Note this assay was carried out with help from Dr Simon Wigfield.

2.8: Electron Microscopy techniques

Cells were harvested by trypsin digestion and fixed in 2.5% glutaraldehyde in phosphate buffer. After spinning down, pellets were washed, post-fixed in 1% osmium tetroxide, pre-embedding stained with 2% uranyl acetate, dehydrated and embedded in Spurr's resin (all from Agar Scientific, UK). Ultrathin sections were cut onto nickel grids, contrast enhanced with 2% uranyl acetate and lead citrate and viewed using a Joel 1010 electron microscope. Please note that after initial sample preparation, images were taken by Prof David Ferguson.

2.9: Protein extraction and analysis

At the end of treatment, cells were washed once with cold PBS and scraped in lysis buffer (20mM Tris-HCl (pH 7.5), 150mM NaCl, 100nM NaF, 100mM Na2P2O7, 10nM EDTA, supplemented with1% (v/v) Triton X-100, 10% (v/v) Complete Mini Protease Inhibitor Cocktail solution [Roche], 1% (v/v) Phosphatase inhibitor cocktail 2 and 3 [Sigma]). Samples were centrifuged at 4°C, at 13500 rpm for 10min before supernatants were transferred into new tubes and protein content measured using a Bradford assay. Samples were normalized and mixed with a 4x loading buffer (Invitrogen, with 10% β-mercaptoethanol [Sigma]. Samples were loaded on Bis-Tris Gels (4-12%, Invitrogen) and run using a MOPS SDS running buffer (Invitrogen) for 2h at 120V.

Gels were then transferred using semi-dry transfer for 2h at 12V. Membranes were blocked in 5% BSA in TBS-Tween (0.2%) for 1h at room temperature or overnight at 4°C. Primary antibodies (see table 2) were applied in the same solution either for 3h at room temperature or overnight at 4°C. This was followed by a wash and the addition of the appropriate secondary antibody (see table 2) for 1h at room temperature. After a second wash step, ECL detection reagents (GE Healthcare) were added onto the membranes.

2.10: In vitro proliferation assays

2.10.1: CyQUANT™ cell proliferation assay

Cells were seeded in a 96 well plate with 1000-2000 cells varying according to the cell lines. They were then left to recover overnight prior to change of media next morning. BT was added in varying concentration and at varying time periods as mentioned in the text (5 replicates per condition per plate). Cyquant NF cell proliferation assay was performed according to the manufacturers instructions. The Cyquant master mix was prepared with 22µl of Cyquant NF dye, 8.8ml of deionized water, and 2.2 ml of 5x Hank's balanced salt solution (HBSS). Prior to the assay, the media was removed and 50µl of the mastermix was added in each well, before incubating in the dark for 30 minutes at 37^0C. Fluorescence intensity was measured using a fluorescent micro plate reader at excitation of 485nm and emission detection at 530nm.

2.10.2: Clonogenic assay

Cells were trypsinised and reseeded at a density of 500 cells per 6cm dish. Cells were grown in normoxia for 24 hours and then exposed to BT for 24 hours. The media was changed after 24 hours of exposure to BT and then cells were grown in DMEM with 5mM glucose for 12 days. At the end of the experiment, the media was aspirated and cells were washed with PBS. The PBS was replaced with 3ml of fixation solution (Acetic acid/methanol 1:7 vol/vol) and the cells were kept at room temperature for 5 min. After 5 minutes, the fixation solution was removed and the cells were treated with 0.5% crystal violet solution and cells were incubated at room temperature for 2 hours. The crystal violet solution was aspirated carefully and the plates were washed with water after immersing the plates in a sink filled with tap water. The plates were air-dried and the colonies were counted manually.

2.10.3: 3 D spheroid formation

Cells were removed from flask by trypsinising, and centrifuged in a 50ml falcon tube. Simultaneously matrigel (BD Biosciences) was kept on ice. Cells were counted and a cell matrigel mixture was prepared (there is 5 µl of matrigel per 100microlitres of media (i.e. 1 in 20)). 5000 cells per well were calculated in 100µl of media. Pipette 100 microliters of cell + media + matrigel per well so there are 5000 cells/well. The cells are plated in a 96 well non-adherent plate and then centrifuged at 10G for 10 minutes in 4^0C. BT was added in varying concentration as specified in the text after 24 hours. Spheroids are photographed at baseline and every 48hours for growth curve using a EVOS XL microscope and AxioCam digital camera. The spheroid volume was calculated using the ImageJ software. The images were processed as JPEG

format and a threshold was set to remove any non-spheroid contributions. The spheroid radius was calculated by the number of pixels in the spheroid area and converted to mm^2. 20 spheroids per condition were taken to calculate averages, and the experiment was repeated 3 times. The spheroid growth curve was
Drawn with SEM of 3 independent average readings per spheroid condition. At the end of the experiment the spheroids were collected in ethanol and kept in 4^0C.

2.10.4: Spheroid Immunohistochemistry

15 ml Falcon tubes were used for each spheroid condition. The spheroids are aspirated from each well of 96 well plate by using a 1ml Pipette (cutting the tip of the pipette), e.g. all spheroids in the drug treated well are collected into one falcon tube etc. The spheroids are initially kept overnight in 1ml of 4% formaldehyde/ 10% formalin, and then formaldehyde is removed the next day and replaced with 5ml of 70% ethanol and kept in the cold room.
The spheroids in the ethanol mixture are removed and the ethanol is aspirated to dryness. 150µl of Agarose gel is added to the spheroids to solidify it (Prepare 2% Agarose gel in PBS); Agarose gel has to be kept warm in the water bath. The Agarose gel is then left to solidify on ice. The gel is then put in a cassette, and embedded in hot paraffin. The paraffin is cooled to -2^0C and then processed for IHC.

2.11: Cell cycle and apoptosis

Propidium iodide is a fluorescent dye, which binds to the nucleic acids i.e. DNA stoichometrically, implying that there is a direct correlation between the quantity of the DNA binding dye and the amount of DNA present in the cell. As a result, we are able to estimate the fraction of cells in each phase of the cell cycle.

3-5 x 10^5 cells are washed in cold iced PBS and then re-suspended in 1 ml of PBS and fixed in 3ml of 100% ethanol for 20 minutes at 4^0 C. Following this, the cells are washed in ice cold PBS twice and then re-suspended in 500µl of PI containing DNAase free RNAase. The suspension in then incubate at Room temperature for 15 minutes and then analysed by FACS analyzer cyan ADP (Dako). At first the single cell population was gated using pulse width versus pulse area and then this gate was applied to the PI histogram plot. The percentage of cells in each cycle, are then plotted after quantification is done using markers set within the analysis program.

2.11.1: Annexin V Flow Cytometry

To measure viability, cells were stained with Annexin V and Propidium iodide (PI) (Molecular Probes). Annexin V binds to the phospholipid phosphatidylserine, which is located in the cytoplasmic surface of the plasma membrane in viable cells or necrotic cells, whereas it translocates to the outer leaflet of the plasma membrane in apoptotic cells. To discriminate between dead and apoptotic cells, the membrane impermeable PI was added simultaneously (van Engeland et al., 1998). Cells were harvested with trypsin after the incubation period and washed in cold PBS. Cells were then resuspended in 100µl of Annexin-binding buffer (10mM Hepes, 140mM NaCl, and 2.5mM $CaCl_2$, pH 7.4), 5µl of Annexin Fluor 647 conjugate and 5µl of PI, and incubated at RT for 15 minutes. Subsequently, 400µl of annexin-binding buffer were added, and samples were kept on ice until analysis. Analysis was performed in a FACS

analyzer cyan ADP (Dako). Note this assay was carried out with help from Dr Esther Bridges.

2.11.2: Cell cycle analysis using Propidium iodide DNA staining

Propidium iodide (PI) is a DNA binding enzyme stoichometrically, implying that the DNA content correlates with the quantity of DNA bound dye. Cell cycle distribution can be measured with PI using flow cytometry. To evaluate cell cycle distribution, 5 x 10^5 cells were washed with ice-cold PBS, resuspended in 1ml of PBS and fixed by the drop wise addition of 3 ml of 70% ethanol for 30 minutes at 4^0C. Cells are then treated with DNase-free ribonuclease (add 50 µl of a 100 µg/ml sock of RNase), this will ensure only DNA and not RNA, is stained. Cells are then resuspended in 200 µl PI (from 50 µg/ml stock solution). After 15 minutes of incubation at RT, cells are analysed in a FACS analyser Cyan ADP.

2.12: Reactive Oxygen Species (ROS) assay

Mitochondrial ROS was assayed using the MitoSOX™ Red (Molecular Probes). MitoSOX Red is a fluorogenic dye for highly selective detection of superoxide in the mitochondria of living cells. MitoSOX™ Red reagent is a live cell permeant and rapidly and selectively targeted to the mitochondria. Once it enters the mitochondria, it is oxidized by superoxide and exhibits fluorescence. MitoSOX™ Red is readily oxidized by superoxide and not by other ROS- or reactive nitrogen species (RNS). The oxidation products become highly fluorescent upon binding to nucleic acids. Cells were washed with PBS and subsequently loaded with 5µM

MitoSOX™ Red and incubated for 45 minutes. The reagent was reconstituted by dissolving (50 μg) of one vial of MitoSOX™ mitochondrial superoxide indicator (Component A) in 13μL of dimethylsulfoxide (DMSO) to make a 5 mM MitoSOX™ reagent stock solution.

The cells were then washed twice with cold PBS, scraped in 500μl cold PBS and kept on ice in FACS tubes and immediately analysed in a in a FACS analyser Cyan ADP (using the PE channel). Cells were also cultivated in presence of 25μM of the anti-oxidant MnTMPyP (5,10,15,20-Tetrakis (1-methylpyridinium-4-yl)-21*H*, 23H-porphyrin manganese (III) pentachloride), a cell permeable superoxide dismutase (SOD) mimetic. The experiment was conducted four times and we also used hydrogen peroxide (H_20_2) as control.

2.13: Quantitative Mass Spectrometry assay

2.13.1: Cell harvesting

Cells were grown to 90% confluent in a T175 flask and were treated with BT for 24 hours. The experiment was done in triplicate. The cells were subsequently washed thrice in PBS and scraped and collected in a falcon tube. They were then centrifuged at 0.5 rcf, to avoid lysing cells. The cells are then counted and the PBS is pipetted from the tubes. The cells are then collected in 1.5ml tubes and frozen in -80^0 C until ready for metabolite extraction.

2.13.2: Metabolite extraction

A solution of 80% methanol/ H20 using milli-Q water and HPLC grade Methanol to add 200µl per sample. The solution is cooled in 4^0 C. 80µl of the 80:20 Methanol: Milli-Q solution is added to the cell pellet and the sample is then transferred to a 500µl eppendorf tube. The cells are then spun down in a centrifuge at maximum setting of 13000 rpm for 20 minutes. The supernatant is aspirated and kept in 4^0 C. Another 80µl of the 80:20 Methanol: Milli-Q solution is added to the cell pellet and the cells are then again spun down in a centrifuge at maximum setting of 13000 rpm for 20 minutes. The supernatant is aspirated and collected in the previous vial. The solution is evaporated to dryness for 2 hours in a vacuum evaporator. When the samples are to be processed, they are reconstituted in 100 µl of Milli-Q water and the samples are submitted for LC/MS analysis.

Aqueous metabolites were analyzed using an Agilent 6970 gas chromatograph and an Agilent 5973 mass selective detector. To determine relative metabolite abundance across samples, the area of the total ion current peak for the relevant metabolite was compared to that of an internal standard (2-oxobutyrate) and normalized for protein content. Note this assay was carried out with help from Dr James McCullagh and Dr Alessandro Valli.

2.14: GLUD1 enzyme assay

Enzyme activity of GLUD1 was measured by a colorimetric assay using the Biovision GLUD assay kit, This analyses the enzyme activity of GLUD1, based on the principle that glutamate will be consumed by the GLUD1 as a substrate, and generate NADH stoichometrically, resulting in a proportional colour development. This assay detects GLUD1 activity as low as 0.01mU in serum or tissue and cell extracts.

In brief, cells grown in 6-well plates were collected after 6, 24, or 48 hours of BT treatment and washed with cold PBS, lysed, and supernatant used for analysis. The assay kit consists of GLUD assay buffer, glutamate, GLUD developer, GLUD positive control and NADH. A 96 well plate is used to conduct the experiment.

1) NADH standard curve- Dilute 10 µl of the 10mM NADH stock solution with 90 µl of GDH assay buffer to generate a 1mM NADH standard. Add 0,2,4,6,8,10 nmol/ well standard. Adjust the final volume to 50 µl with the assay buffer.

2) Sample preparation- 1 x 10^6 cells were homogenized in 200 µl ice-cold assay buffer and then centrifuged (13,000 x g for 10 minutes), in order to remove the insoluble material. Test sample was added in the 96 well plate, bringing the final volume to 50 µl/ well with the assay buffer. For the positive control, 2 µl of the positive control solution was added to the well and adjusted the final volume to 50 µl with the assay buffer.

3) Reaction mix- For each well a Reaction mix was prepared (100 µl) containing- 82 µl assay buffer, 8 µl GLUD developer, and 10 µl Glutamate 2M. 100 µl of the reaction mix is added to each well containing the test samples, positive controls and standards. The samples and positive controls were incubated for 3 minutes at 37 C, and then the Optical density (OD) was measured at 450 nm in a microplate reader. Then the samples were incubated for a further 30 minutes and the OD was measured at 450 nm. The OD was measured every 3-5 minutes.

4) The glutamate standard curve was plotted using the formula- GLUD activity = B/T x V x Sample dilution factor.

(B- NADH amount from the standard curve, T- time incubated, V- sample volume added in the reaction well).

2.15: RT-PCR

2.15.1: RNA extraction

The reagents used for PCR were processed with DEPC (diethyl pyrocarbonate) treated water. 1 ml of TRI reagent (Sigma Aldrich) (RNA isolation reagent) was added directly to a 10cm dish, and the suspension containing the cells was transferred to an eppendorf tube. 200 µl of Chloroform was added to the eppendorf ad this was vigorously shaken for 15 seconds, before leaving at Room temperature for 10 minutes. These were then centrifuged at 14000 rpm for 15minutes at 4^0 C. This centrifugation separates the mixture into three phases, however only the supernatant colorless aqueous phase (which contains the RNA) is aspirated. The aqueous phase is transferred to another eppendorf tube, which contains 500 µl of isopropanol. This was then mixed and incubated at rom temperature for 15 minutes, then again centrifuged at 14000 rpm for 15minutes at 4^0 C. The supernatant was discarded and the samples were treated with 75% ethanol solution (1 mL, containing DEPC treated water) and were centrifuged to 7500 rpm for 5minutes at 4^0 C. The supernatant was then aspirated and the RNA pellets were allowed to air dry for 10 minutes at room temperature. The RNA pellets were then re-suspended in 60 µl of DEPC treated water and heated at 60^0 C for 10 minutes before vortexing. A nanodrop ND 1000 spectrophotometer was used to estimate the RNA concentration and quality. Note this assay was carried out with help from Dr Esther Bridges.

2.15.2: cDNA synthesis

High capacity cDNA synthesis kit (Applied biosystems) was used for cDNA synthesis. Using the reaction components and cycling conditions illustrated below, RNA (1 µg per sample) was prepared. In 200 µl of DEPC treated water, 20 µl of

cDNA samples was diluted before use in quantitative real time polymerase chain reactions.

Reagent	**Volume/reaction (µl)**
Random Primers (10x)	2
dNTP mix (100mM)(25x)	0.8
RT buffer (10x)	2
DEPC treated water	4.2
RNA	1
Multiscribe (50U/ µl)	1

Table 2.1: Quantity of reagents used for cDNA synthesis

Cycling conditions	
Temperature	**Time**
25^0 C	10 minutes
37^0 C	120 minutes
85^0 C	5 seconds
4^0 C	Hold

Table 2.2: Cycling conditions used for cDNA synthesis

2.15.3: Quantitative Real-time PCR (qRT-PCR)

Quantification of the mRNA expression was done by real-time reverse transcription PCR using the Taqman PCR master mix kit and 7900HT fast real time PCR system (Applied Biosystems). The mastermix was prepared with 2 µl cDNA and 1x Taqman primer with a final volume of 10 µl with DEPC treated water. The settings for the

PCR reactions were- 2 minutes at 50^{o} C, 10 minutes at 10^{o} C, followed by 50 cycles each consisting of 15 seconds at 95^{o} C and 1 minute at 60^{o} C.

2.16: Lysotracker assay

LysoTracker® Deep Red is a deep red-fluorescent dye for labeling and tracking acidic organelles in live cells.

To evaluate the lysotracker stain, 1000 cells were seeded in 24 well plates and treated with BT for 24 hours. Cells were washed in PBS buffer and pre-warmed 37^{O}C probe containing media 50nM was added to the cells and then incubated at RT for 30 minutes.

Immunofluorescent images of the cells treated with BT were analysed with Image J software, subtracting the background, using threshold, and analyzing a total of 30 cells for each experiment.

2.17: Chromatography for Protein binding

2.17.1:Chromatography method

Samples were analysed by HPLC (High-performance liquid chromatography), using a separation module Samples were analysed by HPLC using a separation module (Waters 2695, Watford, UK) equipped with a mass spectrometry detector (Waters micromass ZQ) and a Waters 2996 photodiode array detector. Separation was achieved using an RPB C18 (5 µm, 3.2 x 100 mm, Hichrom, UK) column maintained at 35 °C with eluent A: 10mM formic acid; eluent B: acetonitrile, using a flow rate of 0.5 mL/ min and a gradient of 45 – 100 % B over 5 min, with a 1 minute hold, returning to starting conditions in 0.1 min with a run time of 11 min. A flow splitter constructed of a short length of 0.0007 inch i.d. PEEK tubing attached to a T-fitting

on the mass spectrometer inlet diverted ~ half of this to waste, the remainder going to the mass spectrometer detector. Flow was diverted away from the mass spectrometer at the beginning and end of each chromatogram. Bithionol was monitored in single ion mode at m/z 355.05 (M-H) with a cone voltage of 30V or UV absorbance at 300 nm and eluted at 5.5 mins. Mass spectrometry settings were; capillary voltage was set at 2.4 kV, extractor lens 5V, RF lens 0.2V, desolvation gas flow 400 L/h, cone gas flow 40 L/h, source temperature 125 °C, and desolvation temperature 475 °C.

2.17.2: Protein binding method

Mouse plasma (citrate as anticoagulant obtained from Seralabs) was spiked with a bithionol stock to give final concentrations of bithionol shown in the table below. The plasma was transferred into Amicon centrifree YM-30 filters for ultrafiltration (free unbound bithionol). These were spun at 2000g for 20 min at 20 °C. The ultra filtrate was diluted by mixing 20 µl with 20 µl 45% acetonitrile and 10 µl injected onto the HPLC for measurement of bithionol. The presence of bithionol in these samples would indicate the presence of free-non-protein bound bithionol as 99.9 % of protein is prevented from passing through these Amicon filters. Any drug bound to plasma proteins would therefore be retained above the filter.

2.18: Measurement of dNTPs

Using HPLC deoxynucleotides and nucleotides were measured after appropriate calibration against commercial standards. Cell numbers need to be quite high (1 e7/sample) to get enough sensitivity.

1) Cells were seeded in 10cm dishes x 2 per condition. They were grown to 60% confluency and then BT was added.

2) After 24 hours of exposure to BT, the media was removed, and the cells were washed with ice cold PBS, the dish was kept on ice and the PBS was removed.

3) Scrape cells into 0.5ml PBS and transfer to an eppendorf, cells number were then counted.

4) The suspension was then spun at 2000rpm for 5 minutes at 4^0 C.

5) The supernatant was removed with a pipette and 50 µl of 6% TCA (trichloroacetic acid) was added to lyse the cells. Cells/ Pellet was vortexed for 1 minute

6) The eppendorf with the cell pellets was stored in -80^0 C before processing for dNTPs.

2.19: In-vivo Experiment

All animal experiments were performed according to protocols approved by the local ethics committee and Home office regulations. Nude mice (Balb-C nu/nu) were subcutaneously injected with 10^7 HCC 1806 cells in 100µl serum free medium (SFM) mixed with equal amount of matrigel (100µl) into the flank of each mouse.

To evaluate the effects of BT, in the initial experiment, 3 mice in the BT treated arm were given 70mg/kg dose of the drug for 5 days consecutively, with 2 days rest. The

drug was dissolved in 1% DMSO/corn oil: with oral gavage daily for 5 days and two days rest. 3 mice were given DMSO/corn oil as oral gavage in the control arm. BT treatment was started when greater than 50% mice had reached a tumour size greater than 150mm^3. Blood was collected from the tail vein 4 hours and 24 hours after drug administration to measure pKa levels. The blood was centrifuged and the plasma was separated and preserved in -80^0 C freezer. Tumour growth was measured twice a week, with Volume calculated as. When tumour volume reached 15 mm GMD (gross measurement diameter) = $(L+W)/2$ ((L= length, W= width, H= height), mice were sacrificed with cervical dislocation.

Mice were sacrificed, and divided in half, with one half snap frozen in liquid nitrogen and the other half fixed in formalin. All the procedures were carried under experienced technicians trained under the home office license. Note that the xenograft experiments were carried out with the help from Esther Bridges.

2.19.1: Sample storage

The xenograft biopsies/ tissue were snap frozen in liquid nitrogen, and transported to -80^0 C freezer in our institute, in the designated freezer. Blood was centrifuged and the plasma separated and stored in -20^0 C.

2.20: Statistical analysis

Prism 6 software (Graph Pad software) was used for statistical analysis. Statistical significance was calculated using one-way ANOVA (Kruskal-Wallis-Test) if more than two conditions were compared.

CHAPTER 3: Effects of GLUD inhibition and Bithionol on breast cancer cell lines in vitro and xenografts in vivo

3.1.1: Introduction

Numerous studies have shown the importance of glutamine in cancer cell survival and proliferation(Newsholme et al., 2003, Matsuno, 1987, Zielke et al., 1984, DeBerardinis et al., 2007, Vander Heiden et al., 2009). Glutaminase and GLUD are the key enzymes involved in the glutamine metabolism(Liu et al., 2015, Hensley et al., 2013, Gross et al., 2014)(Figure 3.1). Although glutaminase inhibitors have shown anti-proliferation activity in pre-clinical models of breast cancer(Gross et al., 2014), the role of GLUD inhibitors in breast cancer is still not clear.

Glutamate dehydrogenase (GLUD/GDH), a mitochondrial inner membrane enzyme, is involved in the final step of catabolism of glutamine metabolism i.e. the deamination of glutamate to α-ketoglutarate. GLUD has been implicated in cancer cell proliferation, transformation and autophagy by its regulation through various oncogenes and tumor suppressors such as mTORC1, SIRT4, K-RAS and p53(Csibi et al., 2014, Jeong et al., 2013, Son et al., 2013, Hu et al., 2010). Several studies have shown a clear relationship between GLUD expression and poorer clinical outcomes (Liu et al., 2015, Pozniak et al., 2016). Glutamate is responsible for supporting several key cellular pathways including the TCA cycle, nucleotide synthesis, amino acid metabolism and redox homeostasis.

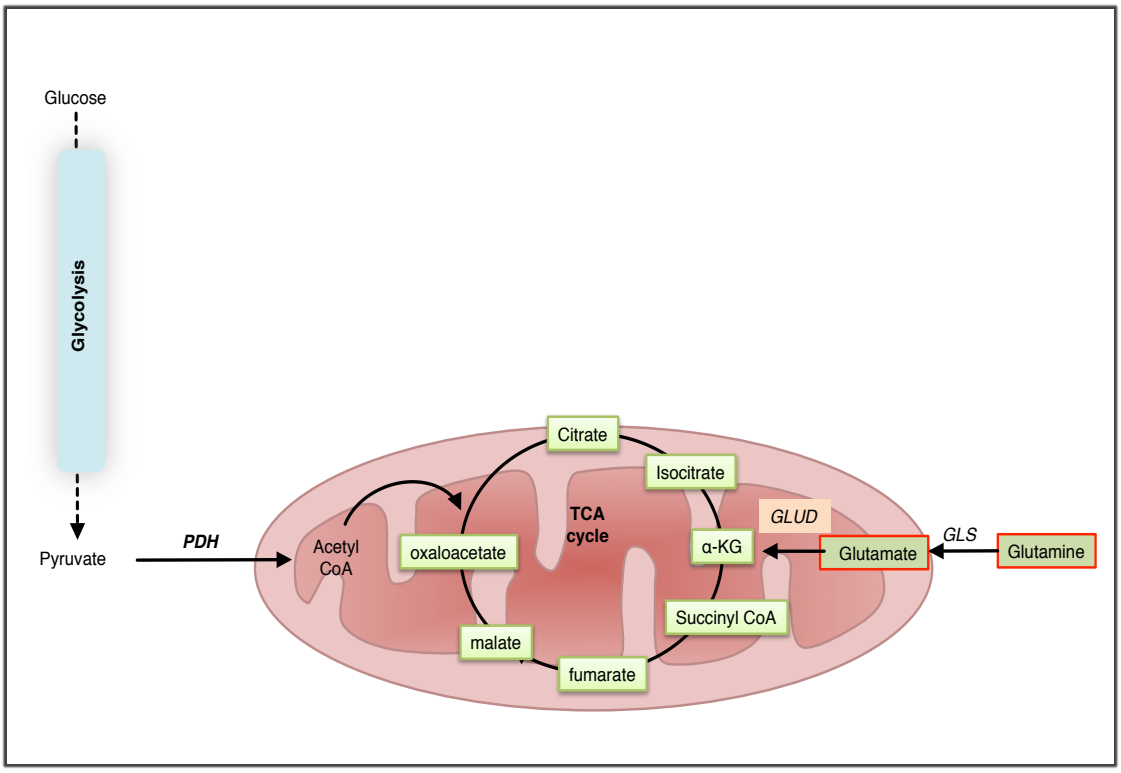

Figure 3.1: Schematic overview of the glutamate metabolism with its interaction with the mitochondrial metabolism. PDH- pyruvate dehydrogenase, TCA- Tricarboxylic acid, -KG- ketoglutarate, GLUD- glutamate dehydrogenase, GLS- glutaminase.

Several GLUD inhibitors have been reported (Li et al., 2011b), among these hexachlorophene (HCP), BT, GW5074 and Epigallocatechin gallate (EGCG) have shown significant GLUD inhibition, but these (Tsai et al., 2015, Choo et al., 2010) drugs have not shown yet been shown to be active in breast cancer. Among these drugs, EGCG has shown to have anticancer activity in glioblastomas(Yang et al., 2009), and also has preclinical activity in tuberous sclerosis(Choo et al., 2010), GW5074 is being studied in renal cancer, and HCP has been studied in colon cancer(Park et al., 2006).

BT (2,2'-thiobis (4,6-dichlorophenol), was originally used as an antiparasitic agent for Fascioliasis infestations(Bacq et al., 1991). Its activity in cancer has been previously

reported in breast, melanoma and ovarian cancer cell lines, but no in vivo experiments have been reported(Braddock, 2010, Saunders et al., 2008, Miller et al., 2010, Ayyagari and Brard, 2014). A recent study by Ayyagari et al. showed that BT exerted cytotoxic effects by autotaxin inhibition (Ayyagari and Brard, 2014), ROS generation, and NF-kB inhibition in ovarian cancer cell lines.

3.2: Results

3.2.1: Enhanced anti-proliferative effects of metformin in glutamine deprived conditions

Our group has previously demonstrated the enhanced activity of metformin in glutamine-deprived conditions. To confirm this, I treated MCF 7 and MDA MB 231 cell lines with 2mM metformin for 96 hours in DMEM supplemented with 10% FCS and 5mM glucose, with and without 4mM glutamine. In order to replenish the nutrients, the media was changed every 24 hours.

At 2mM of metformin, the effect on proliferation was more marked in MCF 7 as compared to MDA MB 231 ($p<0.001$). This has previously been shown by Simon Lord et al (unpublished). The removal of glutamine from media had a significant effect on MCF 7 proliferation with $p< 0.01$)(Figure 3.2).

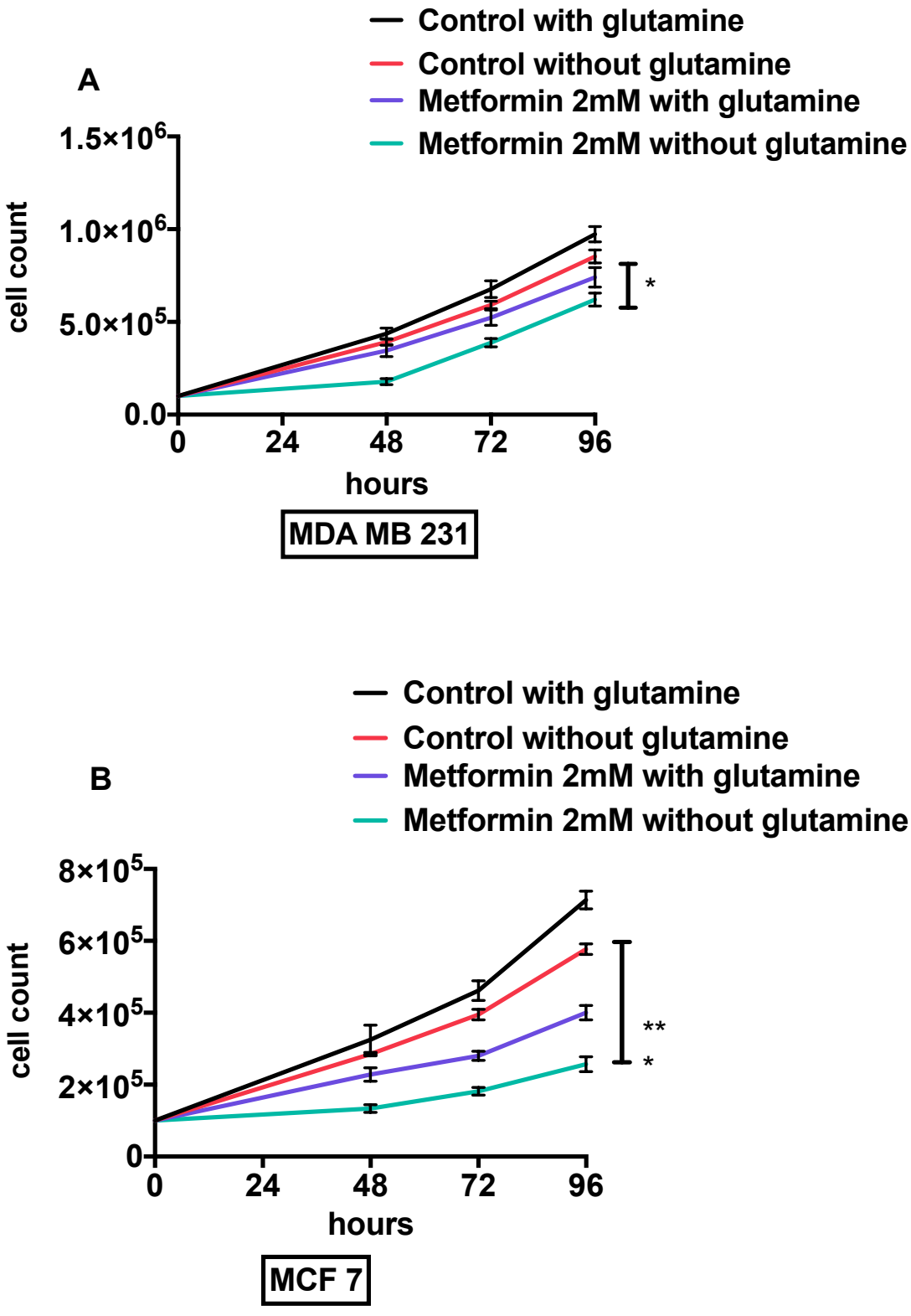

Figure 3.2: Effect of Metformin on MDA MB 231 and MCF 7 in glutamine deprived conditions. (A) MDA MB231 and (B) MCF 7 cells were treated with 2mM metformin with/ without glutamine for 96 hours (n=4). Data shown are mean ± SEM ***p<0.001, **p<0.01, *p<0.05.

3.2.2:Effect of BT on proliferation of a panel of breast cancer cell lines

To assess the effects of BT on a panel of breast cancer cell lines, as a first step, in order to determine a working dose, the effects of BT on 3 different cell lines (MCF 7, MDA MB 231, HCC 1806) was investigated. As seen in Figure 3.3, the IC_{50s} in the three cell lines were similar in MCF 7 (IC_{50} 14μM), MDA MB 231 (IC_{50} 16μM), and HCC 1806 (IC_{50} 17μM). I then treated seven breast cancer cell lines with 10μM and 20μM of BT (MCF 7, T47D- ER+/PR+/HER2-)(MDA MB 231,HCC 1806, MDA MB 468- ER-/PR-/HER2-) (SKBR3- ER-/PR-/HER2+) and (BT474 ER+/PR+/HER2+)(Figure 3.3D). As 20μM concentration of BT caused substantial inhibition, 10μM of BT was used in all subsequent experiments to allow assessment of effect not to be dominated by cell death.

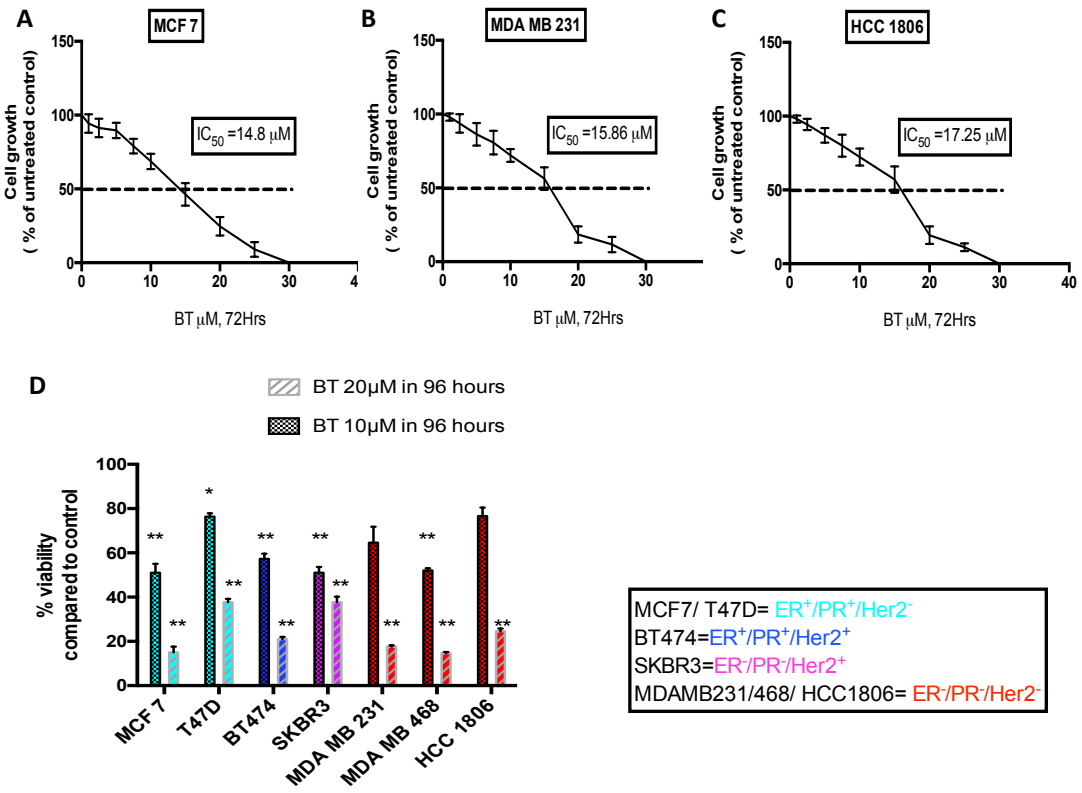

Figure 3.3A-C: Dose response curves of BT to calculate IC_{50} values were plotted using graph pad prism software in MCF 7 (IC_{50} 14.8µM), MDA MB 231 (IC_{50} 15.86µM), and HCC 1806 (IC_{50} 17.25µM), (n=3). **D:** Effect of BT 10 and 20µM at 96 hours of treatment in 7 different cell lines. MCF 7 and T47D are ER positive, BT 474, and SKBR3 are Her 2 +++ cell lines, MDA MB 231, MDA MB468 and HCC 1806 are triple negative cell lines. 1x 10^5 Cells were seeded in 6 well plates and left to settle overnight before being treated with BT for a period of 96 hours in 5mM glucose DMEM. Differences in the treatment groups in comparison to control were analyzed using one-way Annova test and p-values are denoted (n=4, ***p<0.001, **p<0.01, *p<0.05)

3.2.3: BT inhibits spheroid growth through GLUD1 inhibition

Next, we tested the effect of BT on spheroids as a 3 D model of cancer growth. 3 D proliferation studies provide a more realistic model to study anti-tumour drug effects, since they mimic the in vivo avascular tumour architecture(Kim et al., 2004, Ivascu and Kubbies, 2007). Cells were reseeded into a 96-well low adherence round bottom plates before incubating in 37^{o}C. Spheroid growth was measured over a 14-day period, with 15 replicates per condition, taken on 2,4,6,8,10,12 and 14 days after reseeding. Dose response effects were seen on spheroid volumes with volumes of Control (0.35mm^3), 5μM (0.27 mm^3), 10μM (0.21mm^3) and 15μM(0.1 mm^3)(Figure 3.4A, B). There was significant reduction in spheroid volumes from day 6 onwards at BT concentrations higher than 5μM. In representative images of 15 and 20μM the spheroids had evidence of necrosis, with complete disruption of spheroid architecture in both these groups. Spheroids were treated with BT dose of 15 & 20 μM in order to be closer to the IC_{50} values seen in the initial experiment. Also the experiment was done to understand the drug penetration in a 3D model prior to undertaking the in vivo experiment.

Furthermore, the Immunohistochemical staining showed reduced GLUD1 expression in BT treated spheroids as compared to the controls (Figure 3.4C).

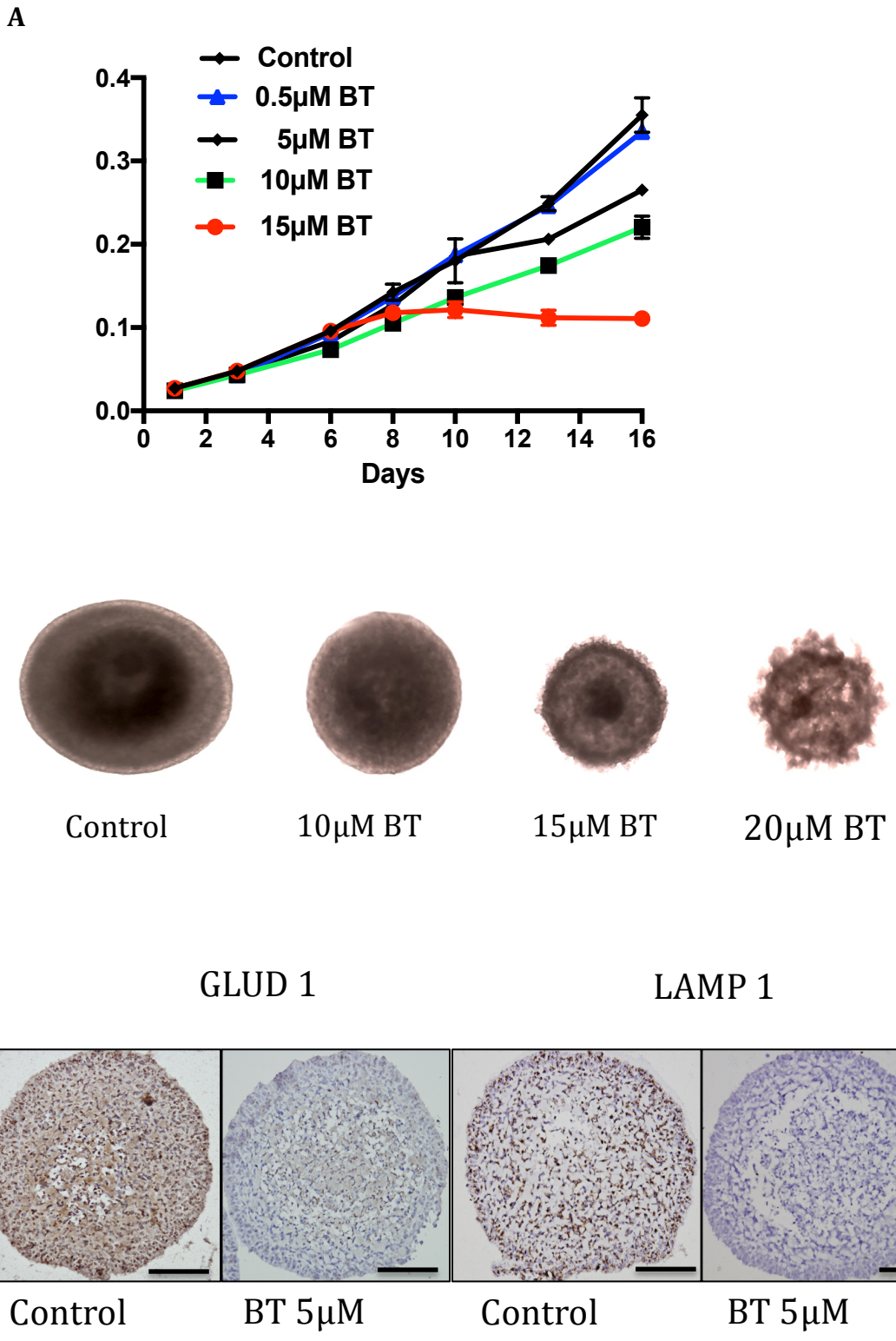

Figure 3.4: Spheroid 3 D proliferation time-course on MDA MB231 with BT drug treatment of 5,10,15 & 20μM. (A) Spheroid volume during a 2-week time course, n=3, **(B)** Representative images of spheroids at the final time point. **(C)** Immunohistochemical staining of GLUD1 and LAMP1 on spheroids shows reduced expression of both the proteins in the BT treated spheroids.

3.2.4: Breast cancer cell lines MDA MB231 and MCF 7 show a decrease in clonogenic survival after BT exposure

Clonogenic survival assays showed a significant decrease in colony formation of MCF 7 and MDA MB231 cells with increasing concentration of BT (Fig.3.5). The two cell lines were exposed to the drug for 24 hours and colony count was done after 10 days. All results are reported after normalizing to untreated controls. Detached cells were excluded form these assays.

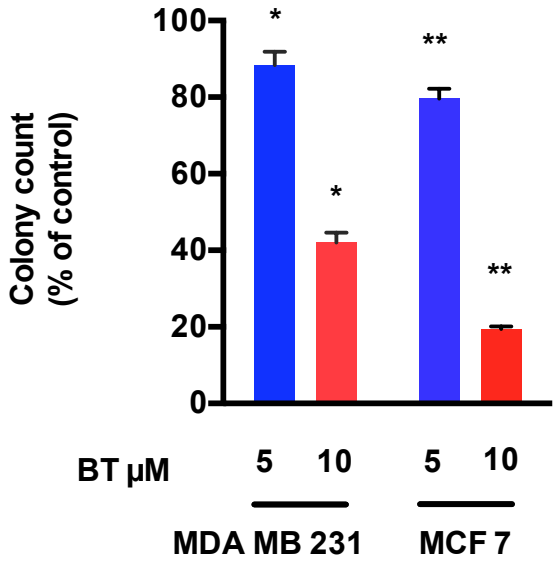

Figure 3.5: Effect of BT on clonogenic survival. MDA MB 231 and MCF 7 cell lines were treated with 5µM and 10µM of BT for 24 hours and colony count done in 10days as compared with control. n=3, Data shown are mean ± SEM ***p<0.001, **p<0.01,*p<0.05.

3.2.5: Effect of glucose depletion on BT treated cells

The observation that BT depleted the glutamine in the cultured breast cancer cell lines, raised the question whether altering the availability of glutamine, increases the reliance on glucose in these cells. Hence to understand the effects of glucose deprivation on BT cytotoxicity on breast cancer cells, we first treated MCF and MDA MB 231 cell lines with BT in media with and without glucose. The concentration of glucose was kept at 5mM in order to mirror the glucose concentration in the tumour microenvironment and close to the physiological levels of glucose in the serum. In both these cell lines, the effects on cell proliferation were significantly increased in glucose-deprived conditions ($p<0.001$)(Fig.3.6 A, B).

To investigate this reliance on glucose, we used a glycolytic inhibitor 2-deoxy-D-glucose (2DG) and evaluated its anti-tumour activity in vitro. 2DG is phosphorylated by hexokinase and subsequently inhibits the ATP generated by the glycolytic pathway and thus inhibits glycolysis(Cheong et al., 2011, Mullen et al., 2011, Vander Heiden, 2011). The combination of 2DG and BT significantly decreased cell proliferation 80% as compared to 12% and 9% with BT and 2DG respectively ($p<0.001$)(Fig. 3.6C, D).

These results signify, increased dependence of cancer cells on glucose on GLUD1 inhibition, as a means of providing alternate fuel for survival, implying the cells rely more on glucose for growth in glutamine deprived condition.

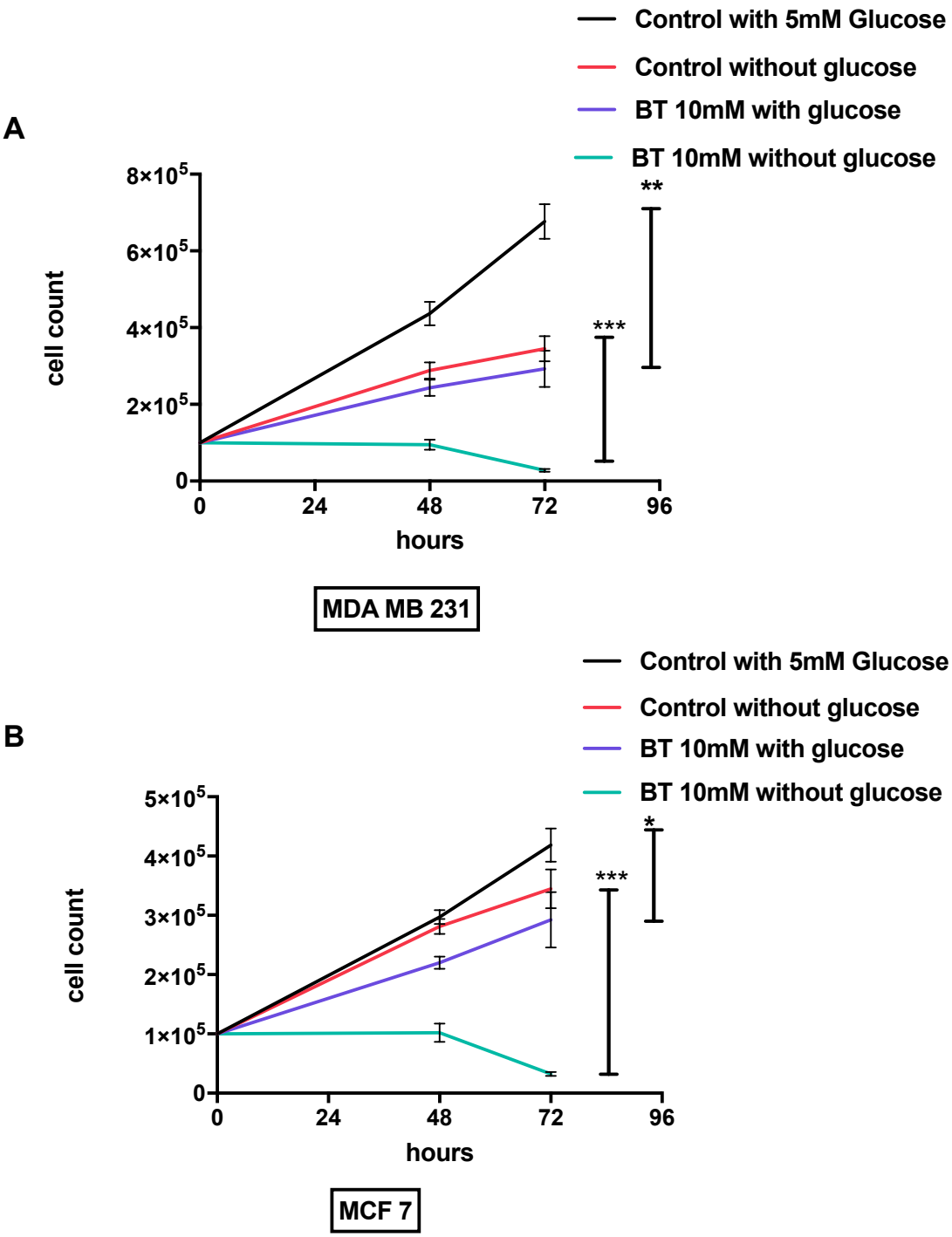
A
Control with 5mM Glucose
Control without glucose
BT 10mM with glucose
BT 10mM without glucose
cell count
8×10^5
6×10^5
4×10^5
2×10^5
0
0
24
48
72
96
hours
**
***
MDA MB 231
B
Control with 5mM Glucose
Control without glucose
BT 10mM with glucose
BT 10mM without glucose
cell count
5×10^5
4×10^5
3×10^5
2×10^5
1×10^5
0
0
24
48
72
96
hours
*
***
MCF 7

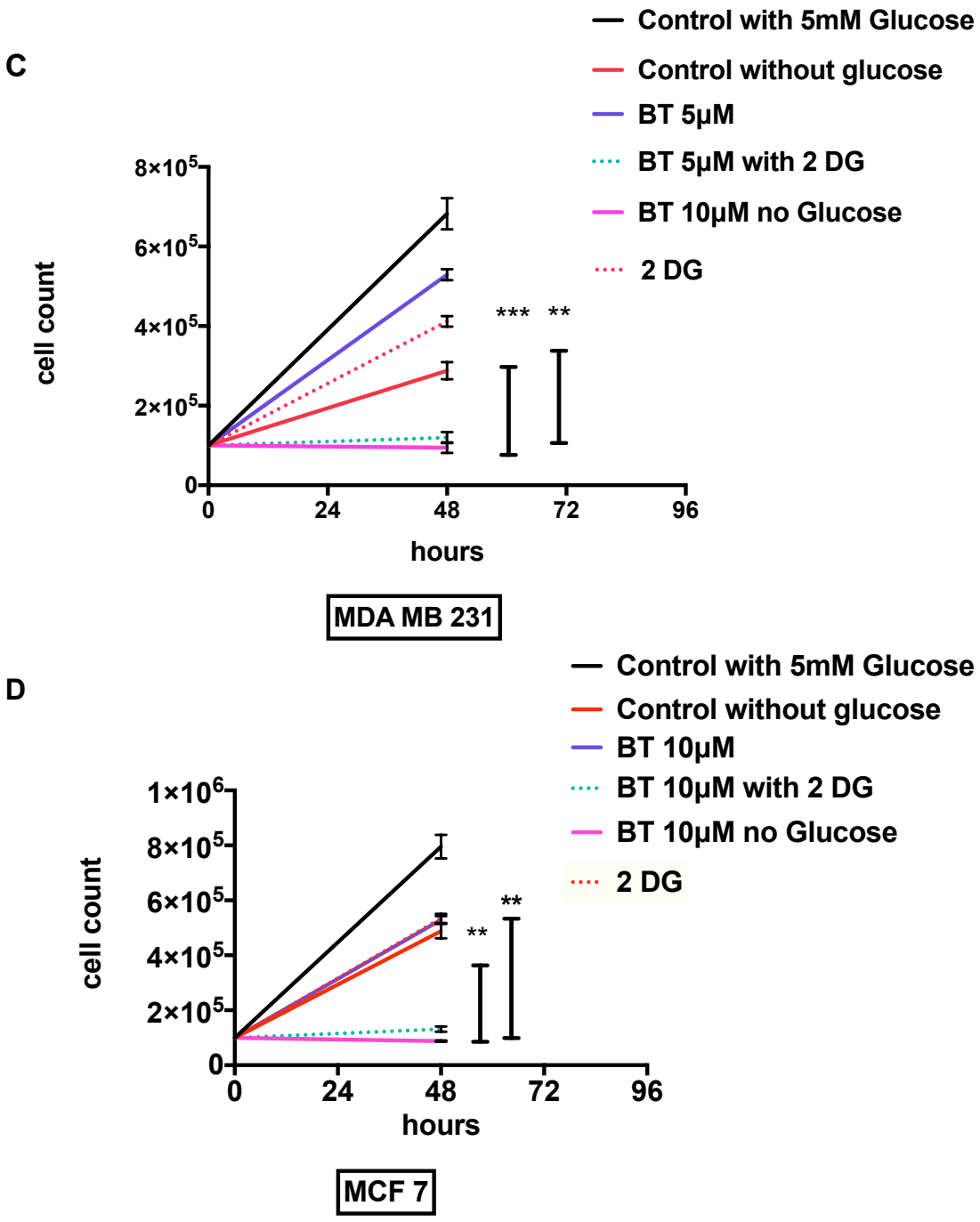

Figure 3.6: Effect of Glucose depletion on cell growth in BT treated cells. (**A**)& (**B**) MDA MB 231 and MCF 7 treated with BT with +/- DMEM containing 5mM Glucose. (**C**)& (**D**) MDA MB 231 and MCF 7 treated with BT with +/- DMEM containing 5mM Glucose and 2 Deoxyglucose. n=4, Data shown are mean ± SEM ***p<0.001, **p<0.01,*p<0.05.

3.2.6: GLUD1 knockdown reduced cell growth in vitro

To better understand how GLUD1 inhibition affects mitochondrial metabolism and growth of cancer cells, we examined the effect of siRNA targeting GLUD1 gene on the MDA MB231 cell line. Commercially available siRNA pools (combination of 4 individual sequences) for GLUD1 were used (Dharmacon) and their activity and GLUD1 specificity confirmed in a reverse transfection experiment with MDA MB 231 cells. This particular cell line was selected, as MDA MB 231 is a triple negative breast cancer cell line, and our earlier experiments have shown good response to BT on inhibition of proliferation and reproducibility in spheroid experiments. siRNA knockdown of GLUD1 resulted in decreased cell number and was significantly more effective than 5uM Bithionol (60% vs 76% $p<0.01$)(Figure 3.7A).

BT inhibited Lysosomal associated membrane protein-1 (LAMP-1) expression and similar inhibition was seen with the GLUD1 knockdown (Figure 3.7B). LAMP-1 is a glycosylated protein present on the lysosomal membranes and in mice deficient with this protein there is an increase in the number of autophagic vacuoles, suggesting their role in autophagy(Rajapakshe et al., 2015). LAMP-1 also functions in stabilization of the lysosomes(Eskelinen et al., 2004).

To elucidate the effects of BT on GLUD enzyme levels, we measured the GLUD1 levels in both MDA MB 231 and MCF 7 cell lines treated with BT 10μM for 24 hours. There was 45% and 50% reduction in the GLUD1 enzyme activity in both MDA MB 231 and MCF 7 cells treated with BT (Figure 3.7 C). siRNA GLUD1 knockdown cells also showed a significant reduction in the GLUD 1 activity $p<0.001$.

Taken together, these results suggest a strong effect of BT on GLUD1 enzyme activity to mediate cytotoxicity. No changes were seen in mRNA expression in BT treated cells, suggesting, the effect on GLUD1 suppression in BT treatment was at the protein level (Figure 3.7D).

A

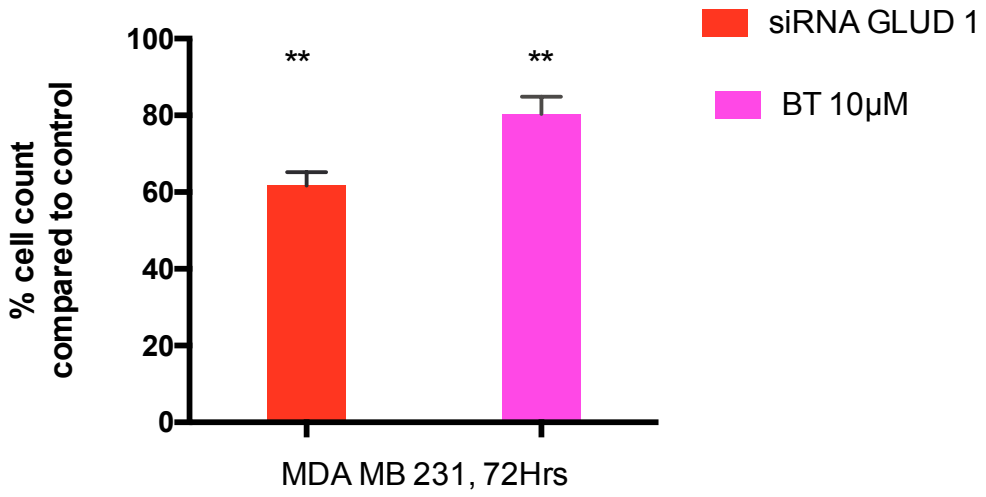

B

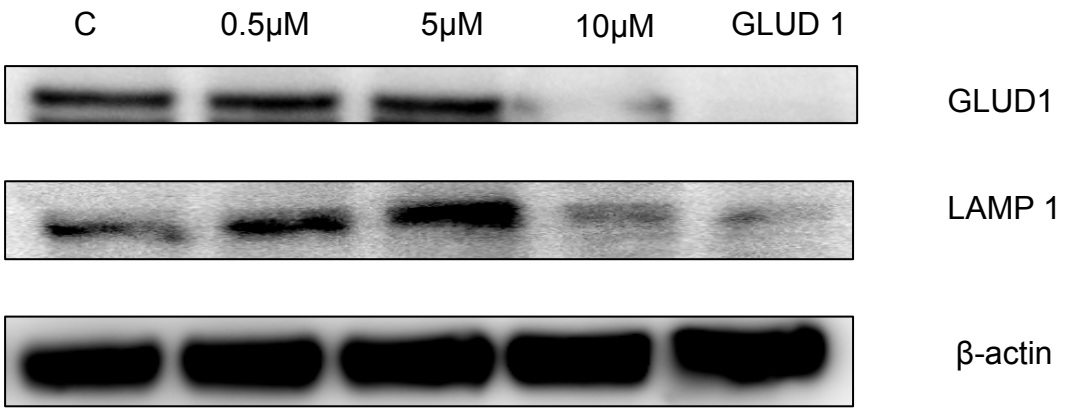

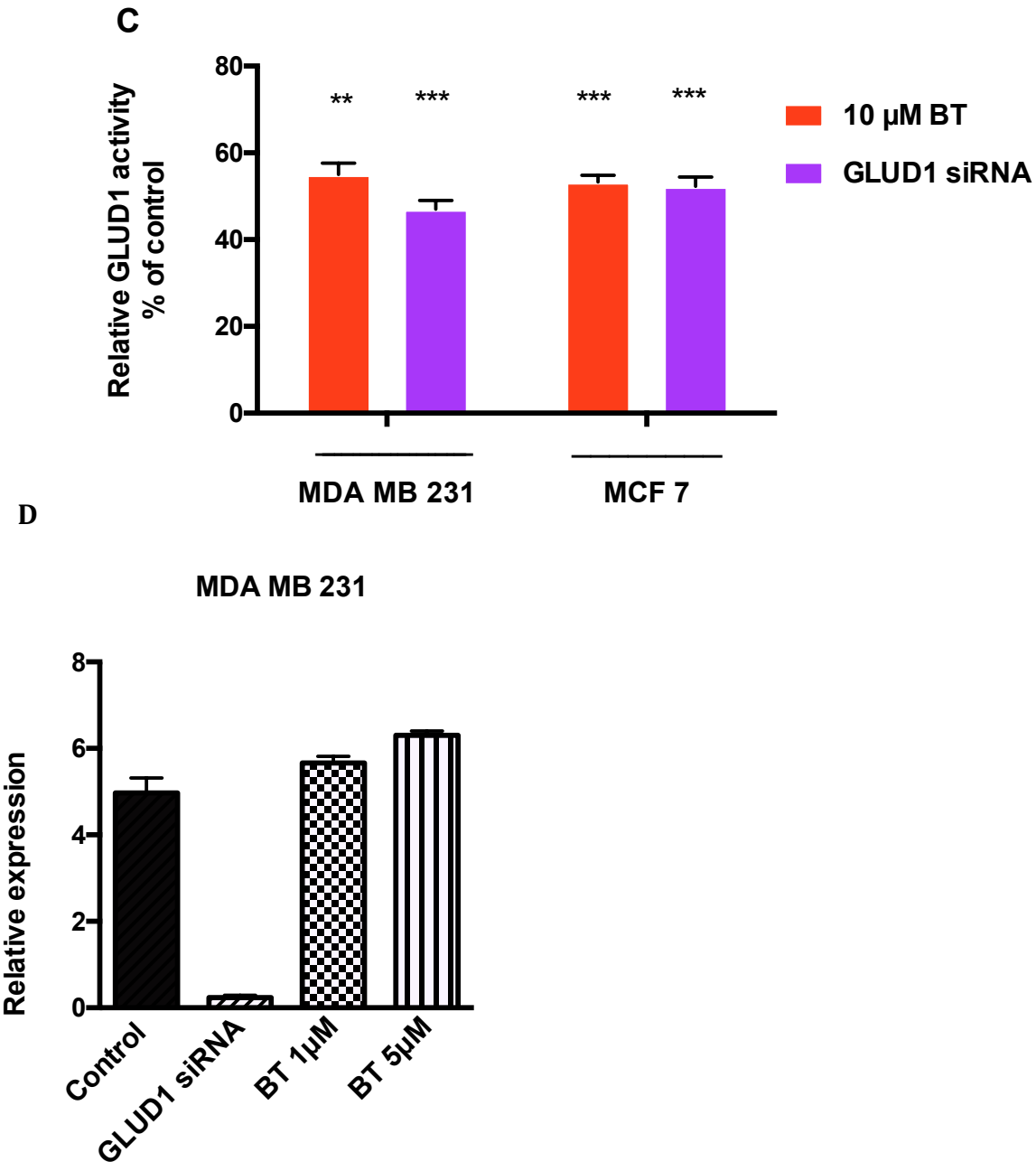

Figure 3.7: Effect of GLUD 1 knock down on cell proliferation. **(A)** Cell growth comparing siRNA GLUD1 knockdown with BT treated MDA MB 231 cells, cell count done at 72 hours. n=3, (**p<0.01).
(B) Western blot validation of siRNA GLUD1 knockdown at protein level of MDA MB231 cells, and comparison with treatment with BT. Representative images of n=3 images. **(C)** Effect of GLUD1 knockdown and BT on GLUD1 enzyme activity in MDA MB 231 and MCF 7 cell lines. **(D)** mRNA expression in GLUD1 siRNA knockdown and in BT treated MDA MB 231 cell line. n=3, Data shown are mean ± SEM *p<0.05, **p<0.01, ***p<0.001. (Control- Scramble si RNA)

3.2.7: BT increases cell dependency on transamination for survival

Aminooxyacetate, a pan transaminase inhibitor has been shown to have antitumour effects in preclinical models of breast cancer(Korangath et al., 2015). In our study, we have seen increasing levels of TCA cycle metabolites on Mass spectroscopy of BT treated cells (Chapter 4.5). Interestingly, the levels of aspartate were also elevated in our analyses (Figure 4.5 A-C). We treated MDA MB 231 and MCF 7 cell lines with AOA 1mmol and BT 5μM. BT and AOA on their own showed modest effects on cell death, however a combination of AOA and BT induced a significant effect on cell count as compared to the individual treatments (Figure 3.8). The effects of combination therapy were more significant in MCF 7 with even BT 5μM showing considerable cytotoxicity with AOA (Figure 3.11 A & B).

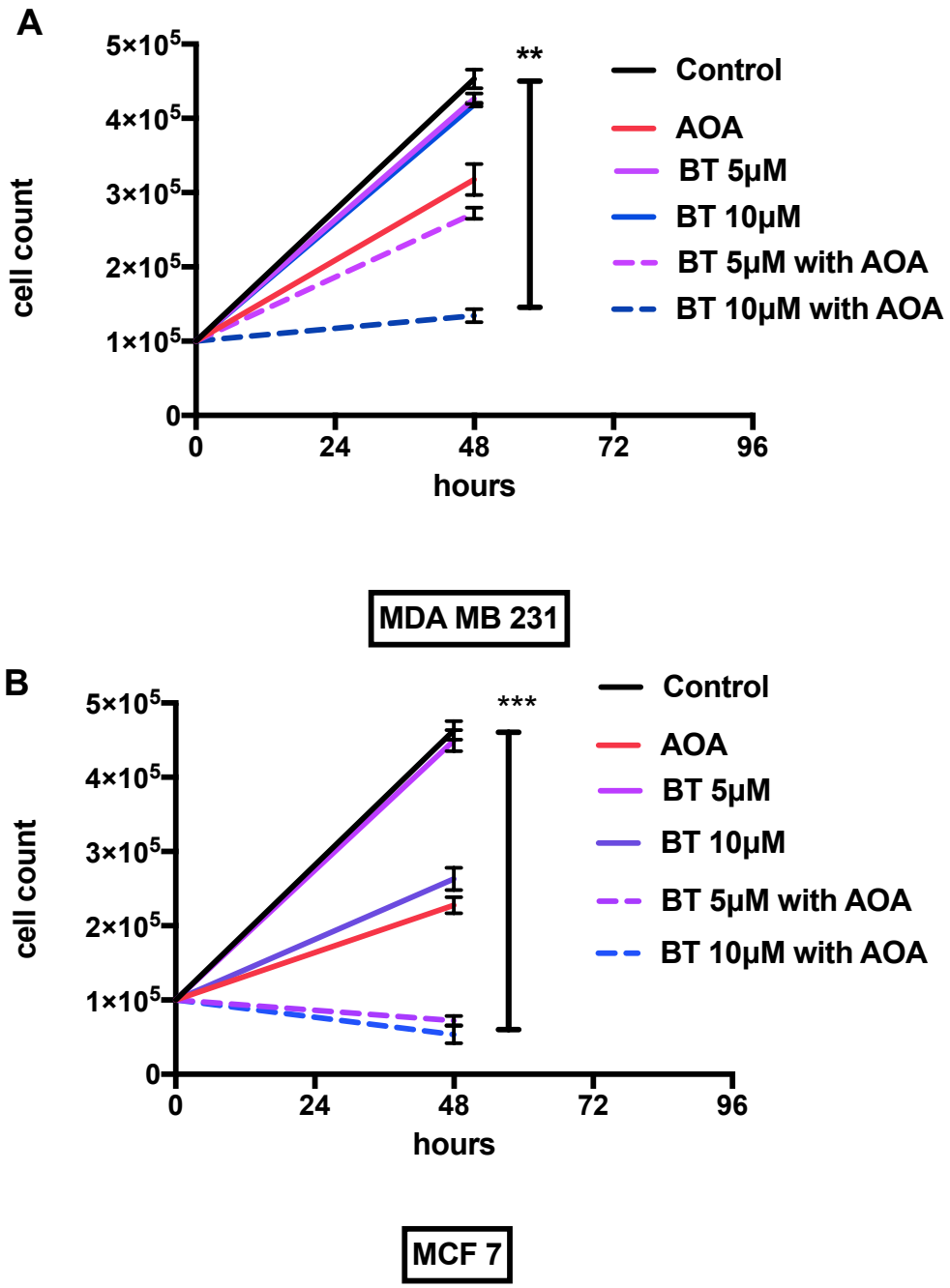

Figure 3.8: Effect of BT 5µM and 10µM on cell proliferation in combination with a transaminase inhibitor AOA 1mmol, at 48 hours in MDA MB 231 **(A)** and MCF 7 **(B)** cell lines (n=3). Data shown are mean ± SEM *p<0.05, **p<0.01.

3.2.8: BT treatment results in cell cycle arrest in G1 phase

FACS analysis on MDA MB 231 and MCF 7 cells 24 hours treatment with BT resulted in significant cell cycle differences, between the control and BT treated cells. Cells were fixed in ethanol and stained with PI, and then cell cycle distribution was analysed with flow cytometry. In the MDA MB 231 cell lines, control group there were 50% cells in the G phase, 23% cells in S phase and 27% cells in the M phase. However, in the 10μM BT treated group, the percentage in G phase increased to 62%, and the percentage in S and M phase decreased to 17.5% and 20.5% respectively ($p<0.01$). Exposure to 5μM BT also showed similar but less marked effects. Similar results were also seen in MCF 7 cells, with the control showing G phase 50%, S phase 22.5% and M phase 27.5%. In the 10μM BT treated cells, G phase increased to 69%, M phase decreased to 16% and S phase was 15% (Figure 3.9B and C)(Table 3.1). These results suggested that the cytotoxicity of BT was associated with cell cycle arrest in the G1/S phase, which is in keeping with the role of nucleotides in ATP production and GI/S transition(Kondo et al., 2000, Lane and Fan, 2015). In chapter 4.8 it is clearly evident that GLUD1 inhibition, reduces the nucleotide synthesis, which also affects the cell cycle arrest at G1 phase.

MDA MB 231			
	G	S	M
Control	50%	23%	27%
BT 10μM	62%	17.5%	20.5%
MCF 7			
Control	50%	22.5%	27.5%
BT 10μM	69%	15%	16%

Table 3.1: Effect of BT on cell cycle, on MDA MB 231 and MCF 7 cell lines.

3.2.9: BT increased apoptosis

Apoptosis is frequently disorganized in cancer progression. Cells from MCF 7 and MDA MB 231 were analysed after treatment with 10μM BT for 24 hours. Apoptosis was analysed using Annexin V-PE staining and flow cytometry. As seen in the figure 3.9A, on quantification of percentage of apoptotic cells, BT treatment showed a significant increase in apoptosis levels, in MCF 7 cells 35% to 60% and 5% to 10% in early and late apoptosis respectively ($p<0.05$).

In MDA MB 231 cells, there was an increase in apoptotic cells from 35% to 63% in early apoptosis and 5% to 17% in late apoptosis following treatment with BT ($p < 0.01$).

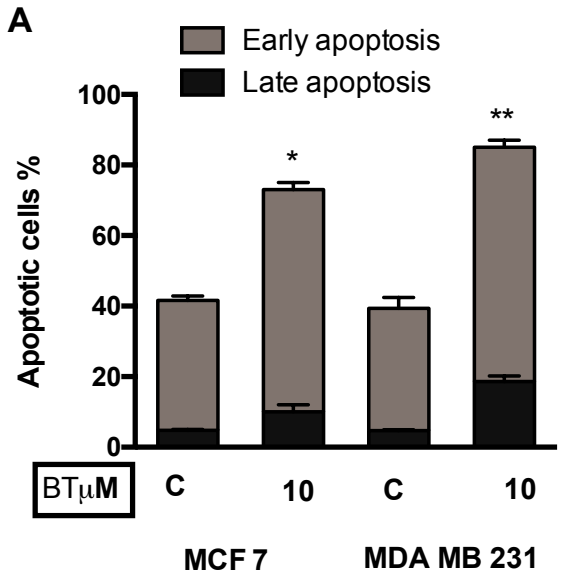

B

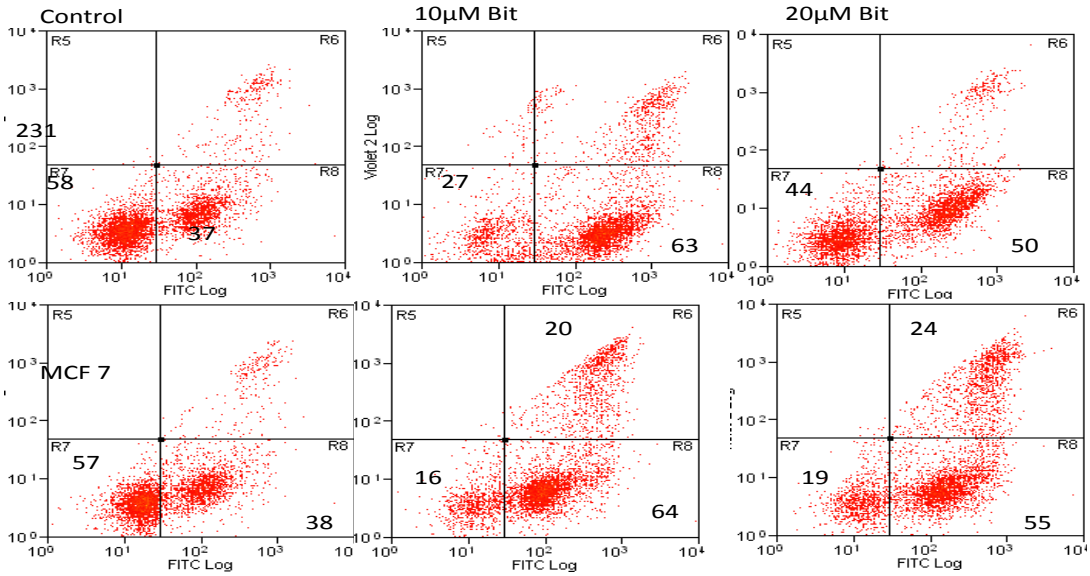
Control
10µM Bit
20µM Bit
R5
R6
R7
R8
231
58
37
27
63
44
50
MCF 7
57
38
20
16
64
24
19
55
FITC Log
Violet 2 Log

C

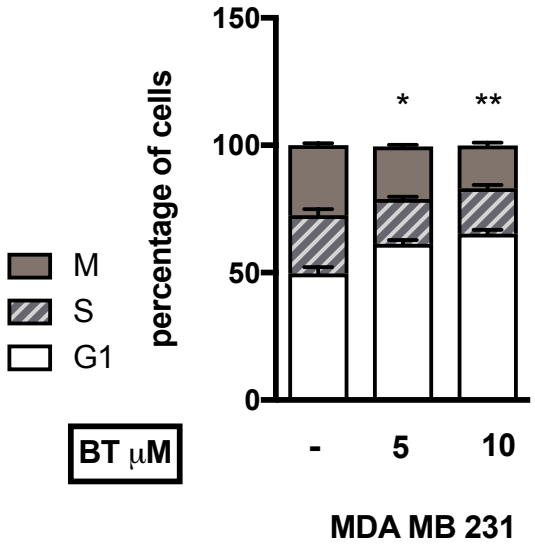
150
100
50
0
percentage of cells
M
S
G1
*
**
BT µM
-
5
10
MDA MB 231

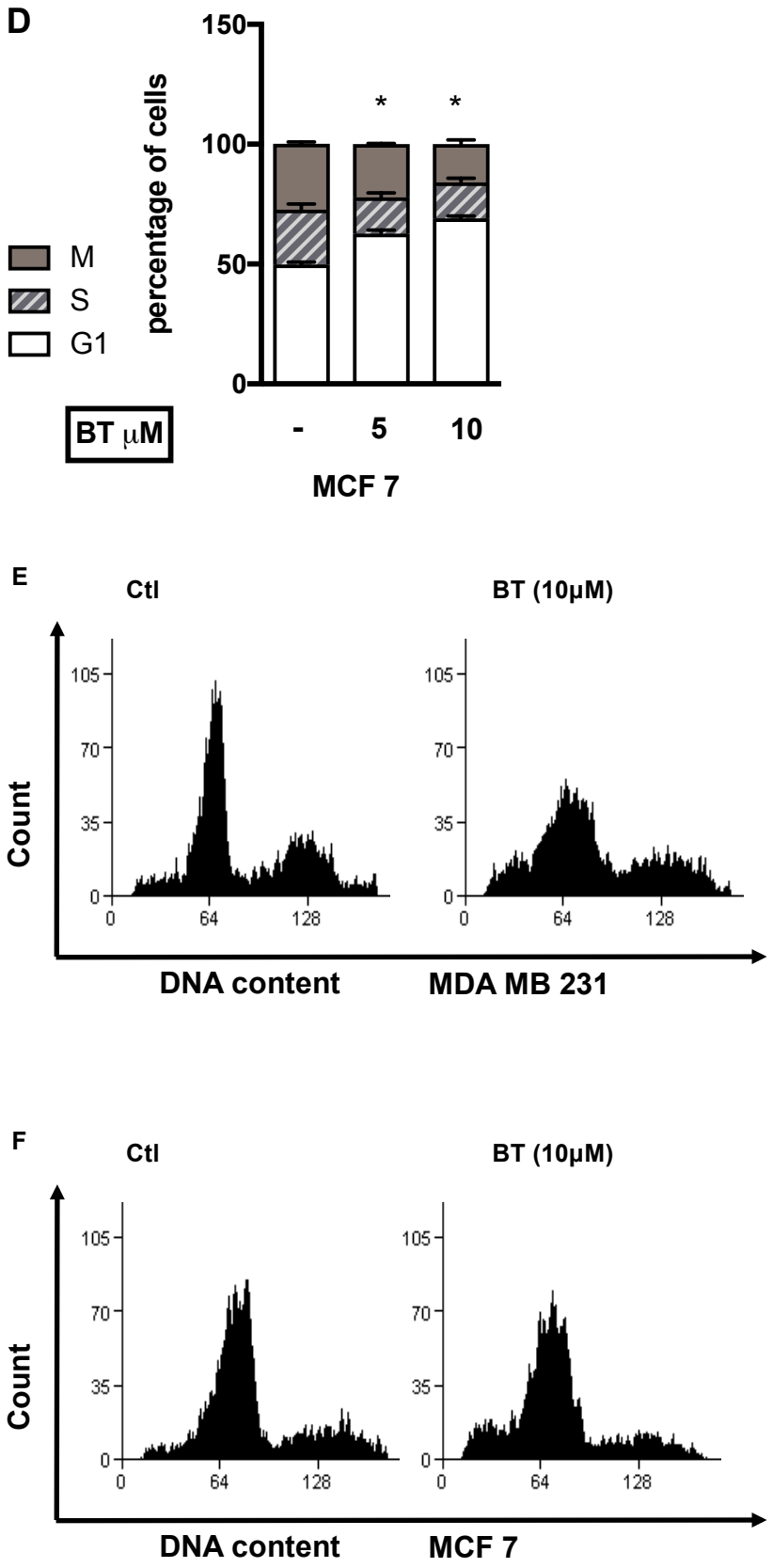

Figure 3.9: Effect of BT on cell cycle and apoptosis, (A) & (B) Flow cytometric analysis of BT on apoptosis induced by BT 10μM for 24 hours in MCF 7 and MDA MB 231 cell lines. **(C) -(E)** BT effected cell cycle distribution in both MCF 7 and

MDA MB231 cell lines. The percentages of cells in each cycle phase were summarized. n=3, Data shown are mean ± SEM *p<0.05, **p<0.01.

3.2.10: Effect of BT in vivo

The effects of BT on HCC 1806 cell lines grown as xenograft tumours on CD1 nu/nu mice was assessed. In the first part of the experiment mice were treated with BT 70mg/kg on 5 days on and 2 days off regime. No mice experienced any adverse effect, however there were no effects on tumour growth. The BT dose was then increased to 100mg/kg with 5 days on and 2 days off regime. In the 100mg/kg cohort, 4 mice were treated with BT and 3 were control. THE 100mg/kg BT arm, showed a consistent greater inhibition of tumour growth compared to all other treatment arms. GLUD1 expression in the xenografts was further investigated by immunohistochemistry (Figure 3.10). The GLUD1 expression in BT treated tumours was significantly reduced. Plasma was collected after 6 hours of dosing for measurement of BT levels. Plasma concentration of BT was 27 and 43 μM in the xenograft treated with 70mg/kg and 100mg/kg respectively.

Mouse plasma was spiked with a bithionol to measure the free unbound bithionol. The ultra filtrate was diluted by mixing 20 μl with 20 μl 45% acetonitrile and 10 μl injected onto the HPLC for measurement of bithionol. The presence of bithionol in these samples would indicate the presence of free-non-protein bound bithionol as 99.9 % of protein is prevented from passing through these Amicon filters. Any drug bound to plasma proteins would therefore be retained above the filter. The concentration of bithionol in the ultra filtrate was calibrated using LCM except for the 2000 μM sample, which was calibrated using the absorption at 300 nm. Bithionol was found to be tightly bound to the plasma with < 2% free drug after spiking control plasma with 2 mM bithionol. Figure 1 shows the concentration of bithionol detected in the ultra filtrate and figure 2 shows the percentage free drug based upon the concentration added to the plasma.

A

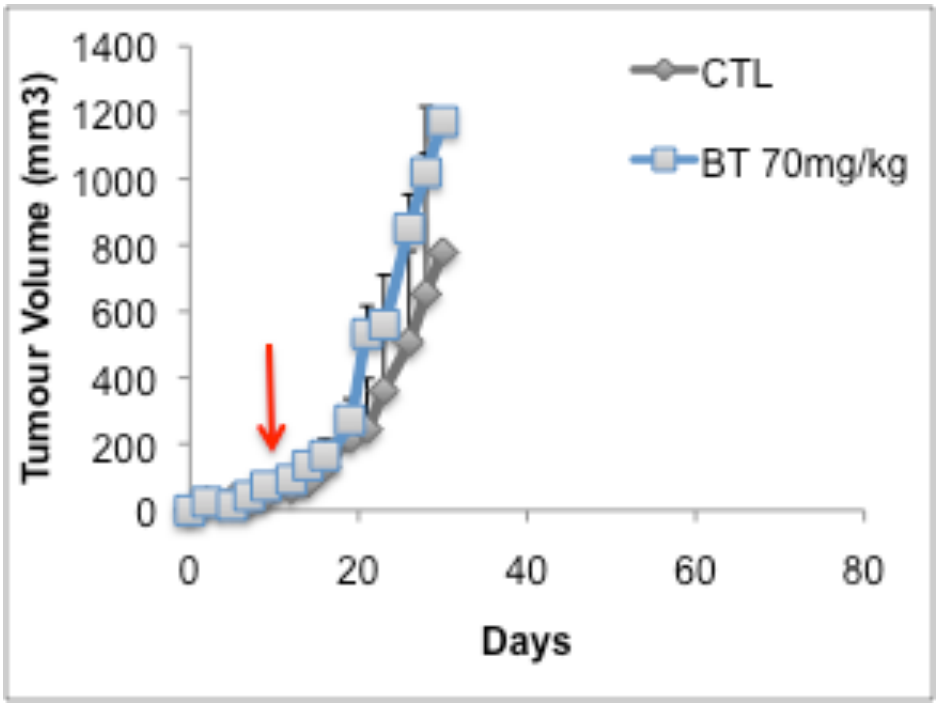
Tumour Volume (mm3)
1400
1200
1000
800
600
400
200
0
0
20
40
60
80
Days
CTL
BT 70mg/kg

B

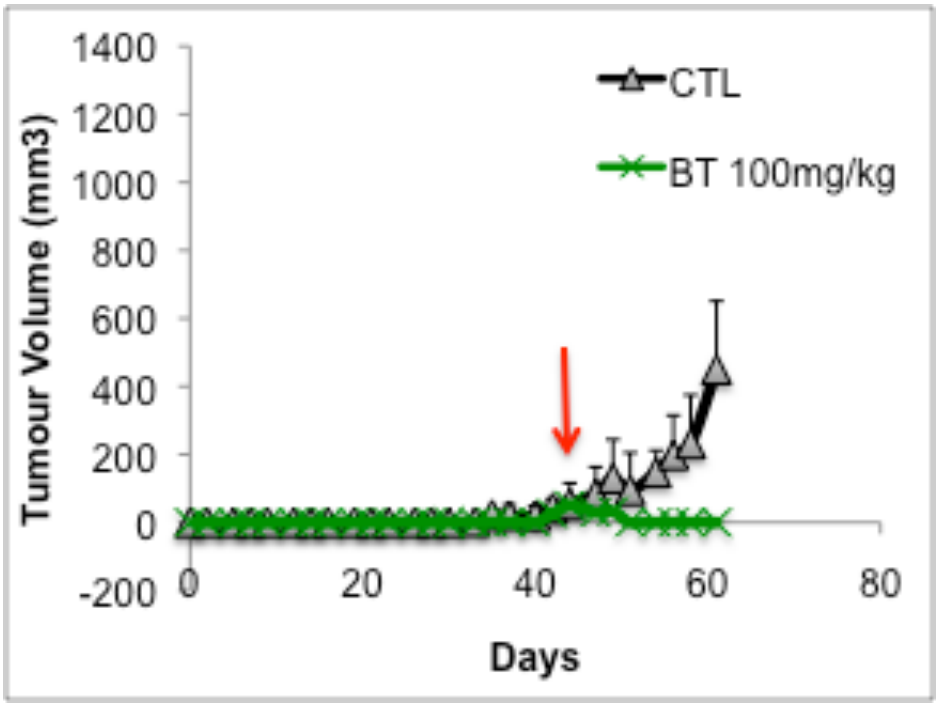
Tumour Volume (mm3)
1400
1200
1000
800
600
400
200
0
-200
0
20
40
60
80
Days
CTL
BT 100mg/kg

C

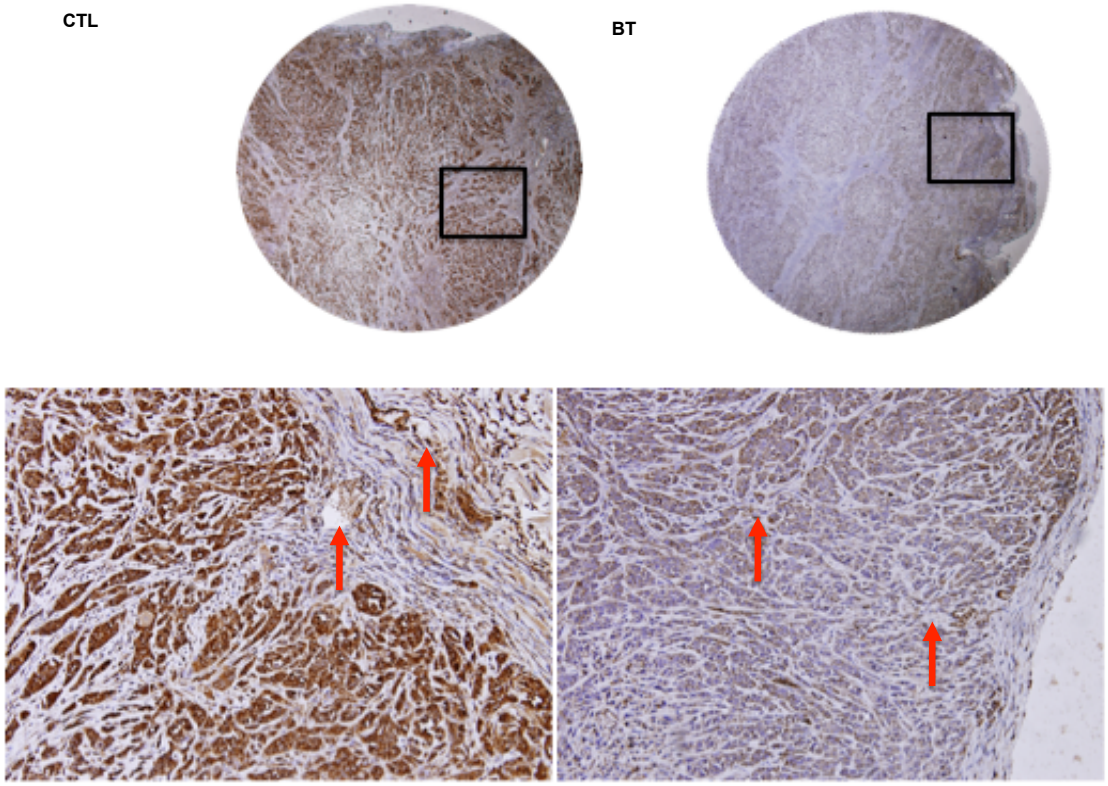

D

Sample no.	Dose mg/kg	Time (h)	Bithionol (µM)
1	70	6	27
2	70	6	28
3	70	6	25
4	100	6	34
5	100	6	51
6	100	6	47
7	100	6	40

E

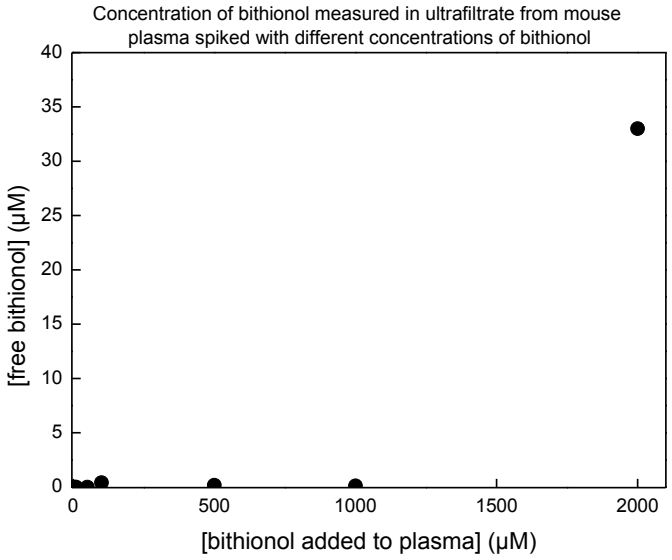

F

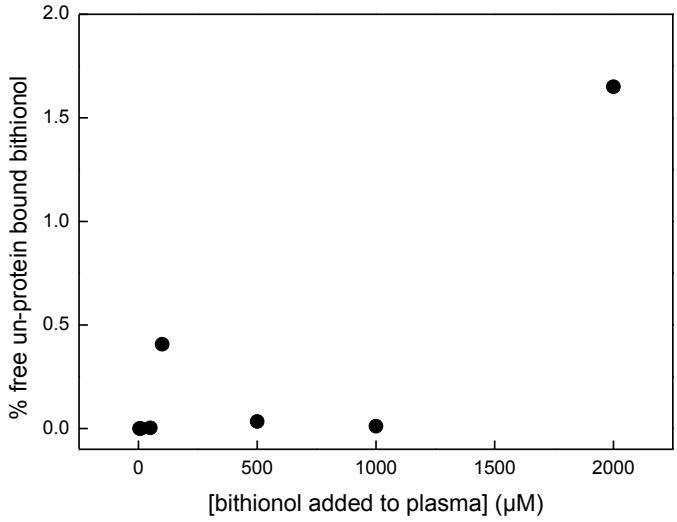

G

[Bithionol] (µM)	[bithionol in filtrate] (µM)	% free drug
5	< 0.01	0
10	< 0.01	0
50	< 0.01	<0.01
100	0.41	0.41
500	0.17	0.03
1000	0.11	0.01
2000	33.0	1.65

Figure 3.10: (A& B) Mean tumour volume over duration of BT minimum effective dose finding study. The curves of the group illustrating the mean tumour volume of mice non treated, and drug treated arm (70mg/kg – A, 100mg/kg- B) for the HCC 1806 breast cancer xenograft model. **(C)** Immunohistochemical analysis of GLUD1 expression in xenografts. Representative photomicrographs of FFPE xenograft sections stained with GLUD1 antibody. **(D)** BT levels measured by HPLC in plasma 6 hours after oral dosing of 70mg/kg and 100mg/kg of BT to mice bearing HCC 1806 tumours (n=7). **(E)** Concentration of bithionol in ultra filtrate from mouse plasma spiked with different concentration of BT. **(F)** Percentage of free bithionol in 'spiked' plasma. **(G)** Concentrations of bithionol in ultra filtrate and % free drug in 'spiked' control plasma.

3.3: Discussion

Investigation into the anticancer potential of BT has been reported in various cell lines, but the role of GLUD1 has not been exploited in any of them(Braddock, 2010, Saunders et al., 2008, Miller et al., 2010, Ayyagari and Brard, 2014). In the present study, the inhibition of GLUD1 by BT in MCF 7 and MDA MB 231 cell lines and the dose dependent cytotoxic effects on breast cancer cell lines, suggesting an important role of GLUD1 in maintaining cell viability. Although BT suppressed the proliferation on a panel of breast cancer cell lines, the effects were similar across all the cell lines. Glucose deprivation increased the cytotoxic effects of BT and this effect was also seen when a glycolytic inhibitor 2DG was used along with BT. This suggests that GLUD1 inhibition, switches cells dependence on glutamine for ATP production to rely on glycolysis for their energy metabolism.

The combination of transaminase inhibitor AOA and BT in inhibiting cell proliferation suggested that tumour bioenergetics can be targeted and this combination deserves further clinical evaluation. Increased synergy between transaminase inhibitor and GLUD1 inhibition represents a promising strategy for cancer therapy. Activation of the transaminase pathway was shown recently in proliferating epithelial mammary cells, so this is potentially an important rescue pathway (Coloff et al., 2016).

BT treatment suppressed GLUD1 protein expression, whereas it had no effect on GLUD1 mRNA expression. In addition to inducing apoptotic death, BT also caused cell cycle arrest at the G1/S checkpoint. BT and GLUD1 siRNA knockdown attenuated the GLUD1 enzyme levels to a similar extent. On western blot analysis, suppression of GLUD1 was shown in cancer cell lines, this was also seen in

immunohistochemistry in xenograft tumours and in spheroids treated with BT. The most notable finding on western blot in BT treated cancer cell lines and Immunohistochemical analysis in spheroids was suppression of expression of LAMP1 protein. The LAMP proteins LAMP-1 & 2 play an important function of positioning of lysosomes and mitochondria(Rajapakshe et al., 2015). A 50kDa protein previously isolated from lysosomal membrane was postulated to be GLUD. It has previously been reported that in mice with deficient LAMP proteins, there is an increased accumulation of autophagic vacuoles, suggesting a significant role in autophagy. This unique function of GLUD protein has also been further studied in chapter 4.4.Through this GLUD lysosomal interaction; BT directly or indirectly is associated with inhibition of proliferation, invasion, survival and degradation of the cancer cells.

To further investigate the safety and efficacy of BT in xenografts, 2 doses of BT were used and there was no toxicity seen in the mice treated with BT. Tumour suppression was seen in 100mg/kg doses, which could probably be due to the high protein binding of BT. In humans BT has been given with a dose of 25-100mg/k/day with minimal toxicity(Bacq et al., 1991) with pKa values of 0.12-0.18mg/ml(Yokogawa et al., 1962). The pKa values of BT in rabbits that were given a dose of 100mg/kg was 0.05mg/l and in dogs who were given 50mg/kg the pKa values was 0.20mg/ml(Nihon Kiseich¿± Gakkai.). The side effects of BT in humans have been few with transient digestive disorders reported including nausea, vomiting, anorexia, occasionally it can cause urticarial or skin photosensitivity(Gutman et al., 1969). These side effects are dose dependent and transient and disappear when the medication was stopped(Bassiouny et al., 1991, Singh et al., 1986). This, when coupled with the data presented in this chapter indicated that BT has good clinical activity in early xenograft

studies, which need further evaluation in a larger xenograft experiment. It also shows that this drug is safe to use in xenografts and in humans and this warrants further evaluation in clinical studies.

CHAPTER 4:

Effects of GLUD1 inhibition on mitochondrial metabolism

4.1:Introduction

Most studies with BT to date have focused on its cytotoxic effects by altering the cellular redox balance, NF-kB and autotoxin inhibition(Ayyagari and Brard, 2014, Braddock, 2010, Saunders et al., 2008). Not much has been investigated about the role of GLUD1 inhibition and altered mitochondrial function with BT. Glutamine is converted into glutamate and ammonium ions by mitochondrial glutaminase and the glutamate can be further catabolised to α-ketoglutarate by either GLUD1 (Figure 4.1) or via transaminases(Moreadith and Lehninger, 1984). Cancer cells use glutamine as an energy generating substrate and any alteration in its metabolism will lead to mitochondrial dysfunction and altered oxidative phosphorylation(Fan et al., 2013). Mitochondria are an important cellular organelle responsible for synthesis of cellular metabolites like amino acids, nucleotides and fatty acids(Ahn and Metallo, 2015).

In addition to the biosynthetic and bioenergetics function, mitochondria also function as signaling organelles. This function can be performed by the release of various metabolites which, synthesis of ROS (Sena and Chandel, 2012)and recently there has been increasing evidence of the presence of various signaling kinases and phosphatases in the mitochondrial matrix (Pagliarini et al., 2005, Acin-Perez et al., 2011, Huang et al., 1999). Mitochondrial metabolism delivers precursors to build macromolecules in proliferating tumour cells (Lunt and Vander Heiden, 2011, Gao et al., 2009). It has previously been shown that cells with defective electron transport chain which site, similarly compensating for metformin at complex 1, use glutamine

dependent reductive carboxylation and than oxidative metabolism to produce citrate(Mullen et al., 2011).

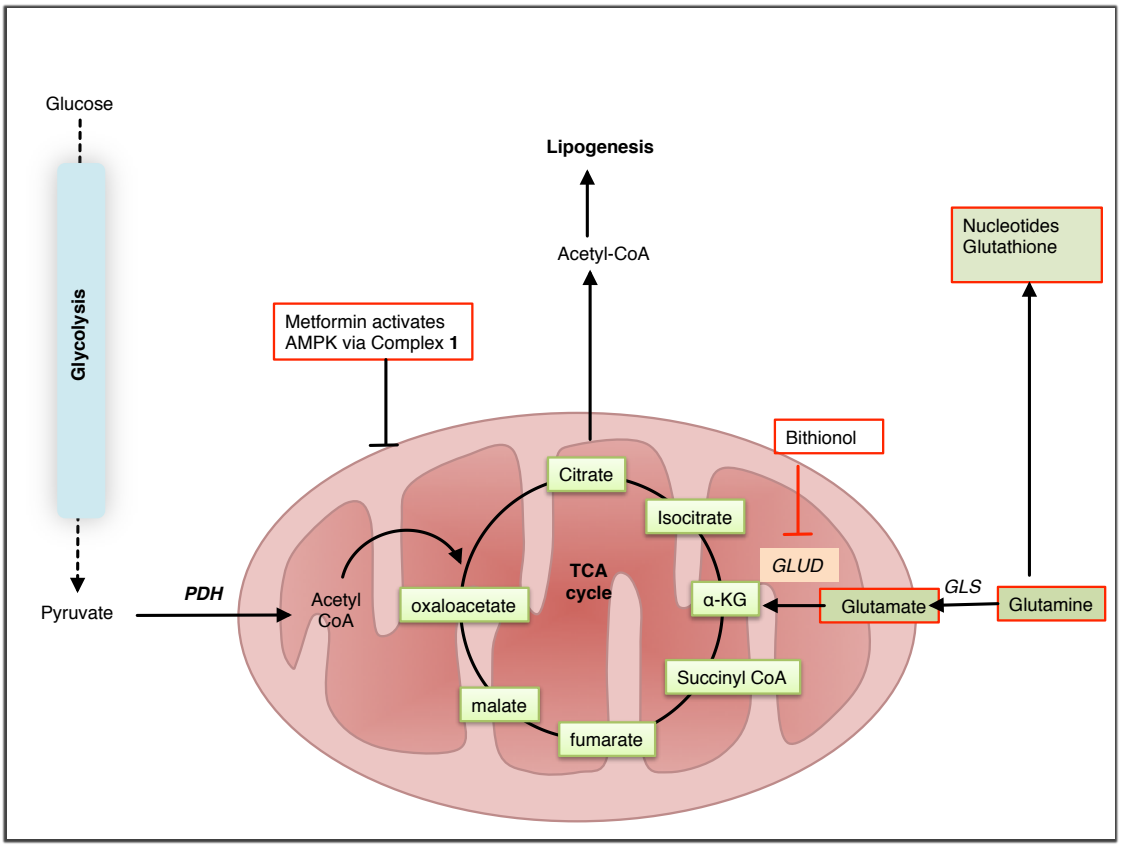

Figure 4.1: Schematic overview of the glutamate, TCA cycle, and the glycolysis pathway. GLS- glutaminase, GLUD- glutamate dehydrogenase, PDH- pyruvate dehydrogenase, TCA- tricarboxylic acid cycle. Glutamine is deaminated to glutamate by the glutaminase enzyme, which further is dehydrogenated to α ketoglutarate, GLUD enzyme is inhibited by BT, which will affect the TCA cycle.

4.2: BT reduces mitochondrial respiration

In order to investigate the effects of GLUD1 inhibition on oxidative phosphorylation, we used the Seahorse™ bioscience XF24-3 extracellular flux analyser to measure the oxygen consumption rates (OCR). This assay measures the rate changes of O_2 and pH in the medium surrounding the adherent cells

cultured in the analyser microplates using optical fluorescent sensors. The cyquant assay was used to standardize the OCR based on the proliferation count. In both MDA MB 231 and MCF 7 cells the dose response curve for OCR was measured using increasing concentration of BT (0.5μM- 20μM).

The baseline OCR was higher in MCF 7 (120±12pMoles/min/cyquant vs 65±10.5pMoles/min/cyquant, respectively). BT increased the OCR at concentrations of <2μM, and reduced the basal OCR at drug concentrations of above 2μM. The effects of BT >2μM on OCR were in a dose dependent manner in both the cell lines, with significant decline of OCR from concentrations of 5μM of BT (Figure 4.2).

The Seahorse assay uses the mitochondrial stress test to gain an insight into cellular bioenergetics and mechanism of mitochondrial toxicity. In the stress test, cells are exposed sequentially to Oligomycin (ATP synthase inhibitor), FCCP (protonophoric uncoupler), and rotenone and antimycin A (electron transport inhibitors). This provides information on basal respiration, proton leak, maximum respiration rate, and non-mitochondrial respiration.

A

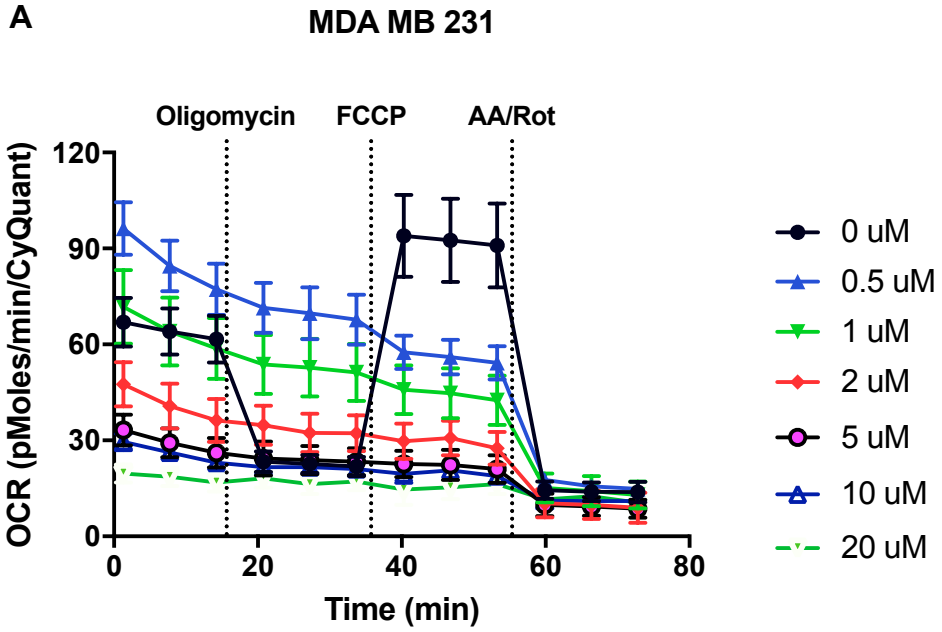
MDA MB 231
Oligomycin
FCCP
AA/Rot
OCR (pMoles/min/CyQuant)
120
90
60
30
0
0
20
40
60
80
Time (min)
0 uM
0.5 uM
1 uM
2 uM
5 uM
10 uM
20 uM

B

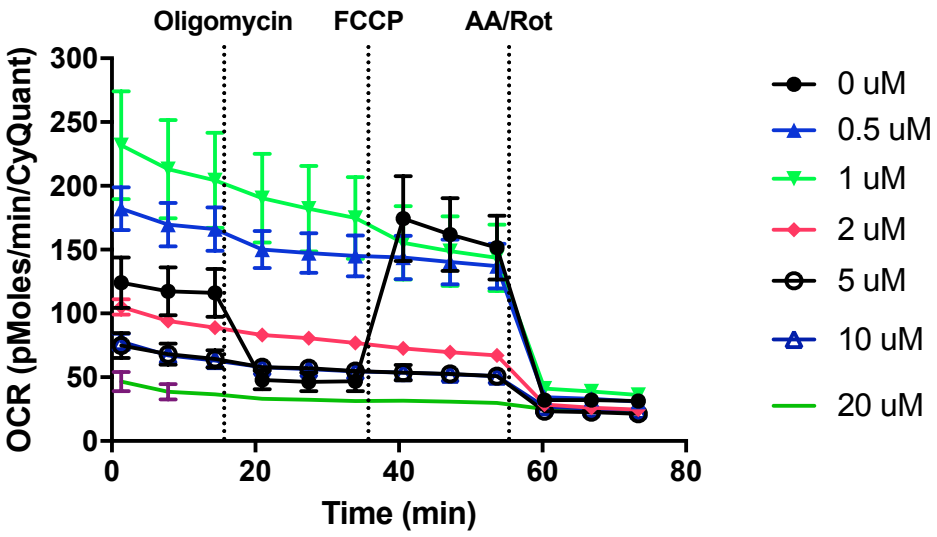
MCF7
Oligomycin
FCCP
AA/Rot
OCR (pMoles/min/CyQuant)
300
250
200
150
100
50
0
0
20
40
60
80
Time (min)
0 uM
0.5 uM
1 uM
2 uM
5 uM
10 uM
20 uM

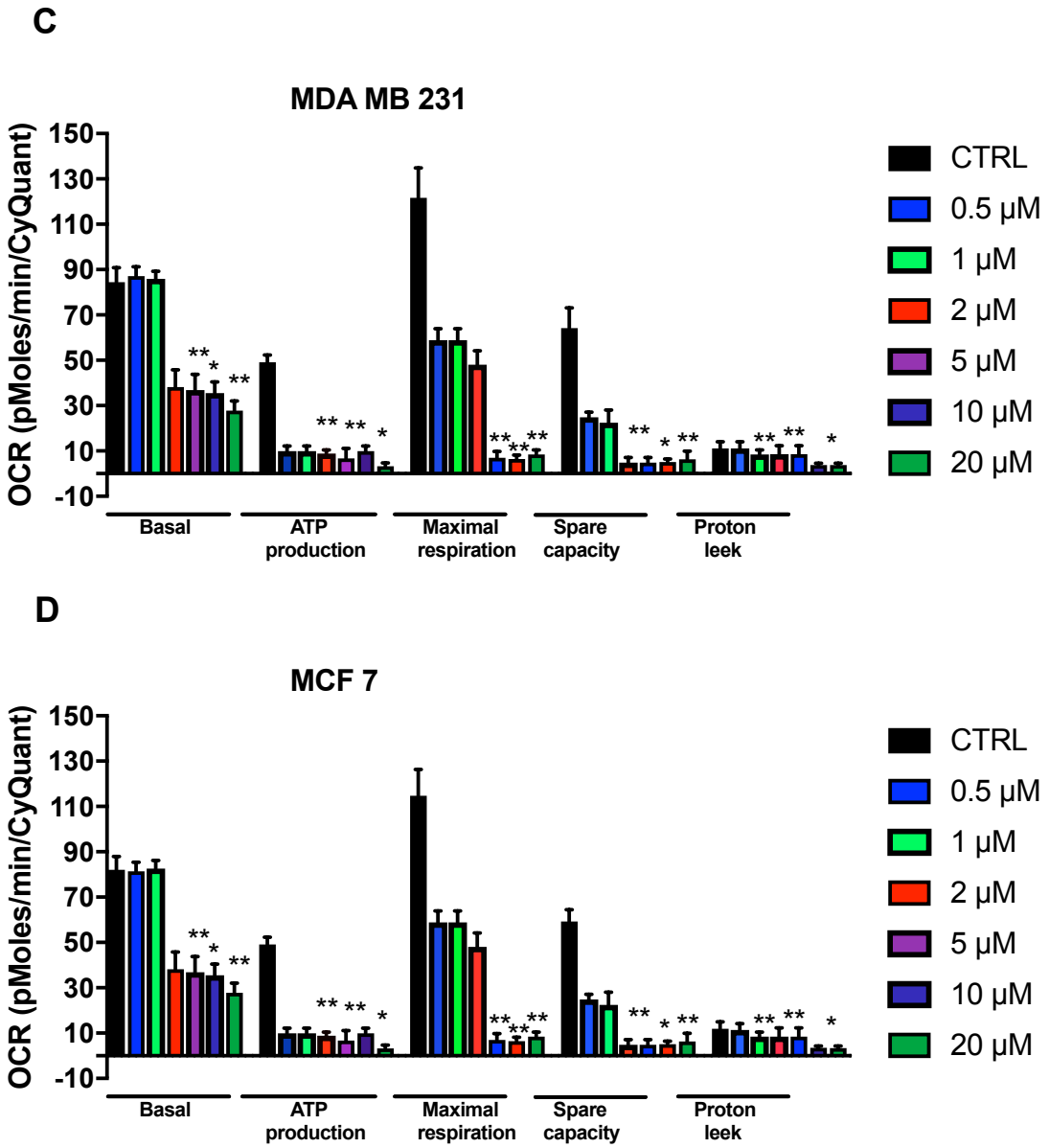

Figure 4.2A & B: Effect of BT on oxygen consumption in and MDA MB 231 (**A**) cells and MCF 7 (**B**) in a dose dependent manner. The rate of Oxygen consumption rate (OCR) was measured in real-time with the XF24 Extracellular flux analyzer (Seahorse Biosciences) (**C & D)**: Different mitochondrial parameters from the same experiment. The first parameter is the basal respiration, followed by addition of Oligomycin b, which blocks the ATP synthase, and OCR correlates with ATP production; FCCP is an uncoupler of oxidative phosphorylation and depolarizes the mitochondrial membrane, hence maximal respiration can be measured, Rotenone (complex I inhibitor) and Antimycin A (complex III) are mitochondrial toxin, addition of which shuts mitochondrial respiration allowing measurement of non-mitochondrial respiration (superoxide production or proton leak). Data shown are mean ± SEM ***p<0.001, **p<0.01, *p<0.05.

4.3: GLUD1 knockdown inhibits mitochondrial respiration

To determine the role of GLUD1 on mitochondrial metabolism, we examined the effect of siRNA targeting GLUD1 gene on MDA MB231 cell line. Commercially available siRNA pools (combination of 4 individual sequences) for GLUD1 were used (Dharmacon) and their activity and GLUD1 specificity confirmed in a reverse transfection experiment with MDA MB 231 cells. GLUD1 knockdown cells showed a decrease in the OCR in MDA MB231 transfected cells (Figure. 4.3). There was a simultaneous decrease in ATP production in the GLUD1 knockdown cells. These results were similar to the effects seen with BT on MDA MB 231 cell lines. Oxygen consumption is a direct measure of electron transport chain activity, and we observed a 40% decrease in the oxygen consumption in the GLUD1 knockdown cells.

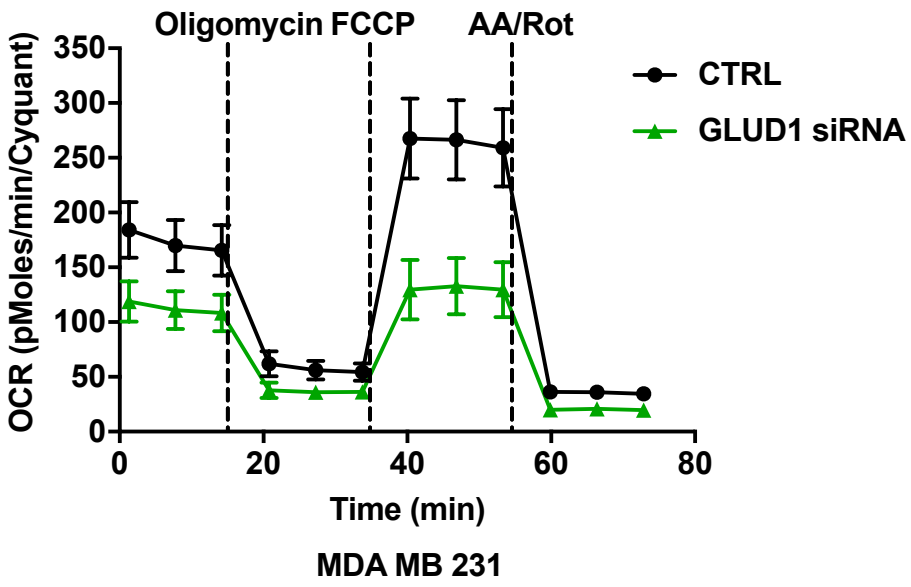

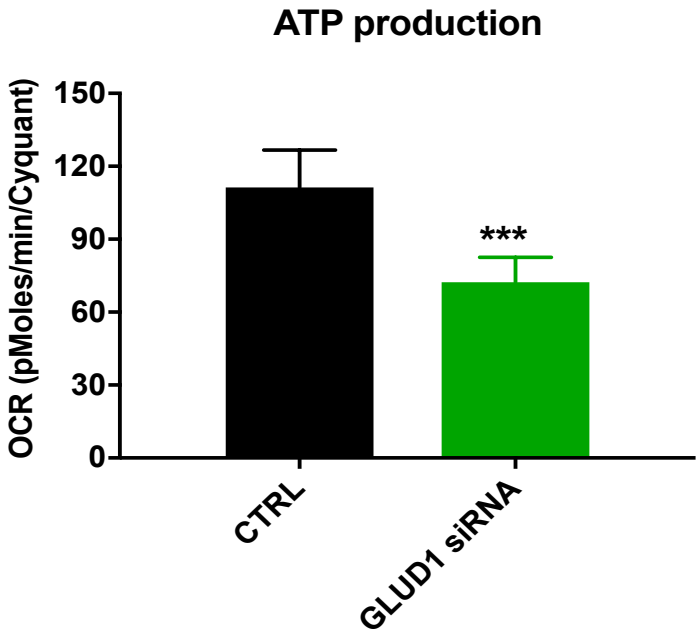

Figure 4.3: GLUD1 siRNA effects on OCR and ATP production in MDA MB 231 cell line. (Control- Scramble si RNA)

4.4: BT triggers autophagy

Preliminary observations with BT treated cells showed a profound increase in vacuolization of MCF 7 and MDAMB 231 cell lines (Figure 4.4.1A). These cell lines were treated with 10μMby electron microscopy. BT induced autophagosome and autolysosome formation. The mitochondria were vacuolated and had a distorted architecture, which implied they underwent mitophagy.

The increased formation of autophagosomes was probably from the mitochondria, as a large number of mitochondria showed pigmented and elongated lysosomal like bodies (Figure 4.4.1B & C). Mitochondria also appeared to be of denser, vacuolated and altered shape.

To investigate the effects of BT on the lysosomes, Immunofluorescent images of the cells treated with and without BT were stained with Lysotracker and analysed by Image J software. Lysotracker red counts showed increased amounts of lysosomes in BT treated MCF 7 and MDA MB231 cell lines l (Figure 4.4.2 A &B). Lysosomal positioning is influenced by starvation or change in nutrient supply (glutamine) and thus controls autophagic flux and impacts autophagosome synthesis(Korolchuk et al., 2011). BT treated cells had increased LC3II flux on western blots. LC3II flux was also increased in GLUD1 knockdown cells (Figure 4.4.2C). Participation of lysosomes in NF-kB degradation was seen in both BT treated and GLUD1 knockdown MDA MB 231 cells, as seen on the Western blots.

A

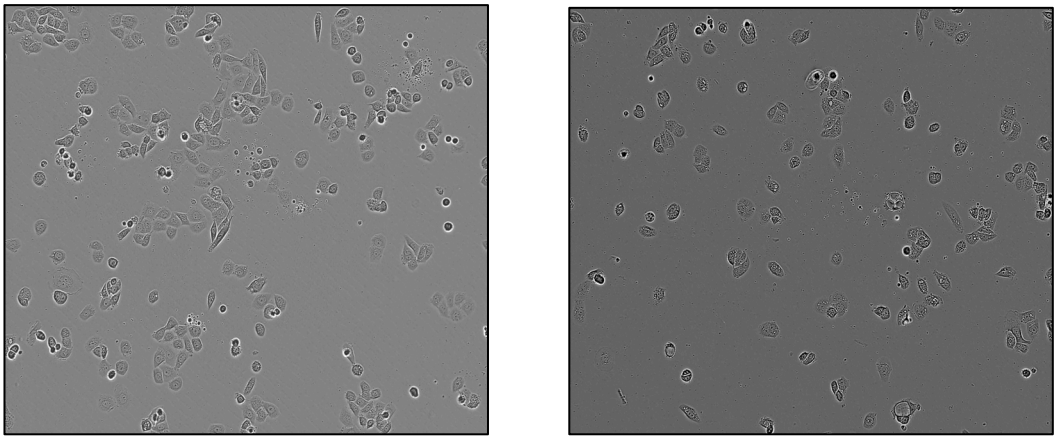

Control BT 10µM

B

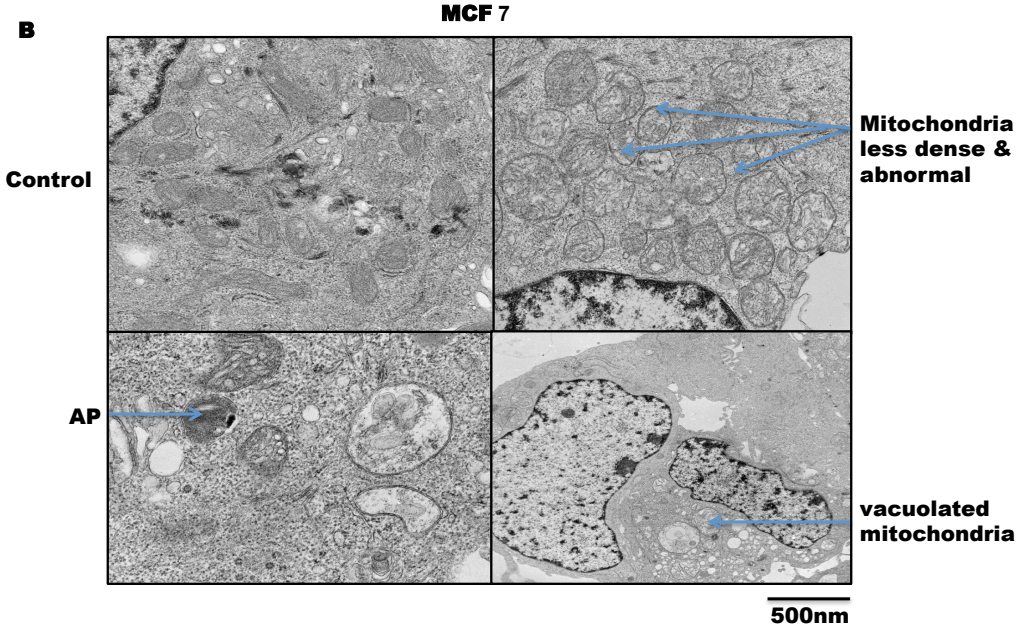

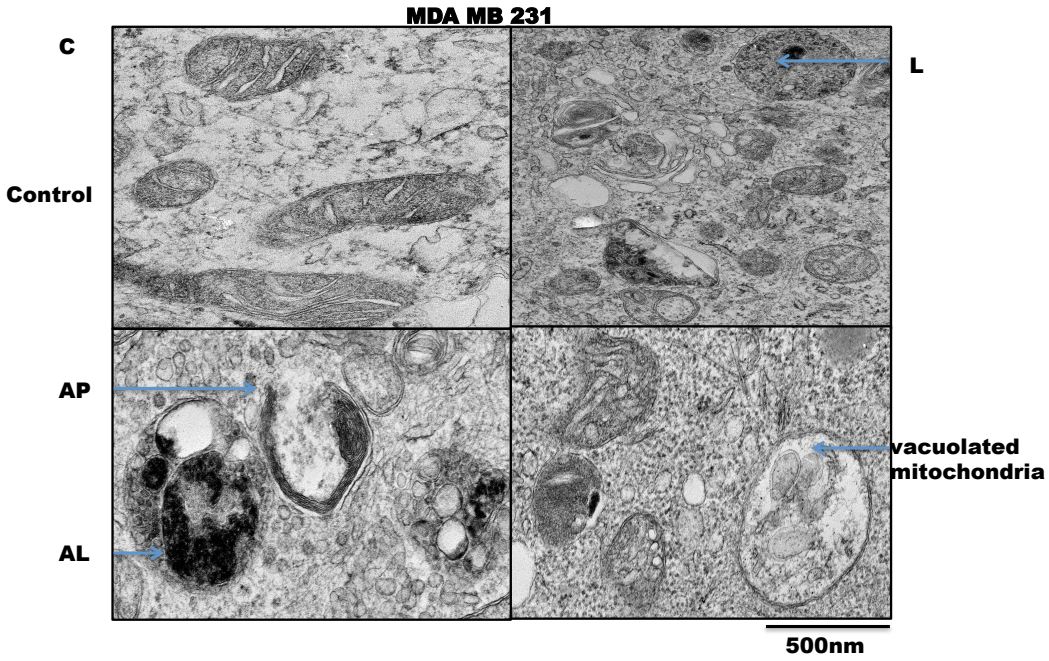

Figure 4.4.1: Effect of BT on mitochondrial morphology. (A) Phase contrast images show increased vacuolization in MDA MB 231 and MCF 7 cells treated with 10µM BT for 24 hours.
(B & C) Electron micrograph of MCF 7 & MDA MB 231 cells treated with 10µM BT for 24 hours. Showing numerous autophagosome (AP), autolysosome (AL), and mitophagy (MP), and vacuolated mitochondria, scale- 500nm

A

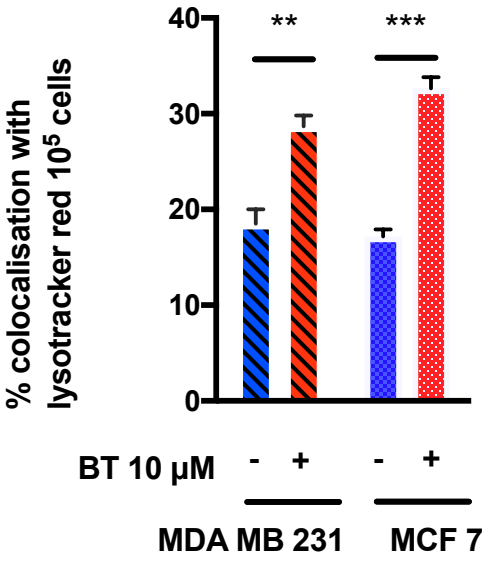

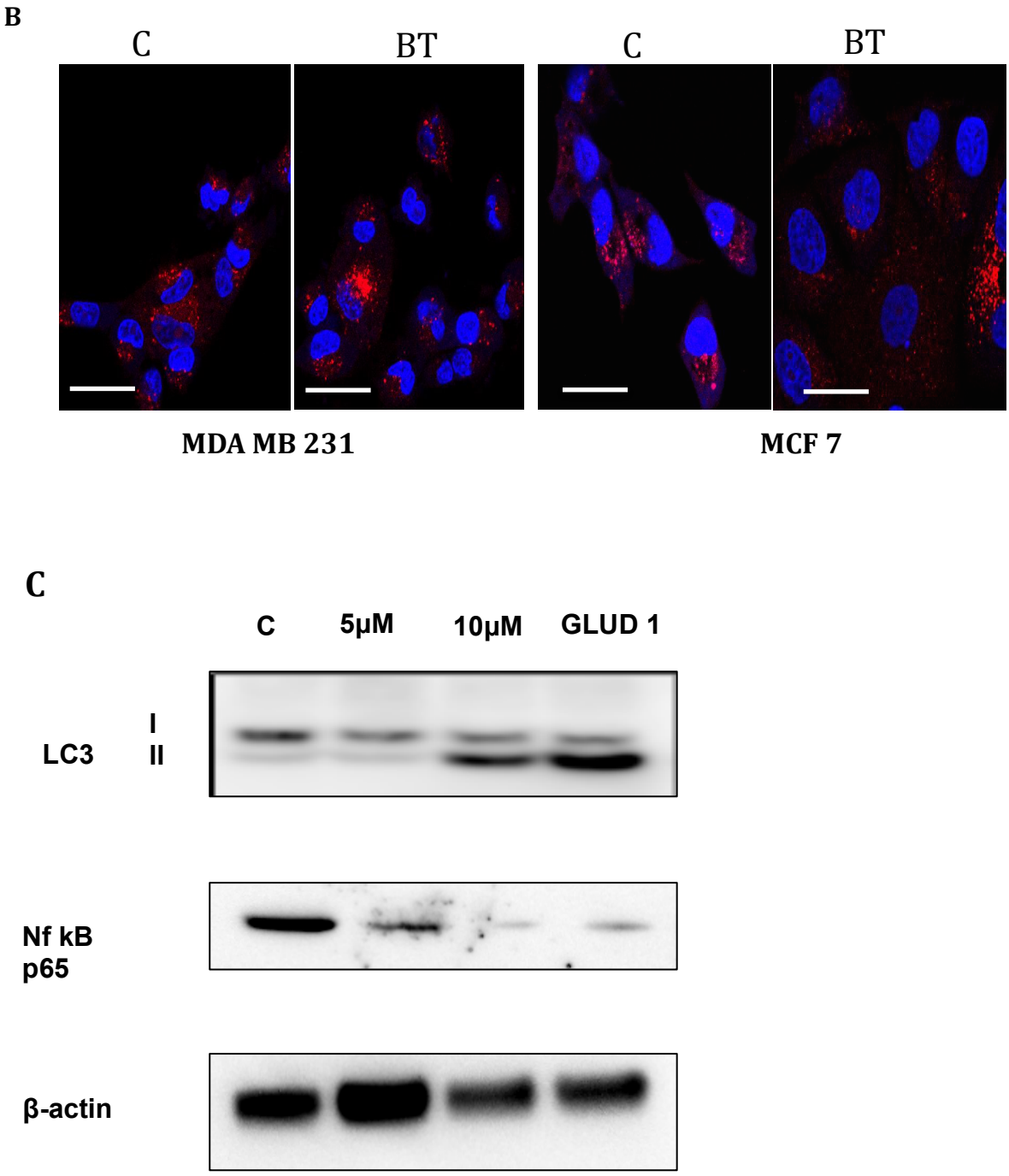

Figure 4.4.2: BT triggers autophagic response. (A-B) Impact of BT on acidification of vacuoles in MCF 7 and MDA MB 231 cell lines, using fluorescence microscopy to determine the colocalisation of BT treated cell lines with LysoTracker red, a fluorescent dye which labels acidified compartments (magnification 1000x). (C) Western blot analysis showing LC3B I & II and Nf kB p65 expression upon treatment with BT and in GLUD1 si RNA knockdown in MDA MB 231 cell line, n=4. (Control- Scramble si RNA)

4.5: BT affects TCA metabolites through increased transamination

To gain insights into the metabolite changes that occur with GLUD1 inhibition, we treated MDA MB 231 cell lines with 10μM of BT for 24 hours. Liquid chromatography- Mass Spectrometry (LC-MS) revealed changes in several metabolites. In BT treated cells, we observed increased levels of TCA cycle metabolites, amongst which there was abundance of α-KG (α-ketoglutarate), fumarate, succinate, fumarate and citrate (Figure 4.5A). Contrary to our expectation, in BT treated cells; we saw significantly lower levels of glutamate. Another striking result amongst amino acids was the, increased abundance of aspartate and decreased levels of serine (Figure 4.5C). Previous studies demonstrated a crucial role of aspartate biosynthesis in proliferating cells(Pusapati et al., 2016, Birsoy et al., 2015) so this increase is unlikely to be relevant to the antiproliferative effects. Reduced levels of glutamate and increased levels of aspartate signified increased transamination leading to increased TCA intermediates. This was further confirmed by use of a transaminase inhibitor AOA, which increasing synthetic lethality in combination with lower doses of BT (Figure 3.7).

As expected in cells with defective oxidative phosphorylation BT treated cells had increased glucose and lactate levels, indicating a shift towards glycolysis (Figure 4.5B).

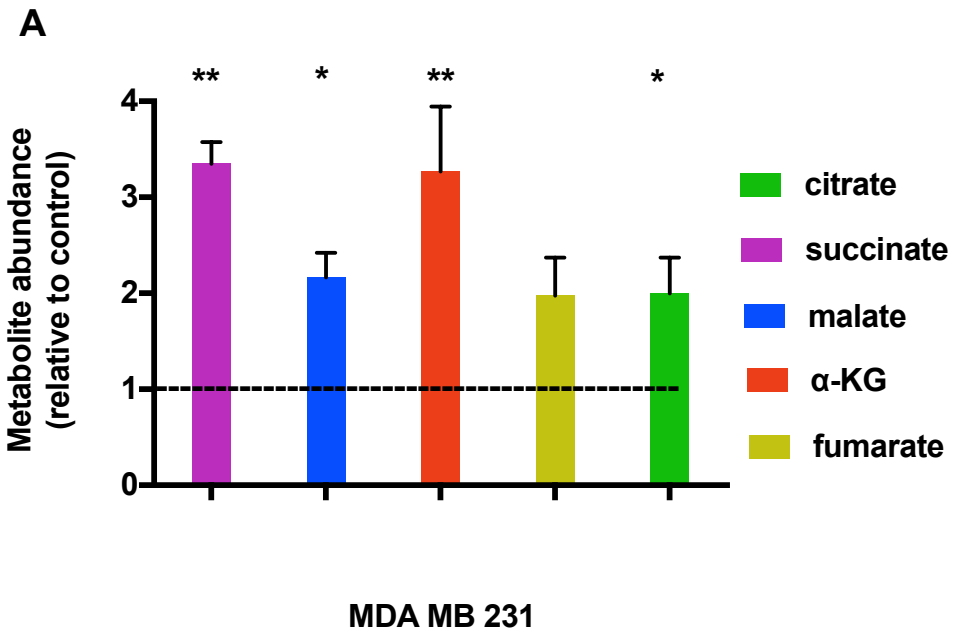
A
**
*
**
*
Metabolite abundance
(relative to control)
4
3
2
1
0
citrate
succinate
malate
α-KG
fumarate
MDA MB 231

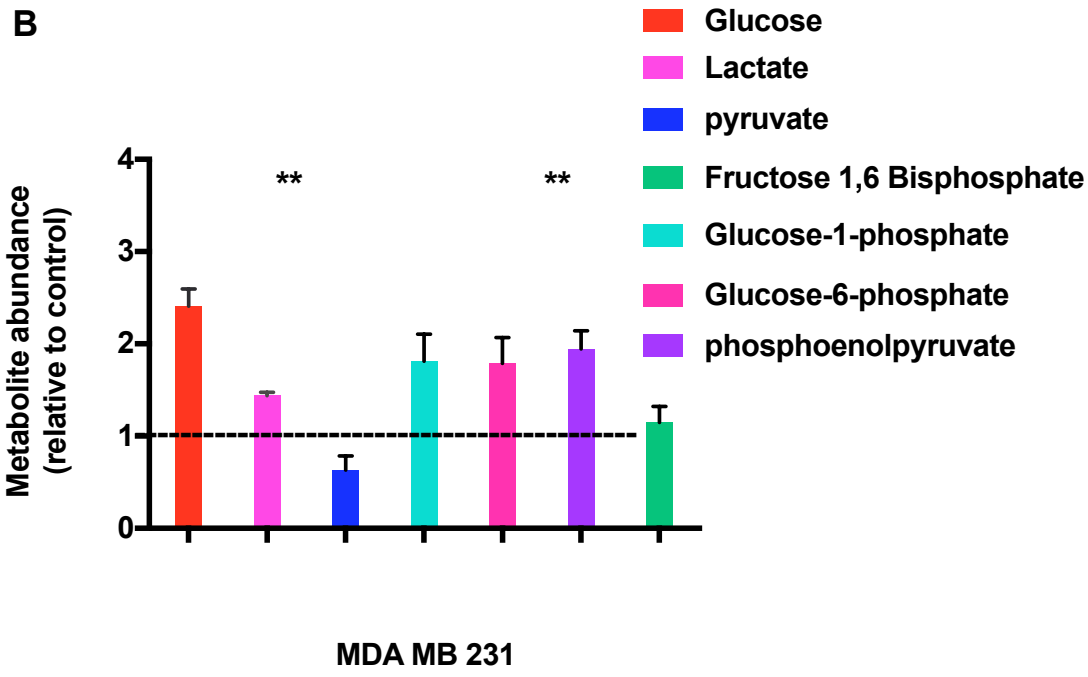
B
Glucose
Lactate
pyruvate
Fructose 1,6 Bisphosphate
Glucose-1-phosphate
Glucose-6-phosphate
phosphoenolpyruvate
**
**
Metabolite abundance
(relative to control)
4
3
2
1
0
MDA MB 231

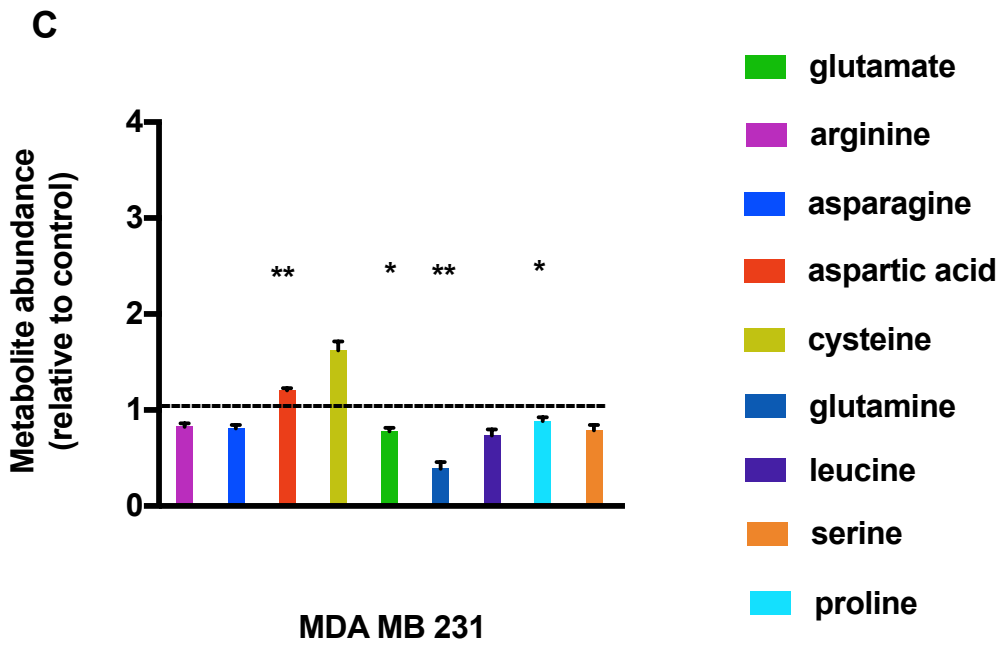

Figure 4.5: Effect of BT on TCA cycle, glycolysis and Amino acid metabolites- Quantitative liquid chromatography- mass spectrometry (LC-MS) analysis of the experiment with MDA MB 231 cell line exposed to BT 10μM over 24 hours. Measuring changes in (A) TCA cycle, (B) Glycolysis and (C) Amino acid concentrations. Data shown are mean ± SEM ***p<0.001, **p<0.01, *p<0.05.

4.6: GLUD1 inhibition increases ROS levels

ROS are formed as by-products of mitochondrial oxidative phosphorylation, (Shigenaga et al., 1994, Turrens, 2003, Zorov et al., 2006). Changes in the ROS levels signify an alteration in the redox state of the tissues. Formation of mitochondrial ROS was assayed using the MitoSOX red (Molecular Probes) a fluorogenic dye that selectively enters the mitochondria and fluoresces upon oxidation by superoxide. ROS was measured by Flow cytometry (FACS). Cells were seeded in 6 well plates and treated with BT 5μM for 24 hours, with H_2O_2 and MnTMPyP (a cell-permeable superoxide dismutase (SOD) mimetic) as controls. Cells were analysed in a FACS analyzer Cyan ADP (using the PE channel). Four different cell lines, MCF 7 & T47D

(ER+) and MDA MB 231 & HCC1806 (ER-) were tested. All four cell lines showed an increase in ROS production as compared to controls, suggesting that the effects on free radicals is caused by defective electron respiratory chain. H_2O_2 increased the ROS levels, whereas MnTMPyP treatments lead to reduced ROS levels (Figure 4.6A). In order to confirm if the effect of mitochondrial ROS production is affected by GLUD1 we measured the ROS levels in si RNA knockdown MDA MB 231 cells. The ROS production in MDA MB 231 was increased in the GLUDI knockdown cells to the same extent as with BT (Figure 4.6C).

A

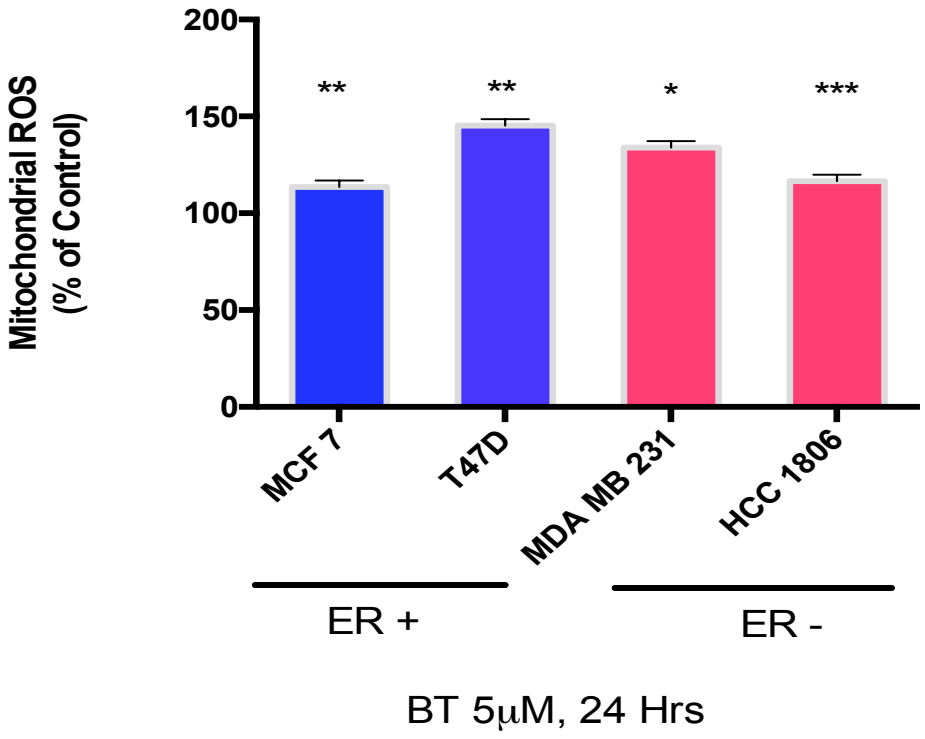

BT 5μM, 24 Hrs

B

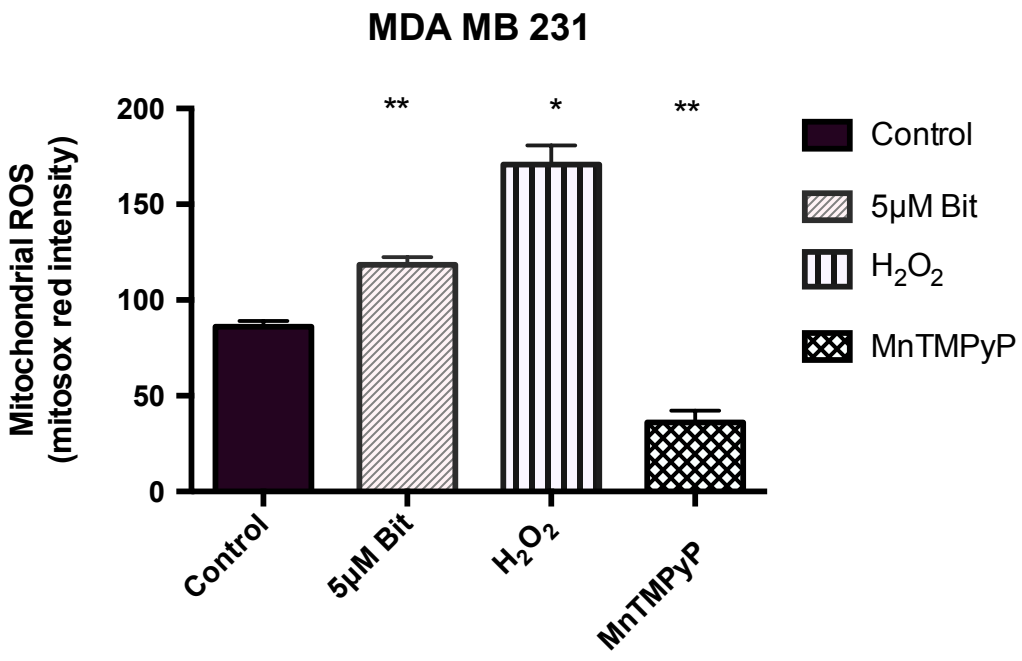

BT 5μM, 24 Hrs

C

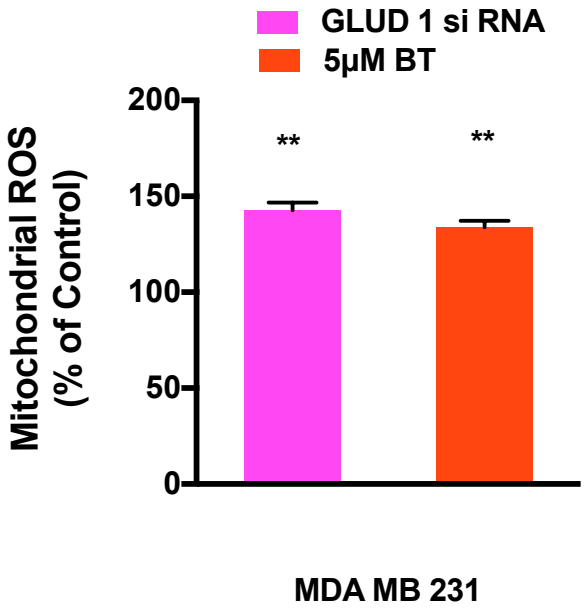

4.6-A: Effect of BT 5μM on mitochondrial ROS production in MCF 7, T47D, MDA MB 231 AND HCC 1806 on 24 hours treatment. **B:** Mitochondrial ROS measured in MDA MB 231 with BT 5μM treatment and H_2O_2 and MnTMPyP as controls. **C:** Effect of BT and GLUD1 siRNA on mitochondrial ROS production. n=3, Data shown are mean ± SEM ***p<0.001, **p<0.01, *p<0.05. (Control- Scramble si RNA)

4.7: BT decreases glutathione

Glutathione (L-γ-glutamyl-L-cysteinyl-glycine, GSH) is synthesized from glutamine, cysteine and glycine (Schulz et al., 2000, Circu and Aw, 2008); hence any metabolic alteration of these metabolites can affect GSH synthesis. The key role of glutathione is in participation in the cell defense against products of oxidative stress. Glutathione is a low molecular antioxidant, which takes part in non-enzymatic antioxidant defense, by working as an efficient scavenger of free radicals(Winterbourn, 1993). By measuring the glutathione levels in MDA MB231 and MCF 7 cell lines treated with BT 10μM for 24 hours it was observed that BT treatment significantly reduced the glutathione levels in both the cancer cell lines (MDA MB 231: 24 vs 18, p<0.01, and MCF7: 31 vs 19, p<0.001, control vs BT treated, respectively, moles/10^6cells)(Figure

4.7). This reduction in glutathione levels in BT treated cells, suggested that GLUD1 is essential for redox homeostasis and hence crucial for maintaining cell viability.

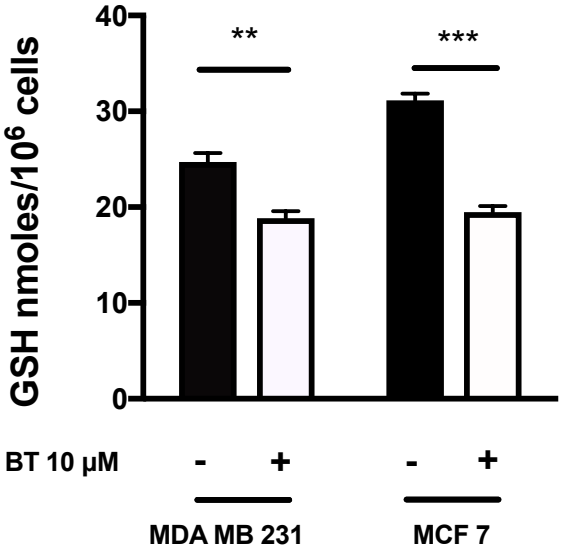

Figure 4.7: MCF 7 and MDA MB 231 cells were treated with BT 10µM for 24 hours and GSH levels were measure by HPLC, n=3, Data shown are mean ± SEM ***p<0.001, **p<0.01, *p<0.05.

4.8: BT inhibits nucleotide synthesis

Nucleotides are the building blocks of DNA and they are an essential requirement to maintain genomic integrity. It is well known that nucleotide pool alteration are linked to mitochondrial disorders and cancer(Aye et al., 2015). Glutamate is an important donor for nucleotide synthesis (Figure 4.8.1-2). Whereas carbon from glutamine is required for amino acid synthesis, the nitrogen contributes to the purines and pyrimidines synthesis(Lane and Fan, 2015). The key role of glutamine in nucleotide synthesis is also evident from the fact that, transformed cells display delayed transit through S phase in glutamine deprived conditions(Gaglio et al., 2009, Ardawi et al., 1989).

Having established the effects of GLUD1 inhibition on the TCA and amino acid pathways, it was necessary to understand the effects of BT on the nitrogen pathway. Upon treatment with BT, there was significant depletion of nucleotides with a compensatory increase of dGTP (Figure 4.8.2A-C). GTP is a potent inhibitor of the oxidative deamination of glutamate and the increase in GTP levels in our results is probably due to a compensatory phenomenon(Dieter et al., 1981). The failure of cells to maintain the nucleotide pools, is detrimental to their survival and leads to DNA breaks, mutagenesis and cell death.

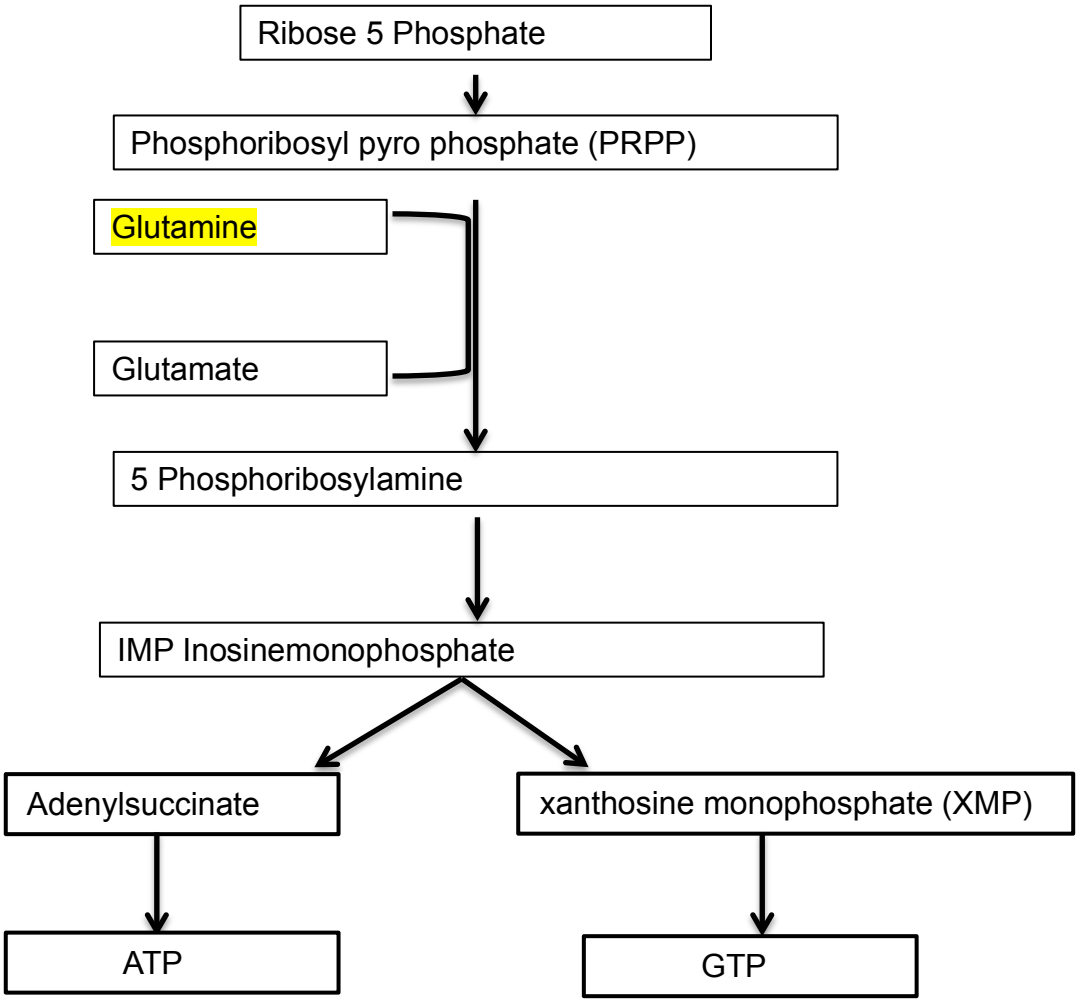

Figure 4.8.1: Role of glutamine in nucleotide synthesis (Purine synthesis)

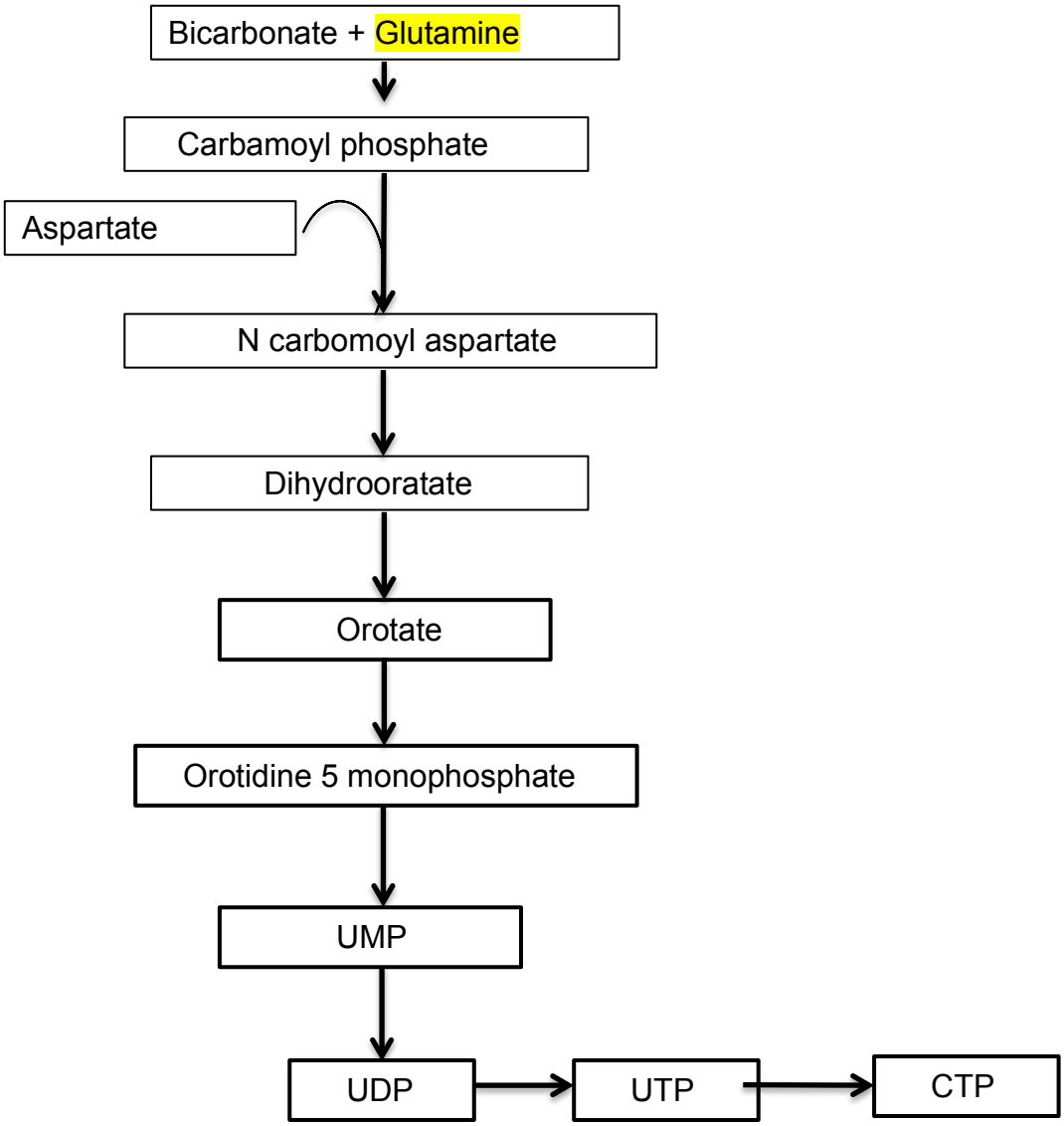

Figure 4.8.2: Role of glutamine in nucleotide synthesis (Purine synthesis)

A

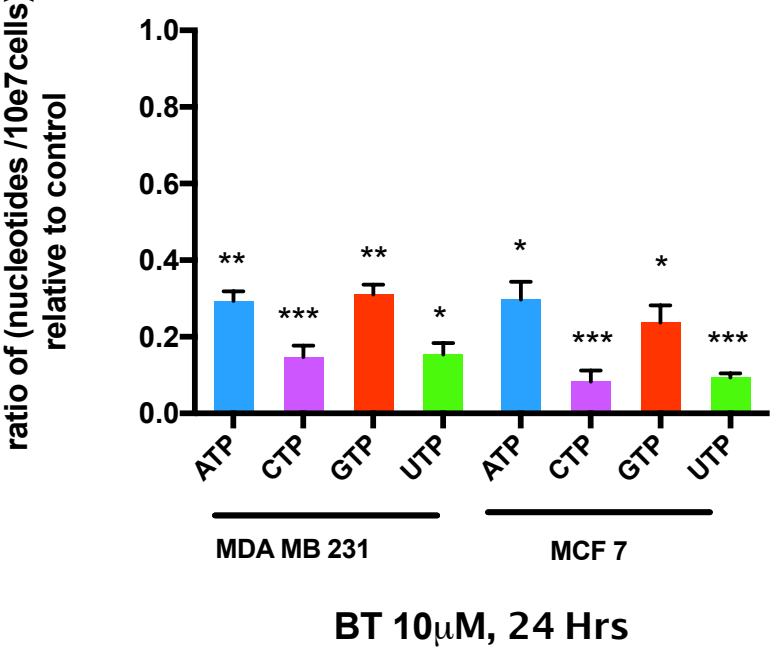

BT 10μM, 24 Hrs

B

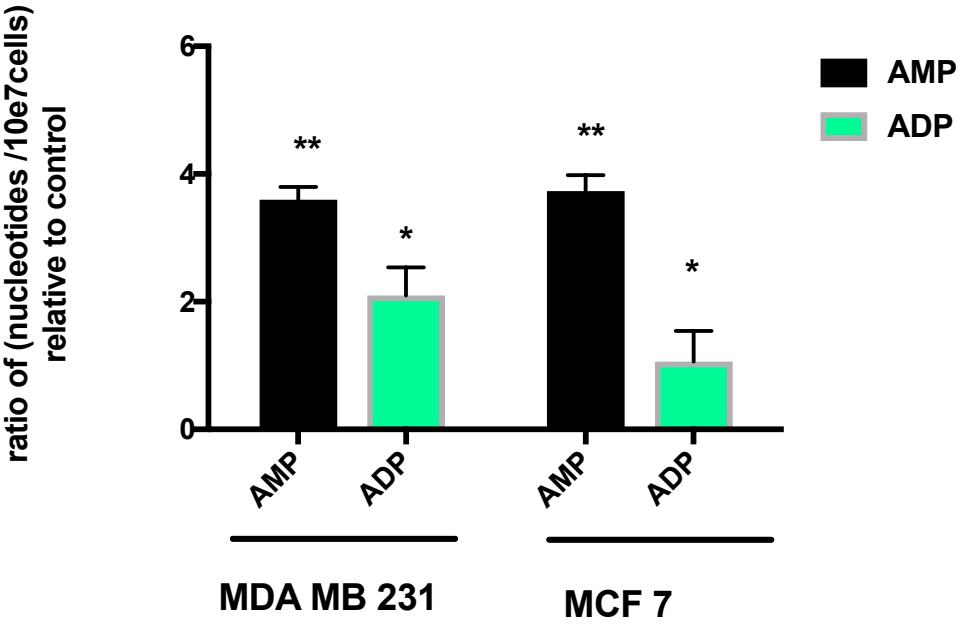

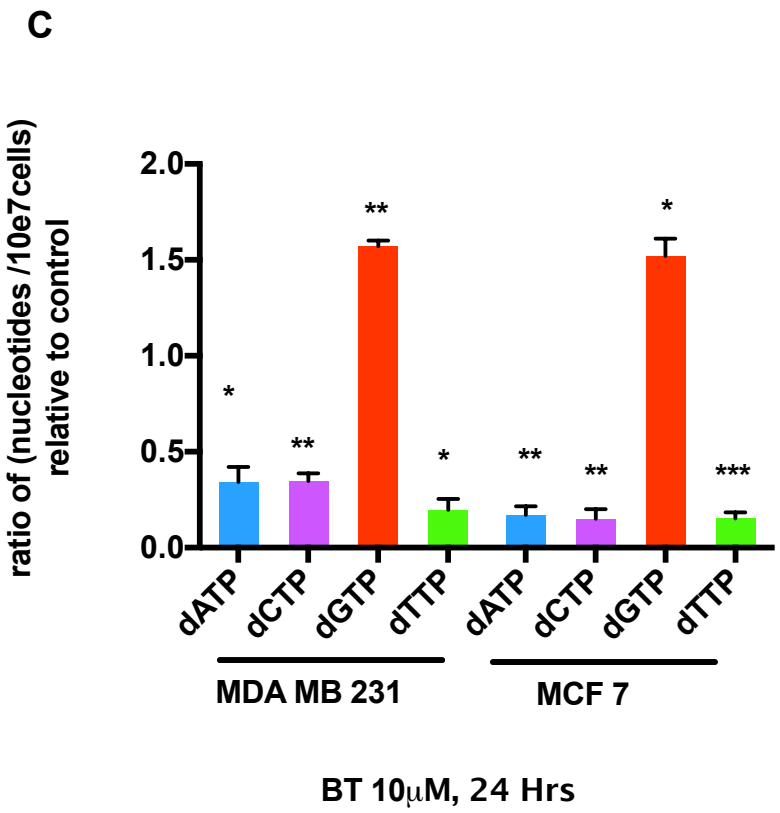

Figure 4.8.2 A-C: Relative levels of triphosphates, monophosphates and deoxynucleotides respectively in BT 10μM treated MCF 7 AND MDA MB 231 cell lines as compared to untreated cell lines, over 24Hrs, n=3, Data shown are mean ± SEM ***p<0.001, **p<0.01, *p<0.05.

4.9: Discussion

Bithionol caused an inhibition of oxygen consumption in both MDA MB-231 and MCF 7 cells, furthermore BT also showed a massive autophagic response with structural changes in mitochondria. GLUD1 knockdown showed similar effects on mitochondrial oxygen consumption, suggesting a role for GLUD1 in mitochondrial metabolism. BT also impaired ATP production in both the cell lines.

The effects on GLUD1 inhibition on lysosomal protein disruption were unexpectedly profound both in vitro and in vivo. A 50kDa protein previously isolated from lysosomal membrane was postulated to be GLUD. This protein accounted for the association of lysosomes to microtubules and microtubule- lysosomal interaction(Mithieux and Rousset, 1989). Thus BT by degrading GLUD may affect the positioning of mitochondria and lysosomes, and contribute to cytotoxicity of this drug(Rajapakshe et al., 2015).

Tumour cells are known to induce anti-oxidant mechanisms to set a novel homeostatic equilibrium, and increases in ROS levels can damage this equilibrium(Anastasiou et al., 2011, Cairns et al., 2011, DeNicola et al., 2011). By raising the ROS levels, BT targets the redox balance maintained by mitochondria in tumour cells and works as an important anti tumour strategy (Figure 4.9.1). This increase in ROS leads to free radial induced mitochondrial damage and increased mitophagy. Importantly, targeting of GLUD1, results in glutathione depletion, decreased nucleotide synthesis, and increased levels of ROS, all of which can contribute to mitochondrial damage and inhibition of cell proliferation.

Lysosome associated membrane proteins (LAMP) comprise the major protein components of the lysosomal membrane(Carlsson et al., 1988, Chen et al., 1985). The

LAMP proteins LAMP-1 and 2 play an important function of positioning of lysosomes and mitochondria(Rajapakshe et al., 2015).

NF-kB has been identified as a physiological regulator of mitochondrial respiration and has a significant role in adaptation in cell metabolism(Mauro et al., 2011). In addition NF-kB is also a substrate, which is activated when the lysosomal pathway of proteolysis is activated(Cuervo et al., 1998). Consistent with this association of NF-kB and lysosomal metabolism we observed a strong link between GLUD1 inhibition and lysosomal pathway activation.

Our findings suggest a remarkable degree of coordinated interaction between the glutamine and the Kreb cycle, with the co-regulation furnishes not only glutamine but also aspartate for the synthesis of Kreb cycle intermediates.

Glutamine feeds carbon to the Krebs cycle via the mitochondria as 2-oxoglutarate, either through the glutamic oxaloacetate transaminases or GLUD enzymes.

We were surprised by the observed increase levels of aspartate in the BT treated cells, and can speculate that this is due to increased activity of the transamination (Figure 4.9.2).

Taken together, these data indicate that exposure of MDA MB 231 cells to AOA (transaminase inhibitor) and BT inhibits tricarboxylic acid pathway, and in turn affects the mitochondrial metabolism, which leads to cytostatic effects of these drugs.

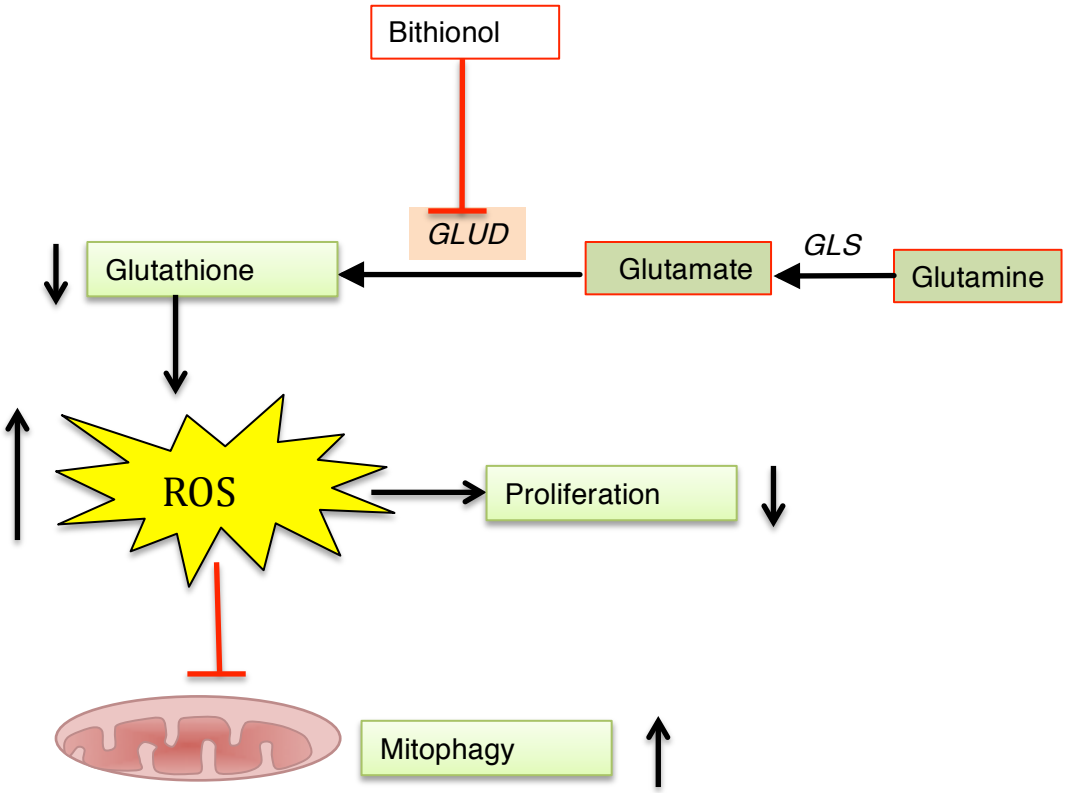

Figure 4.9.1: Schematic detailing aspects of the Glutamine- Redox working model. GLUD inhibition results in reduced glutathione levels, which in turn results in increased ROS levels and cell growth arrest. Increased free radicals, lead to increased mitophagy.

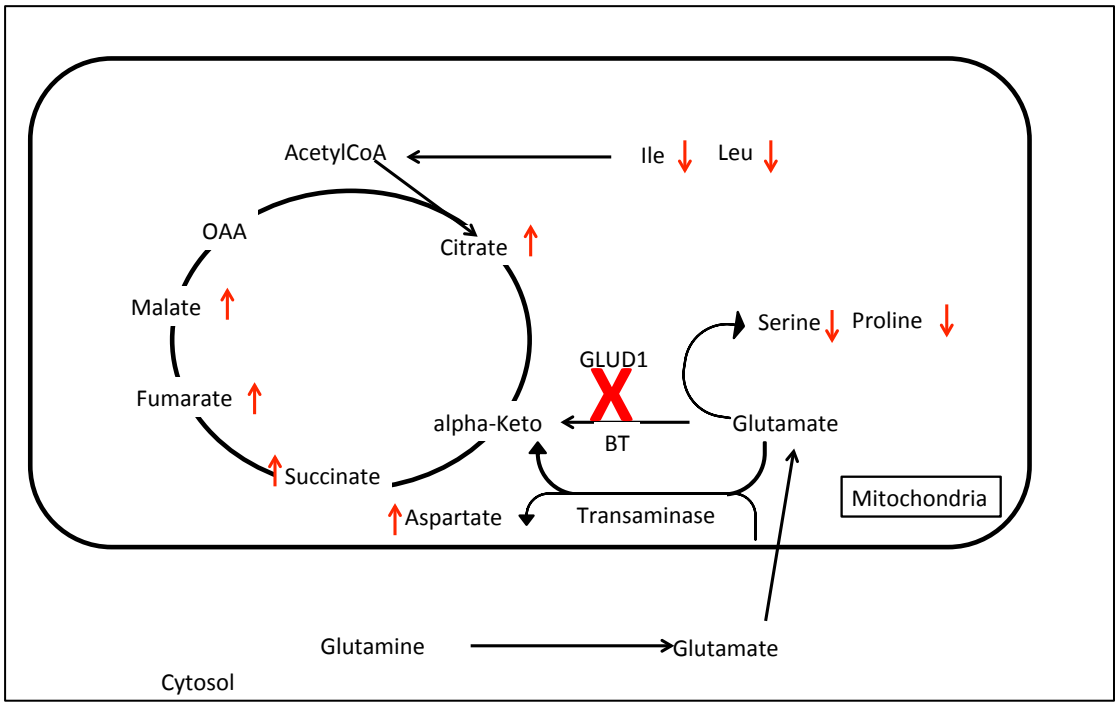

Figure 4.9.2: Schematic detailing aspects of the Glutamine/ TCA cycle pathway that regulate mitochondrial metabolism. Up side arrows represent increase in metabolites and down going arrows represent decrease in the levels of metabolites.

CHAPTER 5: Discussion

5.1 Overview

Our group had previously shown the importance of glutamine as a carbon source in metformin treated breast cancer cells and this raised the possibility of potential synergy between metformin and other agents that more specifically modulated glutamine metabolism. After a literature search to identify potential drugs that would inhibit different steps of the glutaminolysis and reductive carboxylation pathways, we investigated the effects of BT on breast cancer cell lines.

In this thesis the GLUD inhibitor BT was shown to inhibit cell growth in cell lines of different subtypes of breast cancer. It was also shown that BT induces autophagy as a means of inducing cell death. The preliminary data from this study indicates that this drug affects mitochondrial oxygen consumption in both estrogen positive and negative breast cancer cell lines.

Hence the overall aims of the of this DPhil project were met:

1. To study the role of GLUD1 inhibition on the glutamine pathway, and its effect on mitochondrial metabolism
2. To investigate the consequences of GLUD1 inhibition on cell line growth in vitro.
3. To investigate the consequences of GLUD1 inhibition on tumour growth in vivo
4. To investigate the pharmacokinetics of BT
5. To investigate potential synergistic strategies for enhancing the effectiveness of BT.

The work on this thesis has improved our understanding about role of GLUD1 in glutamine metabolism.

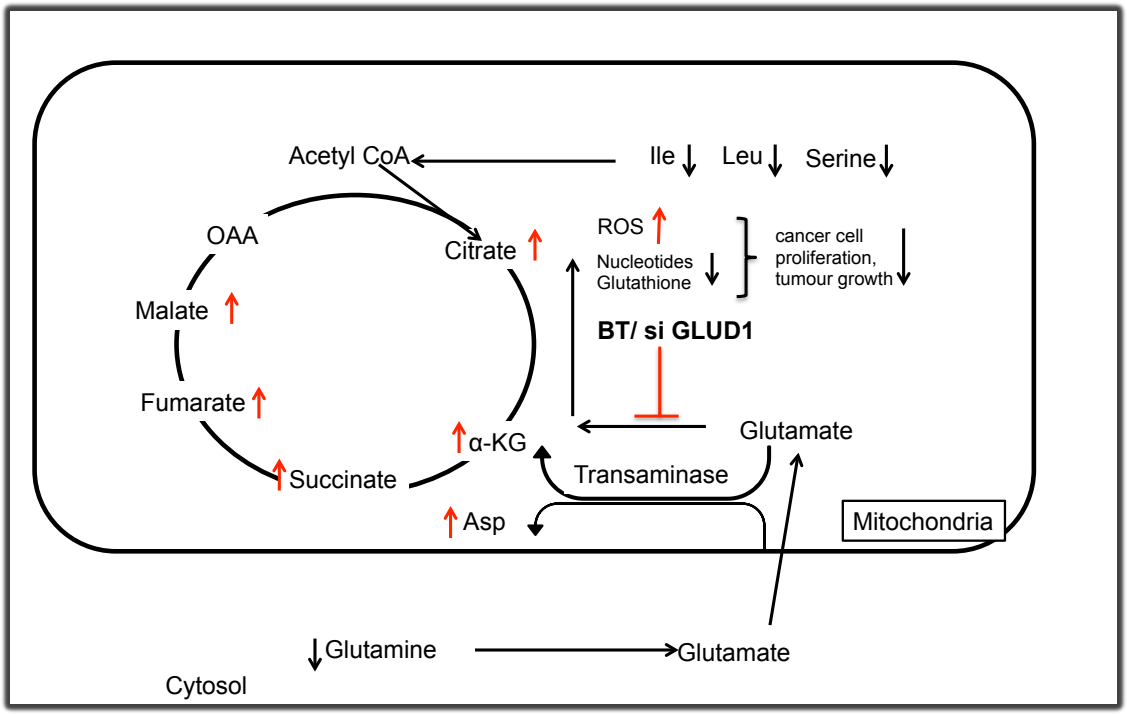

Figure 5.1- Schematic representation of the effects of BT and GLUD1 inhibition on the mitochondrial metabolism and cancer cell proliferation. α-KG- α-ketoglutarate, OAA- oxaloacetate, Ile-isoleucine, Leu- leucine, ROS- reactive oxygen species, Asp-aspartate. ⬇Black arrows – reduced level, red arrows- increase levels of metabolites.

5.2: Targeting glutamine metabolism by GLUD1 inhibition should be pursued as a treatment strategy

In chapter 3, the data presented showed that by inhibiting GLUD1, BT had profound effects on the proliferation of the breast cancer cell lines. This reduced proliferation also resulted in impaired mitochondria function and inhibition of oxidative phosphorylation. BT's effects on mitochondria were associated with increase in ROS levels (Figure 5.1), which could have significant consequences on tumour growth, and increasing cytotoxicity. BT also attenuated glutathione levels, with resultant effects on the redox homeostasis. It was also observed that BT increased the levels of α-ketoglutarate, succinate, malate, and citrate and resulted in reduced levels of glutamine, serine and leucine (Figure 5.1). The fact that the level of aspartate increased suggested activation of an alternate pathway to feed the TCA cycle metabolites. Such metabolic adaptation has been seen in cells with activation of the transaminase enzyme, in pancreatic cancer the glutamine derived aspartate is transported into the cytoplasm where it can be converted into oxaloacetate by glutamate-aspartate transaminase(Son et al., 2013, Gaglio et al., 2011). In addition, treatment with AOA a transaminase inhibitor resulted in an additive antiproliferative effect. A growing number of studies have shown that cancer cells prefer the transaminase pathway to GLUD in some tumour contexts(Son et al., 2013, Coloff et al., 2016). Activation of the transaminase pathway is potentially an important rescue pathway. This observation is of particular interest in future research with a combination of a GLUD1 and transaminase inhibitor to increase cancer cell death.

Mitochondrial reserve capacity is vital in maintaining normal cell functioning, and in periods of oxidative stress or metabolic instability, depletion of this capacity can eventually be lethal(Kingsley-Hickman et al., 1990, Hill et al., 2009). The data presented in chapter 4 showed that GLUD1 inhibition resulted in reduced oxidative phosphorylation. However, at a lower dose (<2μM) BT stimulated oxidative phosphorylation, indicating a uncoupling effect.

The metabolic fate of glutamine is highly dependent on the two key enzymes of GLS and GLUD. Significance of glutaminase inhibition as a therapeutic agent in anticancer activity in breast cancer has been published previously, most recently being a study of CB-839 a glutaminase inhibitor as anti-proliferative effect in triple negative breast cancer(Gross et al., 2014, Gao et al., 2009).

The two important nutrients utilized by cancer cells grown in culture are glucose and glutamine(Vander Heiden et al., 2009). GLUD1 inhibition by Bithionol, resulted in increased reliance of the cells on glucose, hence when 2-DG was combined with BT, there was significant further inhibition of cell proliferation. This deprivation of tumour bioenergetics by the dual inhibition of energy pathways may be a novel therapeutic approach for cancer therapy. Similar effects have previously been reported with 2 DG and metformin(Cheong et al., 2011). This data suggests that defective glutaminolysis with GLUD1 inhibition, makes cells further rely on glucose for their survival.

Lysosome associated membrane proteins (LAMP) comprise the major protein components of the lysosomal membrane(Carlsson et al., 1988, Chen et al., 1985). The LAMP proteins LAMP-1 and 2 play an important function of positioning of

lysosomes and mitochondria(Rajapakshe et al., 2015). The effects of GLUD1 inhibition on lysosomal protein disruption were unexpectedly profound both in vitro and in vivo. A 50kDa protein previously isolated from lysosomal membrane was postulated to be GLUD. This protein had an ATP dependent microtubule activity and also accounted for the association of lysosomes with microtubules and microtubule-lysosomal interaction(Mithieux and Rousset, 1989, Rajas et al., 1996). Thus BT by degrading GLUD may affect the positioning of mitochondria and lysosomes, and contribute to cytotoxicity of this drug(Rajapakshe et al., 2015). The data presented in this study, has shown that by inhibiting LAMP1, BT disrupted the lysosomal activity and this in turn increased autophagy. This effect of GLUD1 inhibition has not been noted before. It could signify that GLUD1 has different functions besides enzyme activity. There is increasing evidence that upon nutrient deprivation, there is an increase in the catabolic processes, and autophagy is one of them(Knecht et al., 2009). Autophagy is extremely sensitive to levels of amino acids, growth factors, cytokines, hormones and insulin(Esteban et al., 2007). There is clear evidence of glucose regulating autophagy, and in this thesis we have shown that in conditions of glutamine depletion there is increased evidence of autophagy and mitophagy(Moruno et al., 2012, Moruno-Manchon et al., 2013). However, it is still unclear, whether autophagy is a defensive or a suicidal phenomenon.

Previously, it has been reported that cancer cells often have much smaller, fragmented mitochondria as compared to normal cells(Rehman et al., 2012). BT treated cells showed various abnormal shaped mitochondria, which were eliminated by either mitophagy or were further encapsulated by the lysosomes to form autophago-

lysosomes. This dysfunctional mitochondrial would have consumed more ATP, and generate harmful ROS, thus contributing to cytotoxicity(Gomes and Scorrano, 2013).

In this thesis, we show a novel effect of an antimetabolism drug-targeted degradation of GLUD protein, to a similar level achievable with siRNA. This specific depletion was also achieved in vivo at non-toxic levels and could be a potential biomarker of drug effects and tissue penetration in Phase I or window studies.

The in vivo activity of BT was clearly seen in the xenograft tumour mouse models. Although the initial dose of 70mg/kg/day did not show much of an antitumour effect, the GLUD1 inhibition was clearly demonstrated on immunohistochemistry on the tumour specimens. Increasing the dose of BT to 100mg/kg/day on 5 days on and 2 days off regime, showed significant tumour growth suppression as compared to the control mice, with minimal toxicity.

In in-vitro experiments, BT showed a very high plasma protein binding, with < 2% free drug after spiking control plasma with 2 mM bithionol, which explains its increased activity at a higher dose. These results suggest that BT works by GLUD1 inhibition with encouraging antiproliferative outcomes in cancer and negligible toxicity both in vivo and in vitro.

GLUD1 influence encompasses much of the mitochondrial function, through the diversity of its proven targets. However, a substantial number of its targets which include- effects on lysosomal proteins, NFkB inhibition, autophagy, still need to be confirmed and their physiological significance needs to be established.

5.3: Future directions

The data presented in the chapters 3 and 4 of this study underscore the point that glutamine metabolism is a key pathway that is altered following metabolic reprogramming. Inhibition of GLUD1 results in glutamine accumulation, which then enters the Krebs cycle via transamination. Furthermore, combination of a transaminase inhibitor (AOA) and GLUD1 inhibitor (Bithionol), showed increased synthetic lethality on the cancer cells. This should be confirmed in vivo.

Finally, it will also be important to develop our own GLUD1 inhibitors, similar in pharmacokinetics and use a similar route of testing as demonstrated in this study. Interestingly, not much research has been done in drugs affecting GLUD1 pathway and this is a good opportunity to maximize the potential of this pathway and developing a compound for rapid effective anti cancer efficacy. This information, combined with a strong induction of autophagy and apoptosis, reinforces the central role of glutamine in the metabolism of breast cancer. In summary, this project has generated a great deal of interest in the role of GLUD1 in both using in vitro and in vivo models of breast cancer.

6: References

1998. Intensive blood-glucose control with sulphonylureas or insulin compared with conventional treatment and risk of complications in patients with type 2 diabetes (UKPDS 33). UK Prospective Diabetes Study (UKPDS) Group. *Lancet,* 352**,** 837-53.

ACIN-PEREZ, R., GATTI, D. L., BAI, Y. & MANFREDI, G. 2011. Protein phosphorylation and prevention of cytochrome oxidase inhibition by ATP: coupled mechanisms of energy metabolism regulation. *Cell Metab,* 13**,** 712-9.

AHN, C. S. & METALLO, C. M. 2015. Mitochondria as biosynthetic factories for cancer proliferation. *Cancer Metab,* 3**,** 1.

ALLEN, R. W., ENZIE, F. D. & SAMSON, K. S. 1962. The effects of bithionol and other compounds on the fringed tapeworm, Thysanosoma actinioides, of sheep. *Am J Vet Res,* 23**,** 236-40.

ANASTASIOU, D., POULOGIANNIS, G., ASARA, J. M., BOXER, M. B., JIANG, J. K., SHEN, M., BELLINGER, G., SASAKI, A. T., LOCASALE, J. W., AULD, D. S., THOMAS, C. J., VANDER HEIDEN, M. G. & CANTLEY, L. C. 2011. Inhibition of pyruvate kinase M2 by reactive oxygen species contributes to cellular antioxidant responses. *Science,* 334**,** 1278-83.

ANSO, E., MULLEN, A. R., FELSHER, D. W., MATES, J. M., DEBERARDINIS, R. J. & CHANDEL, N. S. 2013. Metabolic changes in cancer cells upon suppression of MYC. *Cancer Metab,* 1**,** 7.

ARDAWI, M. S., MAJZOUB, M. F., MASOUD, I. M. & NEWSHOLME, E. A. 1989. Enzymic and metabolic adaptations in the gastrocnemius, plantaris and soleus muscles of hypocaloric rats. *Biochem J,* 261**,** 219-25.

AYE, Y., LI, M., LONG, M. J. & WEISS, R. S. 2015. Ribonucleotide reductase and cancer: biological mechanisms and targeted therapies. *Oncogene,* 34**,** 2011-21.

AYYAGARI, V. N. & BRARD, L. 2014. Bithionol inhibits ovarian cancer cell growth in vitro - studies on mechanism(s) of action. *BMC Cancer,* 14**,** 61.

BACQ, Y., BESNIER, J. M., DUONG, T. H., PAVIE, G., METMAN, E. H. & CHOUTET, P. 1991. Successful treatment of acute fascioliasis with bithionol. *Hepatology,* 14**,** 1066-9.

BALDERAMOS, M., ANKATI, H., AKUBATHINI, S. K., PATEL, A. V., KAMILA, S., MUKHERJEE, C., WANG, L., BIEHL, E. R. & D'MELLO, S. R. 2008. Synthesis and structure-activity relationship studies of 3-substituted indolin-2-ones as effective neuroprotective agents. *Exp Biol Med (Maywood),* 233**,** 1395-402.

BANERJEE, S., SCHMIDT, T., FANG, J., STANLEY, C. A. & SMITH, T. J. 2003. Structural studies on ADP activation of mammalian glutamate dehydrogenase and the evolution of regulation. *Biochemistry,* 42**,** 3446-56.

BASSIOUNY, H. K., SOLIMAN, N. K., EL-DALY, S. M. & BADR, N. M. 1991. Human fascioliasis in Egypt: effect of infection and efficacy of bithionol treatment. *J Trop Med Hyg,* 94**,** 333-7.

BERGSTROM, J., FURST, P., NOREE, L. O. & VINNARS, E. 1974. Intracellular free amino acid concentration in human muscle tissue. *J Appl Physiol,* 36**,** 693-7.

BIRSOY, K., WANG, T., CHEN, W. W., FREINKMAN, E., ABU-REMAILEH, M. & SABATINI, D. M. 2015. An Essential Role of the Mitochondrial Electron Transport Chain in Cell Proliferation Is to Enable Aspartate Synthesis. *Cell,* 162**,** 540-51.

BOROMPOKAS, N., PAPACHATZAKI, M. M., KANAVOURAS, K., MASTORODEMOS, V., ZAGANAS, I., SPANAKI, C. & PLAITAKIS, A. 2010. Estrogen modification of human glutamate dehydrogenases is linked to enzyme activation state. *J Biol Chem,* 285**,** 31380-7.

BOZA, J. J., MOENNOZ, D., BOURNOT, C. E., BLUM, S., ZBINDEN, I., FINOT, P. A. & BALLEVRE, O. 2000. Role of glutamine on the de novo purine nucleotide synthesis in Caco-2 cells. *Eur J Nutr,* 39**,** 38-46.

BRADDOCK, D. T. 2010. Autotaxin and lipid signaling pathways as anticancer targets. *Curr Opin Investig Drugs,* 11**,** 629-37.

CAIRNS, R. A., HARRIS, I. S. & MAK, T. W. 2011. Regulation of cancer cell metabolism. *Nat Rev Cancer,* 11**,** 85-95.

CARLSSON, S. R., ROTH, J., PILLER, F. & FUKUDA, M. 1988. Isolation and characterization of human lysosomal membrane glycoproteins, h-lamp-1 and h-lamp-2. Major sialoglycoproteins carrying polylactosaminoglycan. *J Biol Chem,* 263**,** 18911-9.

CHAKRABARTI, G., MOORE, Z. R., LUO, X., ILCHEVA, M., ALI, A., PADANAD, M., ZHOU, Y., XIE, Y., BURMA, S., SCAGLIONI, P. P., CANTLEY, L. C., DEBERARDINIS, R. J., KIMMELMAN, A. C., LYSSIOTIS, C. A. & BOOTHMAN, D. A. 2015. Targeting glutamine metabolism sensitizes pancreatic cancer to PARP-driven metabolic catastrophe induced by ss-lapachone. *Cancer Metab,* 3**,** 12.

CHATGILIALOGLU, C. & O'NEILL, P. 2001. Free radicals associated with DNA damage. *Exp Gerontol,* 36**,** 1459-71.

CHEN, J. W., PAN, W., D'SOUZA, M. P. & AUGUST, J. T. 1985. Lysosome-associated membrane proteins: characterization of LAMP-1 of macrophage P388 and mouse embryo 3T3 cultured cells. *Arch Biochem Biophys,* 239**,** 574-86.

CHEONG, J. H., PARK, E. S., LIANG, J., DENNISON, J. B., TSAVACHIDOU, D., NGUYEN-CHARLES, C., WA CHENG, K., HALL, H., ZHANG, D., LU, Y., RAVOORI, M., KUNDRA, V., AJANI, J., LEE, J. S., KI HONG, W. & MILLS, G. B. 2011. Dual inhibition of tumor energy pathway by 2-deoxyglucose and metformin is effective against a broad spectrum of preclinical cancer models. *Mol Cancer Ther,* 10**,** 2350-62.

CHLEBOWSKI, R. T., MCTIERNAN, A., WACTAWSKI-WENDE, J., MANSON, J. E., ARAGAKI, A. K., ROHAN, T., IPP, E., KAKLAMANI, V. G., VITOLINS, M., WALLACE, R., GUNTER, M., PHILLIPS, L. S., STRICKLER, H., MARGOLIS, K. & EUHUS, D. M. 2012. Diabetes, metformin, and breast cancer in postmenopausal women. *J Clin Oncol,* 30**,** 2844-52.

CHOO, A. Y., KIM, S. G., VANDER HEIDEN, M. G., MAHONEY, S. J., VU, H., YOON, S. O., CANTLEY, L. C. & BLENIS, J. 2010. Glucose addiction of TSC null cells is

caused by failed mTORC1-dependent balancing of metabolic demand with supply. *Mol Cell,* 38**,** 487-99.
CIRCU, M. L. & AW, T. Y. 2008. Glutathione and apoptosis. *Free Radic Res,* 42**,** 689-706.
COLOFF, J. L., MURPHY, J. P., BRAUN, C. R., HARRIS, I. S., SHELTON, L. M., KAMI, K., GYGI, S. P., SELFORS, L. M. & BRUGGE, J. S. 2016. Differential Glutamate Metabolism in Proliferating and Quiescent Mammary Epithelial Cells. *Cell Metab,* 23**,** 867-80.
CORY, J. G. & CORY, A. H. 2006. Critical roles of glutamine as nitrogen donors in purine and pyrimidine nucleotide synthesis: asparaginase treatment in childhood acute lymphoblastic leukemia. *In Vivo,* 20**,** 587-9.
CSIBI, A., FENDT, S. M., LI, C., POULOGIANNIS, G., CHOO, A. Y., CHAPSKI, D. J., JEONG, S. M., DEMPSEY, J. M., PARKHITKO, A., MORRISON, T., HENSKE, E. P., HAIGIS, M. C., CANTLEY, L. C., STEPHANOPOULOS, G., YU, J. & BLENIS, J. 2013. The mTORC1 pathway stimulates glutamine metabolism and cell proliferation by repressing SIRT4. *Cell,* 153**,** 840-54.
CSIBI, A., LEE, G., YOON, S. O., TONG, H., ILTER, D., ELIA, I., FENDT, S. M., ROBERTS, T. M. & BLENIS, J. 2014. The mTORC1/S6K1 pathway regulates glutamine metabolism through the eIF4B-dependent control of c-Myc translation. *Curr Biol,* 24**,** 2274-80.
CUERVO, A. M., HU, W., LIM, B. & DICE, J. F. 1998. IkappaB is a substrate for a selective pathway of lysosomal proteolysis. *Mol Biol Cell,* 9**,** 1995-2010.
DEBERARDINIS, R. J. & CHENG, T. 2010. Q's next: the diverse functions of glutamine in metabolism, cell biology and cancer. *Oncogene,* 29**,** 313-24.
DEBERARDINIS, R. J., LUM, J. J., HATZIVASSILIOU, G. & THOMPSON, C. B. 2008. The biology of cancer: metabolic reprogramming fuels cell growth and proliferation. *Cell Metab,* 7**,** 11-20.
DEBERARDINIS, R. J., MANCUSO, A., DAIKHIN, E., NISSIM, I., YUDKOFF, M., WEHRLI, S. & THOMPSON, C. B. 2007. Beyond aerobic glycolysis: transformed cells can engage in glutamine metabolism that exceeds the requirement for protein and nucleotide synthesis. *Proc Natl Acad Sci U S A,* 104**,** 19345-50.
DECENSI, A., PUNTONI, M., GOODWIN, P., CAZZANIGA, M., GENNARI, A., BONANNI, B. & GANDINI, S. 2010. Metformin and cancer risk in diabetic patients: a systematic review and meta-analysis. *Cancer Prev Res (Phila),* 3**,** 1451-61.
DENICOLA, G. M., KARRETH, F. A., HUMPTON, T. J., GOPINATHAN, A., WEI, C., FRESE, K., MANGAL, D., YU, K. H., YEO, C. J., CALHOUN, E. S., SCRIMIERI, F., WINTER, J. M., HRUBAN, R. H., IACOBUZIO-DONAHUE, C., KERN, S. E., BLAIR, I. A. & TUVESON, D. A. 2011. Oncogene-induced Nrf2 transcription promotes ROS detoxification and tumorigenesis. *Nature,* 475**,** 106-9.
DIETER, H., KOBERSTEIN, R. & SUND, H. 1981. Studies of glutamate dehydrogenase. The interaction of ADP, GTP, and NADPH in complexes with glutamate dehydrogenase. *Eur J Biochem,* 115**,** 217-26.
DROGE, W. 2002. Free radicals in the physiological control of cell function. *Physiol Rev,* 82**,** 47-95.
EAGLE, H. 1955. Nutrition needs of mammalian cells in tissue culture. *Science,* 122**,** 501-14.

ESKELINEN, E. L., SCHMIDT, C. K., NEU, S., WILLENBORG, M., FUERTES, G., SALVADOR, N., TANAKA, Y., LULLMANN-RAUCH, R., HARTMANN, D., HEEREN, J., VON FIGURA, K., KNECHT, E. & SAFTIG, P. 2004. Disturbed cholesterol traffic but normal proteolytic function in LAMP-1/LAMP-2 double-deficient fibroblasts. *Mol Biol Cell,* 15**,** 3132-45.

ESTEBAN, I., AGUADO, C., SANCHEZ, M. & KNECHT, E. 2007. Regulation of various proteolytic pathways by insulin and amino acids in human fibroblasts. *FEBS Lett,* 581**,** 3415-21.

EVANS, J. M., DONNELLY, L. A., EMSLIE-SMITH, A. M., ALESSI, D. R. & MORRIS, A. D. 2005. Metformin and reduced risk of cancer in diabetic patients. *BMJ,* 330**,** 1304-5.

FAHIEN, L. A. & KMIOTEK, E. 1981. Regulation of glutamate dehydrogenase by palmitoyl-coenzyme A. *Arch Biochem Biophys,* 212**,** 247-53.

FAN, J., KAMPHORST, J. J., MATHEW, R., CHUNG, M. K., WHITE, E., SHLOMI, T. & RABINOWITZ, J. D. 2013. Glutamine-driven oxidative phosphorylation is a major ATP source in transformed mammalian cells in both normoxia and hypoxia. *Mol Syst Biol,* 9**,** 712.

FORETZ, M., HEBRARD, S., LECLERC, J., ZARRINPASHNEH, E., SOTY, M., MITHIEUX, G., SAKAMOTO, K., ANDREELLI, F. & VIOLLET, B. 2010. Metformin inhibits hepatic gluconeogenesis in mice independently of the LKB1/AMPK pathway via a decrease in hepatic energy state. *J Clin Invest,* 120**,** 2355-69.

FRANCIOSI, M., LUCISANO, G., LAPICE, E., STRIPPOLI, G. F., PELLEGRINI, F. & NICOLUCCI, A. 2013. Metformin therapy and risk of cancer in patients with type 2 diabetes: systematic review. *PLoS One,* 8**,** e71583.

FREDERICK, J. J., CORNER, T. R. & GERHARDT, P. 1974. Antimicrobial actions of hexachlorophene: inhibition of respiration in Bacillus megaterium. *Antimicrob Agents Chemother,* 6**,** 712-21.

FREZZA, C. & GOTTLIEB, E. 2009. Mitochondria in cancer: not just innocent bystanders. *Semin Cancer Biol,* 19**,** 4-11.

FUNG, M. K. L. & CHAN, G. C. 2017. Drug-induced amino acid deprivation as strategy for cancer therapy. *J Hematol Oncol,* 10**,** 144.

GAGLIO, D., METALLO, C. M., GAMEIRO, P. A., HILLER, K., DANNA, L. S., BALESTRIERI, C., ALBERGHINA, L., STEPHANOPOULOS, G. & CHIARADONNA, F. 2011. Oncogenic K-Ras decouples glucose and glutamine metabolism to support cancer cell growth. *Mol Syst Biol,* 7**,** 523.

GAGLIO, D., SOLDATI, C., VANONI, M., ALBERGHINA, L. & CHIARADONNA, F. 2009. Glutamine deprivation induces abortive s-phase rescued by deoxyribonucleotides in k-ras transformed fibroblasts. *PLoS One,* 4**,** e4715.

GAO, P., TCHERNYSHYOV, I., CHANG, T. C., LEE, Y. S., KITA, K., OCHI, T., ZELLER, K. I., DE MARZO, A. M., VAN EYK, J. E., MENDELL, J. T. & DANG, C. V. 2009. c-Myc suppression of miR-23a/b enhances mitochondrial glutaminase expression and glutamine metabolism. *Nature,* 458**,** 762-5.

GOMES, L. C. & SCORRANO, L. 2013. Mitochondrial morphology in mitophagy and macroautophagy. *Biochim Biophys Acta,* 1833**,** 205-12.

GOULD, B. S., BOSNIAK, M. A., NEIDLEMAN, S. & GATT, S. 1953. Effect of hexachlorophene and related bisphenolic compounds on the

dehydrogenases and cytochrome system of Bacillus subtilis and Escherichia coli. *Arch Biochem Biophys,* 44**,** 284-97.

GRIGORYAN, R. S., PANOSYAN, E. H., SEIBEL, N. L., GAYNON, P. S., AVRAMIS, I. A. & AVRAMIS, V. I. 2004. Changes of amino acid serum levels in pediatric patients with higher-risk acute lymphoblastic leukemia (CCG-1961). *In Vivo,* 18**,** 107-12.

GRIMBLE, G. K. 1993. Essential and conditionally-essential nutrients in clinical nutrition. *Nutr Res Rev,* 6**,** 97-119.

GROSS, M. I., DEMO, S. D., DENNISON, J. B., CHEN, L., CHERNOV-ROGAN, T., GOYAL, B., JANES, J. R., LAIDIG, G. J., LEWIS, E. R., LI, J., MACKINNON, A. L., PARLATI, F., RODRIGUEZ, M. L., SHWONEK, P. J., SJOGREN, E. B., STANTON, T. F., WANG, T., YANG, J., ZHAO, F. & BENNETT, M. K. 2014. Antitumor activity of the glutaminase inhibitor CB-839 in triple-negative breast cancer. *Mol Cancer Ther,* 13**,** 890-901.

GUTH, P. S., RISEY, J., BRINER, W., BLAIR, P., REED, H. T., BRYANT, G., NORRIS, C., HOUSLEY, G. & MILLER, R. 1990. Evaluation of amino-oxyacetic acid as a palliative in tinnitus. *Ann Otol Rhinol Laryngol,* 99**,** 74-9.

GUTMAN, R. A., LIU, J. C., CHENG, J. T. & KUO, C. C. 1969. Radiographic changes accompanying successful therapy of pulmonary paragonimiasis. *Am Rev Respir Dis,* 99**,** 255-60.

HANAHAN, D. & WEINBERG, R. A. 2011. Hallmarks of cancer: the next generation. *Cell,* 144**,** 646-74.

HANKARD, R. G., DARMAUN, D., SAGER, B. K., D'AMORE, D., PARSONS, W. R. & HAYMOND, M. 1995. Response of glutamine metabolism to exogenous glutamine in humans. *Am J Physiol,* 269**,** E663-70.

HARDIE, D. G. 2013. AMPK: a target for drugs and natural products with effects on both diabetes and cancer. *Diabetes,* 62**,** 2164-72.

HARRIS, I. S., TRELOAR, A. E., INOUE, S., SASAKI, M., GORRINI, C., LEE, K. C., YUNG, K. Y., BRENNER, D., KNOBBE-THOMSEN, C. B., COX, M. A., ELIA, A., BERGER, T., CESCON, D. W., ADEOYE, A., BRUSTLE, A., MOLYNEUX, S. D., MASON, J. M., LI, W. Y., YAMAMOTO, K., WAKEHAM, A., BERMAN, H. K., KHOKHA, R., DONE, S. J., KAVANAGH, T. J., LAM, C. W. & MAK, T. W. 2015. Glutathione and thioredoxin antioxidant pathways synergize to drive cancer initiation and progression. *Cancer Cell,* 27**,** 211-22.

HAWK, M. A., MCCALLISTER, C. & SCHAFER, Z. T. 2016. Antioxidant Activity during Tumor Progression: A Necessity for the Survival of Cancer Cells? *Cancers (Basel),* 8.

HENSLEY, C. T., WASTI, A. T. & DEBERARDINIS, R. J. 2013. Glutamine and cancer: cell biology, physiology, and clinical opportunities. *J Clin Invest,* 123**,** 3678-84.

HILL, B. G., DRANKA, B. P., ZOU, L., CHATHAM, J. C. & DARLEY-USMAR, V. M. 2009. Importance of the bioenergetic reserve capacity in response to cardiomyocyte stress induced by 4-hydroxynonenal. *Biochem J,* 424**,** 99-107.

HSU, P. P. & SABATINI, D. M. 2008. Cancer cell metabolism: Warburg and beyond. *Cell,* 134**,** 703-7.

HU, W., ZHANG, C., WU, R., SUN, Y., LEVINE, A. & FENG, Z. 2010. Glutaminase 2, a novel p53 target gene regulating energy metabolism and antioxidant function. *Proc Natl Acad Sci U S A,* 107**,** 7455-60.

HUANG, F., ZHANG, Q., MA, H., LV, Q. & ZHANG, T. 2014. Expression of glutaminase is upregulated in colorectal cancer and of clinical significance. *Int J Clin Exp Pathol,* 7**,** 1093-100.

HUANG, L. J., WANG, L., MA, Y., DURICK, K., PERKINS, G., DEERINCK, T. J., ELLISMAN, M. H. & TAYLOR, S. S. 1999. NH2-Terminal targeting motifs direct dual specificity A-kinase-anchoring protein 1 (D-AKAP1) to either mitochondria or endoplasmic reticulum. *J Cell Biol,* 145**,** 951-9.

HUDSON, R. C. & DANIEL, R. M. 1993. L-glutamate dehydrogenases: distribution, properties and mechanism. *Comp Biochem Physiol B,* 106**,** 767-92.

IVASCU, A. & KUBBIES, M. 2007. Diversity of cell-mediated adhesions in breast cancer spheroids. *Int J Oncol,* 31**,** 1403-13.

IWATSUBO, M. & PANTALONI, D. 1967. [Regulation of the activity of glutamate dehydrogenase by effectors GTP and ADP: study by means of "stopped flow"]. *Bull Soc Chim Biol (Paris),* 49**,** 1563-72.

JANSSEN-HEININGER, Y. M., NOLIN, J. D., HOFFMAN, S. M., VAN DER VELDEN, J. L., TULLY, J. E., LAHUE, K. G., ABDALLA, S. T., CHAPMAN, D. G., REYNAERT, N. L., VAN DER VLIET, A. & ANATHY, V. 2013. Emerging mechanisms of glutathione-dependent chemistry in biology and disease. *J Cell Biochem,* 114**,** 1962-8.

JENSEN, H. A., BUNACIU, R. P., VARNER, J. D. & YEN, A. 2015. GW5074 and PP2 kinase inhibitors implicate nontraditional c-Raf and Lyn function as drivers of retinoic acid-induced maturation. *Cell Signal,* 27**,** 1666-75.

JEONG, S. M., XIAO, C., FINLEY, L. W., LAHUSEN, T., SOUZA, A. L., PIERCE, K., LI, Y. H., WANG, X., LAURENT, G., GERMAN, N. J., XU, X., LI, C., WANG, R. H., LEE, J., CSIBI, A., CERIONE, R., BLENIS, J., CLISH, C. B., KIMMELMAN, A., DENG, C. X. & HAIGIS, M. C. 2013. SIRT4 has tumor-suppressive activity and regulates the cellular metabolic response to DNA damage by inhibiting mitochondrial glutamine metabolism. *Cancer Cell,* 23**,** 450-63.

JIN, L., LI, D., ALESI, G. N., FAN, J., KANG, H. B., LU, Z., BOGGON, T. J., JIN, P., YI, H., WRIGHT, E. R., DUONG, D., SEYFRIED, N. T., EGNATCHIK, R., DEBERARDINIS, R. J., MAGLIOCCA, K. R., HE, C., ARELLANO, M. L., KHOURY, H. J., SHIN, D. M., KHURI, F. R. & KANG, S. 2015. Glutamate dehydrogenase 1 signals through antioxidant glutathione peroxidase 1 to regulate redox homeostasis and tumor growth. *Cancer Cell,* 27**,** 257-70.

JUNGERMANN, E. 1968. Soap bacteriostats. *J Am Oil Chem Soc,* 45**,** 345-50.

KIM, J. B., STEIN, R. & O'HARE, M. J. 2004. Three-dimensional in vitro tissue culture models of breast cancer-- a review. *Breast Cancer Res Treat,* 85**,** 281-91.

KIM, J. S. 1970. Treatment of Paragonimus westermani infections with bithionol. *Am J Trop Med Hyg,* 19**,** 940-2.

KIM, J. W. & DANG, C. V. 2006. Cancer's molecular sweet tooth and the Warburg effect. *Cancer Res,* 66**,** 8927-30.

KIMBROUGH, R. D. & GAINES, T. B. 1971. Hexachlorophene effects on the rat brain: study of high doses by light and electron microscopy. *Arch Environ Health,* 23**,** 114-8.

KINGSLEY-HICKMAN, P. B., SAKO, E. Y., UGURBIL, K., FROM, A. H. & FOKER, J. E. 1990. 31P NMR measurement of mitochondrial uncoupling in isolated rat hearts. *J Biol Chem,* 265**,** 1545-50.

KNECHT, E., AGUADO, C., CARCEL, J., ESTEBAN, I., ESTEVE, J. M., GHISLAT, G., MORUNO, J. F., VIDAL, J. M. & SAEZ, R. 2009. Intracellular protein degradation in mammalian cells: recent developments. *Cell Mol Life Sci,* 66**,** 2427-43.

KOBERSTEIN, R. & SUND, H. 1973. Studies of glutamate dehydrogenase. The influence of ADP, GTP, and L-glutamate on the binding of the reduced coenzyme to beef-liver glutamate dehydrogenase. *Eur J Biochem,* 36**,** 545-52.

KONDO, M., YAMAOKA, T., HONDA, S., MIWA, Y., KATASHIMA, R., MORITANI, M., YOSHIMOTO, K., HAYASHI, Y. & ITAKURA, M. 2000. The rate of cell growth is regulated by purine biosynthesis via ATP production and G(1) to S phase transition. *J Biochem,* 128**,** 57-64.

KORANGATH, P., TEO, W. W., SADIK, H., HAN, L., MORI, N., HUIJTS, C. M., WILDES, F., BHARTI, S., ZHANG, Z., SANTA-MARIA, C. A., TSAI, H., DANG, C. V., STEARNS, V., BHUJWALLA, Z. M. & SUKUMAR, S. 2015. Targeting Glutamine Metabolism in Breast Cancer with Aminooxyacetate. *Clin Cancer Res,* 21**,** 3263-73.

KOROLCHUK, V. I., SAIKI, S., LICHTENBERG, M., SIDDIQI, F. H., ROBERTS, E. A., IMARISIO, S., JAHREISS, L., SARKAR, S., FUTTER, M., MENZIES, F. M., O'KANE, C. J., DERETIC, V. & RUBINSZTEIN, D. C. 2011. Lysosomal positioning coordinates cellular nutrient responses. *Nat Cell Biol,* 13**,** 453-60.

KROEMER, G. & POUYSSEGUR, J. 2008. Tumor cell metabolism: cancer's Achilles' heel. *Cancer Cell,* 13**,** 472-82.

KUHN, K. S., SCHUHMANN, K., STEHLE, P., DARMAUN, D. & FURST, P. 1999. Determination of glutamine in muscle protein facilitates accurate assessment of proteolysis and de novo synthesis-derived endogenous glutamine production. *Am J Clin Nutr,* 70**,** 484-9.

LANDMAN, G. W., KLEEFSTRA, N., VAN HATEREN, K. J., GROENIER, K. H., GANS, R. O. & BILO, H. J. 2010. Metformin associated with lower cancer mortality in type 2 diabetes: ZODIAC-16. *Diabetes Care,* 33**,** 322-6.

LANE, A. N. & FAN, T. W. 2015. Regulation of mammalian nucleotide metabolism and biosynthesis. *Nucleic Acids Res,* 43**,** 2466-85.

LELEIKO, N. S. & WALSH, M. J. 1996. The role of glutamine, short-chain fatty acids, and nucleotides in intestinal adaptation to gastrointestinal disease. *Pediatr Clin North Am,* 43**,** 451-70.

LI, C., LI, M., CHEN, P., NARAYAN, S., MATSCHINSKY, F. M., BENNETT, M. J., STANLEY, C. A. & SMITH, T. J. 2011a. Green tea polyphenols control dysregulated glutamate dehydrogenase in transgenic mice by hijacking the ADP activation site. *J Biol Chem,* 286**,** 34164-74.

LI, M., ALLEN, A. & SMITH, T. J. 2007. High throughput screening reveals several new classes of glutamate dehydrogenase inhibitors. *Biochemistry,* 46**,** 15089-102.

LI, M., LI, C., ALLEN, A., STANLEY, C. A. & SMITH, T. J. 2011b. The structure and allosteric regulation of glutamate dehydrogenase. *Neurochem Int,* 59**,** 445-55.

LI, M., SMITH, C. J., WALKER, M. T. & SMITH, T. J. 2009. Novel inhibitors complexed with glutamate dehydrogenase: allosteric regulation by control of protein dynamics. *J Biol Chem,* 284**,** 22988-3000.

LIBBY, G., DONNELLY, L. A., DONNAN, P. T., ALESSI, D. R., MORRIS, A. D. & EVANS, J. M. 2009. New users of metformin are at low risk of incident cancer: a cohort study among people with type 2 diabetes. *Diabetes Care,* 32**,** 1620-5.

LIU, D., PERKINS, J. T. & HENNIG, B. 2016. EGCG prevents PCB-126-induced endothelial cell inflammation via epigenetic modifications of NF-kappaB target genes in human endothelial cells. *J Nutr Biochem,* 28**,** 164-70.

LIU, G., ZHU, J., YU, M., CAI, C., ZHOU, Y., YU, M., FU, Z., GONG, Y., YANG, B., LI, Y., ZHOU, Q., LIN, Q., YE, H., YE, L., ZHAO, X., LI, Z., CHEN, R., HAN, F., TANG, C. & ZENG, B. 2015. Glutamate dehydrogenase is a novel prognostic marker and predicts metastases in colorectal cancer patients. *J Transl Med,* 13**,** 144.

LLUIS, J. M., MORALES, A., BLASCO, C., COLELL, A., MARI, M., GARCIA-RUIZ, C. & FERNANDEZ-CHECA, J. C. 2005. Critical role of mitochondrial glutathione in the survival of hepatocytes during hypoxia. *J Biol Chem,* 280**,** 3224-32.

LUNT, S. Y. & VANDER HEIDEN, M. G. 2011. Aerobic glycolysis: meeting the metabolic requirements of cell proliferation. *Annu Rev Cell Dev Biol,* 27**,** 441-64.

M, T. 1976. on the metabolic detoxication of bithionol in man. *J Toxicol Sci* 26**,** 26-31.

MA, Z. & VOSSELLER, K. 2013. O-GlcNAc in cancer biology. *Amino Acids,* 45**,** 719-33.

MARKAU, K., SCHNEIDER, J. & SUND, H. 1972. Kinetic studies on the mechanism of the action of ADP on the glutamate dehydrogenase reaction. *FEBS Lett,* 24**,** 32-6.

MARTIN, R. J. 1997. Modes of action of anthelmintic drugs. *Vet J,* 154**,** 11-34.

MATHEWS, C. K. 2006. DNA precursor metabolism and genomic stability. *FASEB J,* 20**,** 1300-14.

MATRE, P., VELEZ, J., JACAMO, R., QI, Y., SU, X., CAI, T., CHAN, S. M., LODI, A., SWEENEY, S. R., MA, H., DAVIS, R. E., BARAN, N., HAFERLACH, T., SU, X., FLORES, E. R., GONZALEZ, D., KONOPLEV, S., SAMUDIO, I., DINARDO, C., MAJETI, R., SCHIMMER, A. D., LI, W., WANG, T., TIZIANI, S. & KONOPLEVA, M. 2016. Inhibiting glutaminase in acute myeloid leukemia: metabolic dependency of selected AML subtypes. *Oncotarget,* 7**,** 79722-79735.

MATSUNO, T. 1987. Bioenergetics of tumor cells: glutamine metabolism in tumor cell mitochondria. *Int J Biochem,* 19**,** 303-7.

MAURO, C., LEOW, S. C., ANSO, E., ROCHA, S., THOTAKURA, A. K., TORNATORE, L., MORETTI, M., DE SMAELE, E., BEG, A. A., TERGAONKAR, V., CHANDEL, N. S. & FRANZOSO, G. 2011. NF-kappaB controls energy homeostasis and metabolic adaptation by upregulating mitochondrial respiration. *Nat Cell Biol,* 13**,** 1272-9.

MCCAULEY, R., KONG, S. E. & HALL, J. 1998. Glutamine and nucleotide metabolism within enterocytes. *JPEN J Parenter Enteral Nutr,* 22**,** 105-11.

MEISTER, A. 1983. Selective modification of glutathione metabolism. *Science,* 220**,** 472-7.

MEISTER, A. 1994. Glutathione, ascorbate, and cellular protection. *Cancer Res,* 54**,** 1969s-1975s.

MESHI, T., YOSHIKAWA, M. & SATO, Y. 1970. Metabolic fate of bis(3,5-dichloro-2-hydroxyphenyl)-sulfoxide (bithionol sulfoxide). *Biochem Pharmacol,* 19**,** 1351-61.

MIHAYLOVA, M. M. & SHAW, R. J. 2011. The AMPK signalling pathway coordinates cell growth, autophagy and metabolism. *Nat Cell Biol,* 13**,** 1016-23.

MILLER, R. A., CHU, Q., XIE, J., FORETZ, M., VIOLLET, B. & BIRNBAUM, M. J. 2013. Biguanides suppress hepatic glucagon signalling by decreasing production of cyclic AMP. *Nature,* 494**,** 256-60.

MILLER, S. C., HUANG, R., SAKAMURU, S., SHUKLA, S. J., ATTENE-RAMOS, M. S., SHINN, P., VAN LEER, D., LEISTER, W., AUSTIN, C. P. & XIA, M. 2010. Identification of known drugs that act as inhibitors of NF-kappaB signaling and their mechanism of action. *Biochem Pharmacol,* 79**,** 1272-80.

MITHIEUX, G. & ROUSSET, B. 1989. Identification of a lysosome membrane protein which could mediate ATP-dependent stable association of lysosomes to microtubules. *J Biol Chem,* 264**,** 4664-8.

MOREADITH, R. W. & LEHNINGER, A. L. 1984. The pathways of glutamate and glutamine oxidation by tumor cell mitochondria. Role of mitochondrial NAD(P)+-dependent malic enzyme. *J Biol Chem,* 259**,** 6215-21.

MORUNO, F., PEREZ-JIMENEZ, E. & KNECHT, E. 2012. Regulation of autophagy by glucose in Mammalian cells. *Cells,* 1**,** 372-95.

MORUNO-MANCHON, J. F., PEREZ-JIMENEZ, E. & KNECHT, E. 2013. Glucose induces autophagy under starvation conditions by a p38 MAPK-dependent pathway. *Biochem J,* 449**,** 497-506.

MULLEN, A. R., WHEATON, W. W., JIN, E. S., CHEN, P. H., SULLIVAN, L. B., CHENG, T., YANG, Y., LINEHAN, W. M., CHANDEL, N. S. & DEBERARDINIS, R. J. 2011. Reductive carboxylation supports growth in tumour cells with defective mitochondria. *Nature,* 481**,** 385-8.

NAGY, P. 2013. Kinetics and mechanisms of thiol-disulfide exchange covering direct substitution and thiol oxidation-mediated pathways. *Antioxid Redox Signal,* 18**,** 1623-41.

NAKAUE, H. S., DOST, F. N. & BUHLER, D. R. 1973. Studies on the toxicity of hexachlorophene in the rat. *Toxicol Appl Pharmacol,* 24**,** 239-49.

NEWSHOLME, P., PROCOPIO, J., LIMA, M. M., PITHON-CURI, T. C. & CURI, R. 2003. Glutamine and glutamate--their central role in cell metabolism and function. *Cell Biochem Funct,* 21**,** 1-9.

NIHON KISEICH¿± GAKKAI. Japanese journal of parasitology. Kiseichugaku zasshi. Tokyo: Japanese Society of Parasitology.

NING, W., WANG, S., DONG, X., LIU, D., FU, L., JIN, R. & XU, A. 2015. Epigallocatechin-3-gallate (EGCG) Suppresses the Trafficking of Lymphocytes to Epidermal Melanocytes via Inhibition of JAK2: Its Implication for Vitiligo Treatment. *Biol Pharm Bull,* 38**,** 1700-6.

NOTO, H., GOTO, A., TSUJIMOTO, T. & NODA, M. 2012. Cancer risk in diabetic patients treated with metformin: a systematic review and meta-analysis. *PLoS One,* 7**,** e33411.

PAGLIARINI, D. J., WILEY, S. E., KIMPLE, M. E., DIXON, J. R., KELLY, P., WORBY, C. A., CASEY, P. J. & DIXON, J. E. 2005. Involvement of a mitochondrial

phosphatase in the regulation of ATP production and insulin secretion in pancreatic beta cells. *Mol Cell,* 19**,** 197-207.

PARK, S., GWAK, J., CHO, M., SONG, T., WON, J., KIM, D. E., SHIN, J. G. & OH, S. 2006. Hexachlorophene inhibits Wnt/beta-catenin pathway by promoting Siah-mediated beta-catenin degradation. *Mol Pharmacol,* 70**,** 960-6.

PERRY, T. L., WRIGHT, J. M., HANSEN, S., ALLAN, B. M., BAIRD, P. A. & MACLEOD, P. M. 1980. Failure of aminooxyacetic acid therapy in Huntington disease. *Neurology,* 30**,** 772-5.

PETERSON, P. E. & SMITH, T. J. 1999. The structure of bovine glutamate dehydrogenase provides insights into the mechanism of allostery. *Structure,* 7**,** 769-82.

PLAITAKIS, A., LATSOUDIS, H. & SPANAKI, C. 2011. The human GLUD2 glutamate dehydrogenase and its regulation in health and disease. *Neurochem Int,* 59**,** 495-509.

POZNIAK, Y., BALINT-LAHAT, N., RUDOLPH, J. D., LINDSKOG, C., KATZIR, R., AVIVI, C., PONTEN, F., RUPPIN, E., BARSHACK, I. & GEIGER, T. 2016. System-wide Clinical Proteomics of Breast Cancer Reveals Global Remodeling of Tissue Homeostasis. *Cell Syst,* 2**,** 172-84.

PROUGH, R. A., CULVER, J. M. & FISHER, H. F. 1973. The mechanism of activation of glutamate dehydrogenase-catalyzed reactions by two different, cooperatively bound activators. *J Biol Chem,* 248**,** 8528-33.

PUSAPATI, R. V., DAEMEN, A., WILSON, C., SANDOVAL, W., GAO, M., HALEY, B., BAUDY, A. R., HATZIVASSILIOU, G., EVANGELISTA, M. & SETTLEMAN, J. 2016. mTORC1-Dependent Metabolic Reprogramming Underlies Escape from Glycolysis Addiction in Cancer Cells. *Cancer Cell,* 29**,** 548-62.

QING, G., LI, B., VU, A., SKULI, N., WALTON, Z. E., LIU, X., MAYES, P. A., WISE, D. R., THOMPSON, C. B., MARIS, J. M., HOGARTY, M. D. & SIMON, M. C. 2012. ATF4 regulates MYC-mediated neuroblastoma cell death upon glutamine deprivation. *Cancer Cell,* 22**,** 631-44.

RAJAPAKSHE, A. R., PODYMA-INOUE, K. A., TERASAWA, K., HASEGAWA, K., NAMBA, T., KUMEI, Y., YANAGISHITA, M. & HARA-YOKOYAMA, M. 2015. Lysosome-associated membrane proteins (LAMPs) regulate intracellular positioning of mitochondria in MC3T3-E1 cells. *Exp Cell Res,* 331**,** 211-22.

RAJAS, F., GIRE, V. & ROUSSET, B. 1996. Involvement of a membrane-bound form of glutamate dehydrogenase in the association of lysosomes to microtubules. *J Biol Chem,* 271**,** 29882-90.

RAMPAZZO, C., MIAZZI, C., FRANZOLIN, E., PONTARIN, G., FERRARO, P., FRANGINI, M., REICHARD, P. & BIANCHI, V. 2010. Regulation by degradation, a cellular defense against deoxyribonucleotide pool imbalances. *Mutat Res,* 703**,** 2-10.

REED, H. T., MELTZER, J., CREWS, P., NORRIS, C. H., QUINE, D. B. & GUTH, P. S. 1985. Amino-oxyacetic acid as a palliative in tinnitus. *Arch Otolaryngol,* 111**,** 803-5.

REHMAN, J., ZHANG, H. J., TOTH, P. T., ZHANG, Y., MARSBOOM, G., HONG, Z., SALGIA, R., HUSAIN, A. N., WIETHOLT, C. & ARCHER, S. L. 2012. Inhibition of mitochondrial fission prevents cell cycle progression in lung cancer. *FASEB J,* 26**,** 2175-86.

REICHARD, P. 1988. Interactions between deoxyribonucleotide and DNA synthesis. *Annu Rev Biochem,* 57**,** 349-74.

REITZER, L. J., WICE, B. M. & KENNELL, D. 1979. Evidence that glutamine, not sugar, is the major energy source for cultured HeLa cells. *J Biol Chem,* 254**,** 2669-76.

SAEKI, K., WATANABE, M., TSUBOI, M., SUGANO, S., YOSHITAKE, R., TANAKA, Y., ONG, S. M., SAITO, T., MATSUMOTO, K., FUJITA, N., NISHIMURA, R. & NAKAGAWA, T. 2015. Anti-tumour effect of metformin in canine mammary gland tumour cells. *Vet J,* 205**,** 297-304.

SAUNDERS, L. P., OUELLETTE, A., BANDLE, R., CHANG, W. C., ZHOU, H., MISRA, R. N., DE LA CRUZ, E. M. & BRADDOCK, D. T. 2008. Identification of small-molecule inhibitors of autotaxin that inhibit melanoma cell migration and invasion. *Mol Cancer Ther,* 7**,** 3352-62.

SCHULZ, J. B., LINDENAU, J., SEYFRIED, J. & DICHGANS, J. 2000. Glutathione, oxidative stress and neurodegeneration. *Eur J Biochem,* 267**,** 4904-11.

SCHUMACKER, P. T. 2015. Reactive oxygen species in cancer: a dance with the devil. *Cancer Cell,* 27**,** 156-7.

SENA, L. A. & CHANDEL, N. S. 2012. Physiological roles of mitochondrial reactive oxygen species. *Mol Cell,* 48**,** 158-67.

SHASHIDHARAN, P., MICHAELIDIS, T. M., ROBAKIS, N. K., KRESOVALI, A., PAPAMATHEAKIS, J. & PLAITAKIS, A. 1994. Novel human glutamate dehydrogenase expressed in neural and testicular tissues and encoded by an X-linked intronless gene. *J Biol Chem,* 269**,** 16971-6.

SHEEN, J. H., ZONCU, R., KIM, D. & SABATINI, D. M. 2011. Defective regulation of autophagy upon leucine deprivation reveals a targetable liability of human melanoma cells in vitro and in vivo. *Cancer Cell,* 19**,** 613-28.

SHERRY, A. D., ZHAO, P., WIETHOFF, A. J., JEFFREY, F. M. & MALLOY, C. R. 1998. Effects of aminooxyacetate on glutamate compartmentation and TCA cycle kinetics in rat hearts. *Am J Physiol,* 274**,** H591-9.

SHIGENAGA, M. K., HAGEN, T. M. & AMES, B. N. 1994. Oxidative damage and mitochondrial decay in aging. *Proc Natl Acad Sci U S A,* 91**,** 10771-8.

SILVERNALE, J. N., JOSWICK, H. L., CORNER, T. R. & GERHARDT, P. 1971. Antimicrobial actions of hexachlorophene: cytological manifestations. *J Bacteriol,* 108**,** 482-91.

SINGH, T. S., MUTUM, S. S. & RAZAQUE, M. A. 1986. Pulmonary paragonimiasis: clinical features, diagnosis and treatment of 39 cases in Manipur. *Trans R Soc Trop Med Hyg,* 80**,** 967-71.

SMITH, T. J., PETERSON, P. E., SCHMIDT, T., FANG, J. & STANLEY, C. A. 2001. Structures of bovine glutamate dehydrogenase complexes elucidate the mechanism of purine regulation. *J Mol Biol,* 307**,** 707-20.

SMITH, T. J., SCHMIDT, T., FANG, J., WU, J., SIUZDAK, G. & STANLEY, C. A. 2002. The structure of apo human glutamate dehydrogenase details subunit communication and allostery. *J Mol Biol,* 318**,** 765-77.

SMITH, T. J. & STANLEY, C. A. 2008. Untangling the glutamate dehydrogenase allosteric nightmare. *Trends Biochem Sci,* 33**,** 557-64.

SON, J., LYSSIOTIS, C. A., YING, H., WANG, X., HUA, S., LIGORIO, M., PERERA, R. M., FERRONE, C. R., MULLARKY, E., SHYH-CHANG, N., KANG, Y., FLEMING, J. B., BARDEESY, N., ASARA, J. M., HAIGIS, M. C., DEPINHO, R. A., CANTLEY, L. C. & KIMMELMAN, A. C. 2013. Glutamine supports pancreatic cancer growth through a KRAS-regulated metabolic pathway. *Nature,* 496**,** 101-5.

SORBI, D., BOYNTON, J. & LINDOR, K. D. 1999. The ratio of aspartate aminotransferase to alanine aminotransferase: potential value in differentiating nonalcoholic steatohepatitis from alcoholic liver disease. *Am J Gastroenterol,* 94**,** 1018-22.

SOUBA, W. W. 1993. Glutamine and cancer. *Ann Surg,* 218**,** 715-28.

STANLEY, C. A. 2009. Regulation of glutamate metabolism and insulin secretion by glutamate dehydrogenase in hypoglycemic children. *Am J Clin Nutr,* 90**,** 862S-866S.

TAKEUCHI, T., KOBAYASHI, S., TANABE, M. & FUJIWARA, T. 1985. In vitro inhibition of Giardia lamblia and Trichomonas vaginalis growth by bithionol, dichlorophene, and hexachlorophene. *Antimicrob Agents Chemother,* 27**,** 65-70.

THOMPSON, R. M., DYTFELD, D., REYES, L., ROBINSON, R. M., SMITH, B., MANEVICH, Y., JAKUBOWIAK, A., KOMARNICKI, M., PRZYBYLOWICZ-CHALECKA, A., SZCZEPANIAK, T., MITRA, A. K., VAN NESS, B. G., LUCZAK, M. & DOLLOFF, N. G. 2017. Glutaminase inhibitor CB-839 synergizes with carfilzomib in resistant multiple myeloma cells. *Oncotarget,* 8**,** 35863-35876.

THORNBURG, J. M., NELSON, K. K., CLEM, B. F., LANE, A. N., ARUMUGAM, S., SIMMONS, A., EATON, J. W., TELANG, S. & CHESNEY, J. 2008. Targeting aspartate aminotransferase in breast cancer. *Breast Cancer Res,* 10**,** R84.

TOWNSEND, D. M., TEW, K. D. & TAPIERO, H. 2003. The importance of glutathione in human disease. *Biomed Pharmacother,* 57**,** 145-55.

TRACHOOTHAM, D., ALEXANDRE, J. & HUANG, P. 2009. Targeting cancer cells by ROS-mediated mechanisms: a radical therapeutic approach? *Nat Rev Drug Discov,* 8**,** 579-91.

TSAI, Y. T., CHUANG, M. J., TANG, S. H., WU, S. T., CHEN, Y. C., SUN, G. H., HSIAO, P. W., HUANG, S. M., LEE, H. J., YU, C. P., HO, J. Y., LIN, H. K., CHEN, M. R., LIN, C. C., CHANG, S. Y., LIN, V. C., YU, D. S. & CHA, T. L. 2015. Novel Cancer Therapeutics with Allosteric Modulation of the Mitochondrial C-Raf-DAPK Complex by Raf Inhibitor Combination Therapy. *Cancer Res,* 75**,** 3568-82.

TURRENS, J. F. 2003. Mitochondrial formation of reactive oxygen species. *J Physiol,* 552**,** 335-44.

VANDER HEIDEN, M. G. 2011. Targeting cancer metabolism: a therapeutic window opens. *Nat Rev Drug Discov,* 10**,** 671-84.

VANDER HEIDEN, M. G., CANTLEY, L. C. & THOMPSON, C. B. 2009. Understanding the Warburg effect: the metabolic requirements of cell proliferation. *Science,* 324**,** 1029-33.

WANG, J. B., ERICKSON, J. W., FUJI, R., RAMACHANDRAN, S., GAO, P., DINAVAHI, R., WILSON, K. F., AMBROSIO, A. L., DIAS, S. M., DANG, C. V. & CERIONE, R. A. 2010. Targeting mitochondrial glutaminase activity inhibits oncogenic transformation. *Cancer Cell,* 18**,** 207-19.

WANG, J. L. & BUHLER, D. R. 1978. Inhibition of dehydrogenase enzymes by hexachlorophene. *Biochem Pharmacol,* 27**,** 2947-53.

WARBURG, O. 1956a. On respiratory impairment in cancer cells. *Science,* 124**,** 269-70.

WARBURG, O. 1956b. On the origin of cancer cells. *Science,* 123**,** 309-14.

WARD, P. S. & THOMPSON, C. B. 2012. Metabolic reprogramming: a cancer hallmark even warburg did not anticipate. *Cancer Cell,* 21**,** 297-308.

WILMORE DW, B. P., MUHLBACHER F 1983. *Injured man:trauma and sepsis.* , New york, Academic press.

WINTERBOURN, C. C. 1993. Superoxide as an intracellular radical sink. *Free Radic Biol Med,* 14**,** 85-90.

WISE, D. R., DEBERARDINIS, R. J., MANCUSO, A., SAYED, N., ZHANG, X. Y., PFEIFFER, H. K., NISSIM, I., DAIKHIN, E., YUDKOFF, M., MCMAHON, S. B. & THOMPSON, C. B. 2008. Myc regulates a transcriptional program that stimulates mitochondrial glutaminolysis and leads to glutamine addiction. *Proc Natl Acad Sci U S A,* 105**,** 18782-7.

WISEMAN, H. & HALLIWELL, B. 1996. Damage to DNA by reactive oxygen and nitrogen species: role in inflammatory disease and progression to cancer. *Biochem J,* 313 (Pt 1)**,** 17-29.

WROBLEWSKI, F. & LADUE, J. S. 1956. Serum glutamic pyruvic transaminase in cardiac with hepatic disease. *Proc Soc Exp Biol Med,* 91**,** 569-71.

YANG, C., SUDDERTH, J., DANG, T., BACHOO, R. M., MCDONALD, J. G. & DEBERARDINIS, R. J. 2009. Glioblastoma cells require glutamate dehydrogenase to survive impairments of glucose metabolism or Akt signaling. *Cancer Res,* 69**,** 7986-93.

YIELDING, K. L. & TOMKINS, G. M. 1960. Structural Alterations in Crystalline Glutamic Dehydrogenase Induced by Steroid Hormones. *Proc Natl Acad Sci U S A,* 46**,** 1483-8.

YIELDING, K. L. & TOMKINS, G. M. 1961. An effect of L-leucine and other essential amino acids on the structure and activity of glutamic dehydrogenase. *Proc Natl Acad Sci U S A,* 47**,** 983-9.

YOKOGAWA, M., YOSHIMURA, H., OKURA, T. & SAITO, M. 1962. Effect of bithionol on Taenia saginata, especially with reference to the detection of eggs with fecal examination and the perianal cellophane tape method. *J Chiba Med Soc,* 37**,** 455-62.

YU, D., SHI, X., MENG, G., CHEN, J., YAN, C., JIANG, Y., WEI, J. & DING, Y. 2015. Kidney-type glutaminase (GLS1) is a biomarker for pathologic diagnosis and prognosis of hepatocellular carcinoma. *Oncotarget,* 6**,** 7619-31.

YUNEVA, M., ZAMBONI, N., OEFNER, P., SACHIDANANDAM, R. & LAZEBNIK, Y. 2007. Deficiency in glutamine but not glucose induces MYC-dependent apoptosis in human cells. *J Cell Biol,* 178**,** 93-105.

ZETTERBERG, A. & ENGSTROM, W. 1981. Glutamine and the regulation of DNA replication and cell multiplication in fibroblasts. *J Cell Physiol,* 108**,** 365-73.

ZIELKE, H. R., ZIELKE, C. L. & OZAND, P. T. 1984. Glutamine: a major energy source for cultured mammalian cells. *Fed Proc,* 43**,** 121-5.

ZOROV, D. B., JUHASZOVA, M. & SOLLOTT, S. J. 2006. Mitochondrial ROS-induced ROS release: an update and review. *Biochim Biophys Acta,* 1757**,** 509-17.